A Study on the Fatigue Crack Growth Characteristics and Mutual Interaction Effect of Micro Defects in Structures

Lee, Hoyeon

(Degree)
博士（工学）

(Date of Degree)
2013-09-25

(Date of Publication)
2014-09-01

(Resource Type)
doctoral thesis

(Report Number)
甲第5972号

(URL)
https://hdl.handle.net/20.500.14094/D1005972

Doctoral Dissertation

A Study on the Fatigue Crack Growth Characteristics and Mutual Interaction Effect of Micro Defects in Structures

構造部材中の微小欠陥群の相互干渉効果及び
疲労き裂進展特性に関する研究

July 2013

Graduate School of Maritime Sciences
Kobe University

Hoyeon LEE

Contents

Abstract

The fracture mechanics is the academic subject that should be handled very importantly for safety, maintenance, repair and the life, in machinery and structures (aircraft, trains, cars, ships, gas turbines, rocket engines, rotary shafts, pipes, pressure vessels, offshore structures, etc.). The loss caused by fracture accident produces the negative consequence in economic and environment as well as human life. In particular, the accidents caused by metal fatigue fracture have been reported as more than 80 % of fracture accidents. Thus, it is thought that prevention of accidents and safety of various machines and structure should be secured through the more detailed studies on the mechanism of fatigue fracture. Therefore, study on fatigue crack growth behavior and interference effects between cracks was conducted with four research themes in machinery and structures.

The first project is to conduct the study on mutual interference between circular hole which is the target of stress concentration and surface crack for fatigue crack growth. In machinery and structures, there are many discontinuous parts for lubrication, riveting, bolting and external design. These are inevitable parts in the design. These discontinuous parts become stress concentration zone. In addition, because fatigue cracks begin to occur mostly on surface, state of surface and environment become very important factors upon fatigue fracture behavior. These surface cracks grow toward the inside of the member by repeated external loads. If surface crack approaches to the stress concentration zone which is already mentioned during this course, fatigue crack behavior should consider the effect caused by stress concentration zone. Thus, in order to investigate the interference effect between surface crack and stress concentration zone during fatigue crack growth, fatigue crack growth experiment has been conducted using experiments with stress concentration zone and initial crack.

The second project is to conduct the study on effect of mutual interference of surface crack on fatigue crack growth. Representative examples of defect and crack are inherent defects in the materials such as inclusion, processing defect caused by processing wound and weld defect. These defects may be unilaterally present in machinery and structures, but many defects are concentrated and occur irregularly. It is pointed out that these defects affect occurrence of new cracks and growth of fatigue crack much. Defects and cracks represent complex and various fracture behaviors due to mutual interaction. Thus, the effect of mutual interaction on defect evaluation is the project which should be considered in aspect of safety. However, experiments and numerical study on the effects of mutual interaction of adjacent cracks and defects have been conducted by many scholars and research institutions. Due to its complexity and diversity, the safety based on quantitative evaluation was not derived but structural preservation based on excessive safety rate was represented much. Thus, in order to quantitatively and precisely investigate the interaction effect of cracks in this study, fatigue crack growth experiments about single crack and multiple cracks were conducted. Mutual interaction effect between cracks was observed by identifying surface crack and internal crack growth behaviors with beach mark method.

The third project is to conduct the study on effect of mixed mode on fatigue crack growth behavior using three point bending specimens and dependence of thickness of specimens. In machinery and structures, inclusion of materials, corrosion or fatigue during use, or slight defect caused by other causes must exist. Direction of load working on such cracks or defects greatly varies depending on kinds of machinery and structures, environment and state. However, load direction working on fatigue crack occurring on the member placed in this state is not always the normal direction. If load working direction is not normal, crack is distorting and progresses to the inside of structure. However, the information on this fracture behavior is insufficient and accurately proven data are very little. Therefore, in order to prevent cracks from progressing to important parts of structures and machinery and prevent the fracture accident in advance, it is very important to establish the fracture path prediction theory about distorting progress phenomenon of various cracks. Thus, this study observed fatigue crack behavior in mixed mode state with consideration of correlation between load working direction and initial crack direction, and it investigated fatigue crack mechanism.

The fourth and last project is to conduct the evaluation of the strength through static load and fatigue test using a crane hook being widely used in construction site or industrial site. The crane hook is being used for several purposes in construction site, industrial site and ship. For example, an overhead hook is being used to repair the engine in ship. A crane hook is being used to move or transport cargo. A hook attached to excavator is being used. As such, fracture and damage of crane hook being used for several purposes have become a problem. In particular, because a hook is being used based on the experience of the worker rather than the rated load at work, a huge load is often given to the hook. If this operation is repeated, a crane hook will be altered and damaged. However, if small alteration or damage occurs on site, it is not immediately replaced but, instead, it is used until it is broken down. Thus, it is more dangerous. Static load test and fatigue test were performed by using a crane hook (specimen 1) being widely used in actual construction site, industrial site and ship and a hook (specimen 2) in which diameter and rounding were changed in parts where damage and alteration were frequently occurring. This study on evaluation of the strength of crane hook was conducted through above tests.

List of symbols

a	Crack length, Depth of surface crack
θ	Crack propagation angle, the angle surface crack and circular hole
da/dN	Fatigue crack propagation rate(fatigue crack growth velocity)
r	Infinitesimal radius from crack tip
C	Material constants
ν	Poisson's ratio
ΔK	Stress intensity factor range
σ_{ij}	Stress tensor
$2c$	Surface crack length
K_I	Mode I
K_{II}	Mode II
K_{II}	Mode II
K_I	Stress intensity factor
N_f	Number of initial fatigue cycles
R	Stress ratio
m	Material constants

E	Young's modulus; input energy
F	Fracture energy
ν	Poisson's ratio
ρ	Material mass density
N_i / N_f	Fatigue life ratio
a / W	Crack growth rate
a / c	Aspect ratio

List of Captions of Figures and Tables

Figures in Chapter 2

Figures in Chapter 3

Figures in Chapter 4

Figures in Chapter 5

Figures in Chapter 6

Figures in Chapter 7

Tables

Chapter 1

Introduction

1.1 Background

Machine or structures are mostly placed in the state of load repeatedly fluctuating during the use. Since damage is accumulated by such repeated load, it shows fatigue fracture phenomenon in which crack occurs and ultimately fracture may occur if repeated load is given under the state of stress even below the yield stress.

Fracture mechanics was established as the academic subject for the first time in the 1920s by Griffith. Interpretation about fatigue fracture equipment and ability to prevent the fracture accident has been rapidly developed after World War II. In addition, it obtained high performance and achievement with efforts of many research organizations and scholars, but many challenges still remain to be solved. It is thought that efforts to apply existing fracture mechanics theory to the actual situation will be needed.

If load condition is changed into unexpected one due to several factors after load condition at the time of the design of machinery and structures has been used for a long time, fracture may occur in the load below the design standards and then parts of machine or structure may collapse. Fracture accidents which cause huge human and material damage are sometimes caused by mistake of design, but most of them are caused by cracks occurring in defect or stress concentration zone which is present in the inside of materials.

Typical examples of defects and cracks are inherent defects of the inside of material such as inclusions, processing defect caused by processing wound and weld defects. These defects exist in machinery and structure by itself, but many defects are concentrated and occur irregularly. These defects have been pointed out to give a significant impact on the growth behavior and the occurrence of new cracks. In adjacent cracks or defects, stress field around the defect has been changed depending on the relative location and size, and it shows complex fracture behavior caused by mutual interaction. Therefore, it is impossible to apply a single crack and the same terms. In addition, a large number of members of machinery or structures should give shape for binding, and have bolt for binding and circular hole for cooling. As a result, stress concentration often occurs at the local zone of member due to action of external forces. Such stress concentration is inhibited under allowable range at the design step, but if slight defect and crack occur in or around stress concentration zone, complex fracture behavior caused by mutual interference may occur. Therefore, prediction of fatigue crack growth becomes the important issue for accident prevention and selection of proper maintenance method.

Stress state working on actual machinery and structures is complex and most of cracks generally represent the aspects of mixed mode load conditions due to complexity. The necessity for studies on mixed mode load has been increased and many scholars are conducting various studies to reveal occurrence and mechanism of mixed mode crack. However, it is difficult to have consistent and unified evaluation because the experimental standards for behavior of mixed mode fatigue cracks are not enacted and results are different due to various experimental methods. Therefore, more detailed and quantitative mixed mode implementation methods are needed to implement occurrence of mixed mode fatigue crack, and the mechanism of crack behavior and fatigue crack behavior needs to be studied.

Therefore, this paper observed fatigue crack initiation and propagation behavior through fatigue crack propagation test with the following purpose for defects and fatigue cracks.

Chapter 2

Basic Concepts in Fatigue and Fracture

Fatigue is a leading cause of failure in mechanical components and structure that are subjected to repeated loads. This chapter presents general theoretical background concerning the initiation and propagation of fatigue crack.

2.1 Stress Analysis of Cracks

For certain cracked configurations subjected to external forces, it is albe to derive closed-form expressions for the stress in the body, assuming isotropic linear elastic material behavior. Westergaard (1939), Irwin (1957), Sneddon (1946) and Williams (1957) were among the firs to publish such solutions. If we defined a polar coordinate axis with the origin at the crack tip (see Figure 2.1), it can be shown that the stress field in any linear elastic cracked body is given by

$$\sigma_{ij} = \left(\frac{k}{\sqrt{r}}\right) f_{ij}\left(\theta\right) + other\ terms \tag{2.1}$$

Where σ_{ij} is the stress tensor, r and θ are as defined in Figure 2.1, k is a constant, and f_{ij} is a dimensionless function of θ. The higher order terms depend on geometry, but the solution for any given configuration contains a leading term that is proportional to $\frac{1}{\sqrt{r}}$. As $r \to 0$, the leading term approaches infinity, but the other terms remain finite or approach zero. Thus stress near the crack tip varies with $\frac{1}{\sqrt{r}}$, regardless of the configuration of the cracked body. It can also be shown that displacement near the crack tip varies with $\sqrt{r}$. Equation (2.1) describes a stress *singularity*, since stress is asymptotic to $r = 0$.

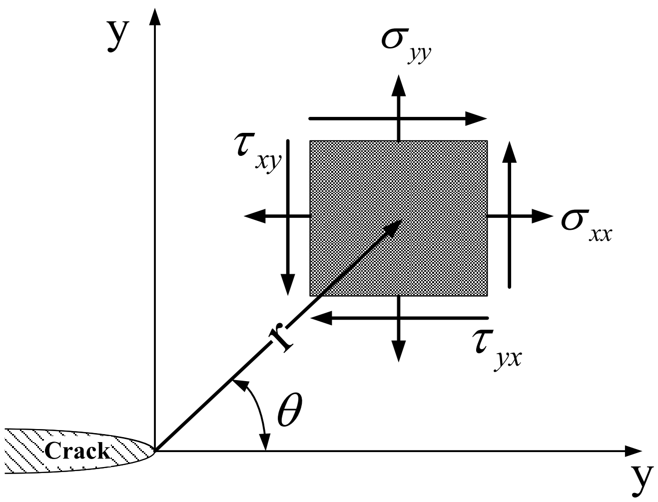

Figure 2.1 Definition of the coordinate axis ahead of a crack tip

There are three type of loading that a crack can experience, as illustrated in Figure 2.2. *Mode I* loading, where the principal load is applied normal to the crack plane, tends to slide on crack. *Mode II* corresponds to in-plane shear loading and tends to slide one crack face with body can be loaded in any one of these modes, or a combination of two or three modes.

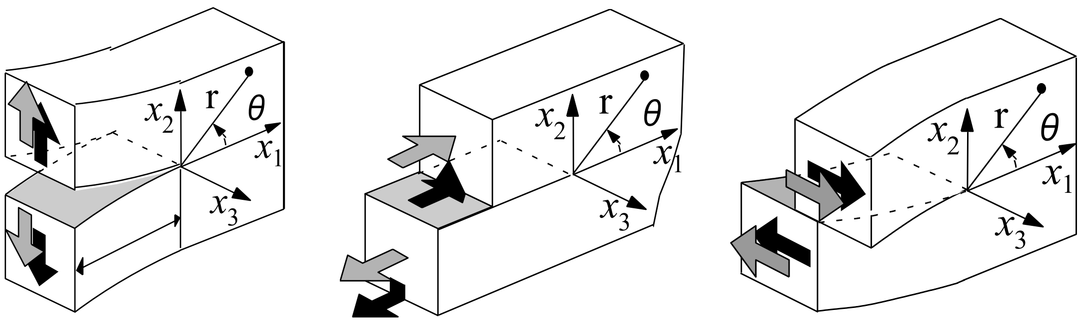

Mode I Mode II Mode III

Figure 2.2 Three modes of loading that can be applied to a crack

2.2 Stress Intensity Factor

Each mode of loading produces the $\frac{1}{\sqrt{r}}$ singularity at the crack tip, but the proportionality constant, k, and f_{ij} depend on mode. It is convenient at this point to replace k by the *stress intensity factor*, K, where $K = k\sqrt{2\pi}$. The stress intensity factor is usually given a subscript to denote the mode of loading; i.e., K_I, K_{II} or K_{III}. Thus the stress fields ahead of a crack tip in an isotropic linear elastic material can be written as

$$\lim_{r \to 0} \sigma_{ij}^{(I)} = \frac{K_I}{\sqrt{2\pi r}} f_{ij}^{(I)}(\theta) \tag{2.2}$$

$$\lim_{r \to 0} \sigma_{ij}^{(II)} = \frac{K_I}{\sqrt{2\pi r}} f_{ij}^{(II)}(\theta) \tag{2.3}$$

$$\lim_{r\to 0}\sigma_{ij}^{(III)} = \frac{K_I}{\sqrt{2\pi r}} f_{ij}^{(III)}(\theta) \tag{2.4}$$

for *Mode I, II, and III,* respectively. In a mixed-mode problem (i.e., when more than one loading mode is present), the individual contributions to given stress component are additive:

$$\sigma_{ij}^{(total)} = \sigma_{ij}^{(I)} + \sigma_{ij}^{(II)} + \sigma_{ij}^{(III)} \tag{2.5}$$

Equation (2.5) stems from the principle of linear superposition.

Detailed expressions for the singular stress fields for *Mode I and Mode II* are given in Table 2.1. Displacement relationships for *Mode I and Mode II* are listed in Table 2.2. Table 2.3 lists the nonzero stress and displacement components for *Mode III*.

Consider the *Mode I* singular field on the crack plane, where $\theta = 0$. According to Table 3.1, the stress in the x_1 and x_2 directions are equal:

$$\sigma_{11} = \sigma_{22} = \frac{K_I}{\sqrt{2\pi r}} \tag{2.6}$$

When $\theta = 0$, the shear is zero, which means that the crack plane is a principal plane for pure *Mode I* loading. Figure 2.3 is a schematic plot of σ_{22}, the stress normal to crack plane, versus distance from the crack tip. Equation (2.6) is only valid near the crack tip, where the $\frac{1}{\sqrt{r}}$ singularity dominates the stress field. Stresses far from the crack tip are governed by the remote boundary conditions. For example, if the cracked structures is subjected to a uniform remote tensile stress, σ_{22} approaches a constant value, σ^{∞}. We can define a *singularity dominated zone* as the region where the equations in Table 2.1 to 2.3 describe the crack tip fields.

The stress intensity factor defines the amplitude of the crack tip singularity. That is, stress near the crack tip increase in proportion to K. Moreover, the stress intensity factor completely defines the crack tip conditions; if K is known, it is possible to solve for all components of stress, description of crack tip conditions turns out to be one of the most important concepts in fracture mechanics.

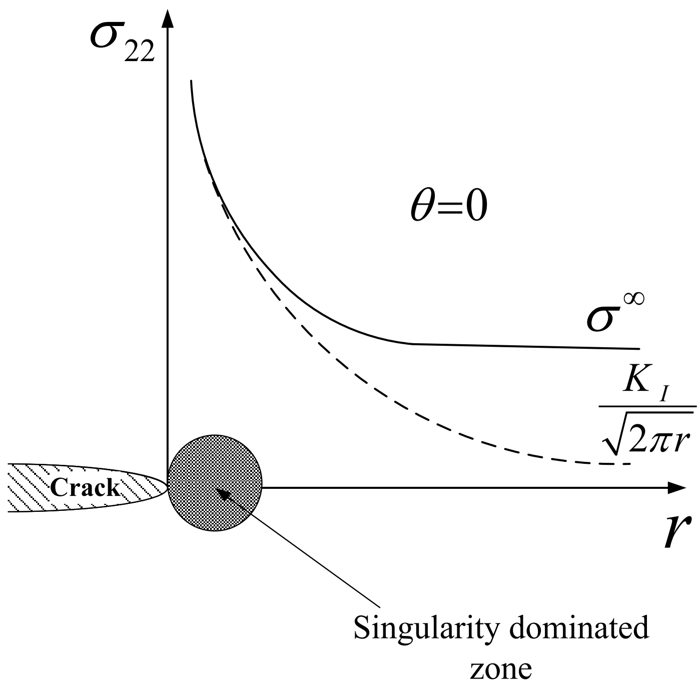

Figure 2.3 Stress normal to the crack plane in *Mode I*

Table 2.1 Stress fields ahead of a crack tip for *Mode I* and *Mode II* (linear elastic, isotropic material)

	Mode I	*Mode II*
σ_{11}	$\frac{K_I}{\sqrt{2\pi r}}\cos\left(\frac{\theta}{2}\right)\left[1-\sin\left(\frac{\theta}{2}\right)\sin\left(\frac{3\theta}{2}\right)\right]$	$\frac{K_{II}}{\sqrt{2\pi r}}\sin\left(\frac{\theta}{2}\right)\left[2+\cos\left(\frac{\theta}{2}\right)\cos\left(\frac{3\theta}{2}\right)\right]$
σ_{22}	$\frac{K_I}{\sqrt{2\pi r}}\cos\left(\frac{\theta}{2}\right)\left[1+\sin\left(\frac{\theta}{2}\right)\sin\left(\frac{3\theta}{2}\right)\right]$	$\frac{K_{II}}{\sqrt{2\pi r}}\sin\left(\frac{\theta}{2}\right)\cos\left(\frac{\theta}{2}\right)\cos\left(\frac{3\theta}{2}\right)$
τ_{12}	$\frac{K_I}{\sqrt{2\pi r}}\cos\left(\frac{\theta}{2}\right)\sin\left(\frac{\theta}{2}\right)\cos\left(\frac{3\theta}{2}\right)$	$\frac{K_{II}}{\sqrt{2\pi r}}\cos\left(\frac{\theta}{2}\right)\left[1-\sin\left(\frac{\theta}{2}\right)\sin\left(\frac{3\theta}{2}\right)\right]$
σ_{33}	0 (Plane Stress) $\nu(\sigma_{11}+\sigma_{22})$ (Plane Strain)	0 (Plane Stress) $\nu(\sigma_{11}+\sigma_{22})$ (Plane Strain)
τ_{13}, τ_{23}	0	0

Table 2.2 Crack tip displacement fields for *Mode I* and *Mode II* (linear elastic, isotropic material)

	Mode I	*Mode II*
u_1	$\frac{K_I}{2\mu}\sqrt{\frac{r}{2\pi}}\cos\left(\frac{\theta}{2}\right)\left[k-1+2\sin^2\left(\frac{\theta}{2}\right)\right]$	$\frac{K_{II}}{2\mu}\sqrt{\frac{r}{2\pi}}\sin\left(\frac{\theta}{2}\right)\left[k+1+2\cos^2\left(\frac{\theta}{2}\right)\right]$
u_2	$\frac{K_I}{2\mu}\sqrt{\frac{r}{2\pi}}\sin\left(\frac{\theta}{2}\right)\left[k+1-2\cos^2\left(\frac{\theta}{2}\right)\right]$	$-\frac{K_{II}}{2\mu}\sqrt{\frac{r}{2\pi}}\cos\left(\frac{\theta}{2}\right)\left[k-1+2\sin^2\left(\frac{\theta}{2}\right)\right]$

* μ is the shear modulus

* ν is Poisson's ratio

* $k = 3-4\nu$ (plane strain)

* $k = (3-\nu)/(1+\nu)$ (plane stress)

Table 2.3 Non-zero stress and displacement components in *Mode III* (linear elastic, isotropic material).

	Mode III
τ_{13}	$-\frac{K_{III}}{\sqrt{2\pi r}}\sin\left(\frac{\theta}{2}\right)$
τ_{23}	$\frac{K_{III}}{\sqrt{2\pi r}}\cos\left(\frac{\theta}{2}\right)$
u_3	$\frac{K_{III}}{\mu}\sqrt{\frac{r}{2\pi}}\sin\left(\frac{\theta}{2}\right)$

2.3 Fatigue: Background

A fatigue fracture is the result of the repeated application of stress below the tensile strength of the material. The failure process consists of the initiation of one or more cracks, the propagation of a dominant crack, and final separation. Fatigue cracks usually initiate at the surface and for this reason, the condition of the surface and the environment are important factors influencing fatigue behavior. Process such as shot-peening or carburizing can improve high cycle fatigue performance by developing surface compressive residual stress that make the initiation of surface crack more difficult. However, when the surface is made highly resistant to the initiation of fatigue cracks, subsurface crack initiation can occur.

In the first half of the nineteenth century, a number of train wrecks occurred as the result of the fatigue failure of railroad car axles. These accidents brought attention to this new failure mode, and as a result, a number of investigations concerning the nature of fatigue were initiated. In 1839, Poncelet spoke of the failure of metals under the repeated action of tension and compression, and used the term "fatigue." Rankine(1843) observed that the growth of fatigue cracks in axles was an important aspect of the fatigue process. McConnell in England (1849) claimed, probably because of the brittle appearance of fatigue fracture surfaces he observed, that "a change from fibrous to crystalline character" occurred during fatigue, and unfounded idea that has long appealed to shop mechanics. Fairbairn (1864) carried out fatigue tests of components and was able to propose allowable stresses for bridge structures subject to fatigue loading. Some of the most important work aimed at characterizing fatigue as a material property was done by Wöhler in Germany during the period from 1858 to 1870. He was the first to carry out extensive fatigue test programs on test specimens rather than actual components, and to use both rotating banding and axial loading test methods. Because of his strong contributions to the field, plots of the stress amplitude versus the log of the fatigue life are commonly referred to in Europe as "Wöhler curves." In the United States, such curves are known as *S/N* curves.

The shape of these *S/N* curves is material-dependant, particularly in the high cycle regime. For low-carbon steels, the *S/N* curves exhibit a well-defined "knee" at about 10^6 cycles, as shown in Figure 2.4. Beyond the knee, the curves are horizontal, and we can speak of a fatigue limit. As indicated in this figure, a useful relationship for steels is that the fatigue limit is about one-self of the tensile strength. For most other alloys, however, as indicated in Figure 2.5, the knee is absent and the *S/N* curve at high numbers of cycles continues to decline slowly with increase in the number of cycles to failure. For such materials, it is customary to define the fatigue strength or endurance limit as the stress amplitude corresponding to a specified number of cycles, often 10^7. Further, there is generally no correlation with other properties such as the tensile strength.

Some components will experience huge numbers of fatigue cycles in their lifetime, and for reliable operation, will be designed such that the stress amplitudes experienced are below the fatigue curve by a margin of safety. Such components are designed for infinite life. Other components, such as aircraft structures, will experience stress above the fatigue strength, and are designed for finite life. However, it is not unusual for the actual life to exceed the original design life.

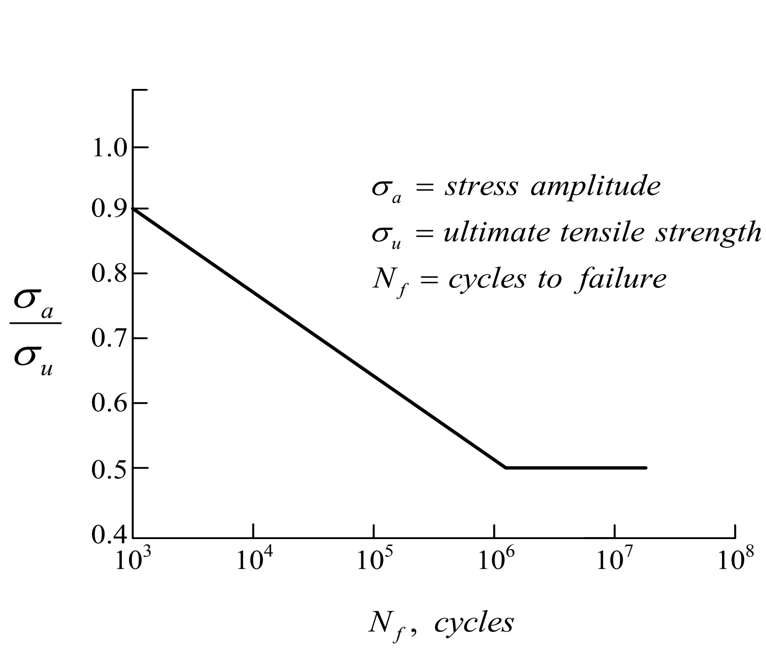

Figure 2.4 Typical *S/N* behavior for steels

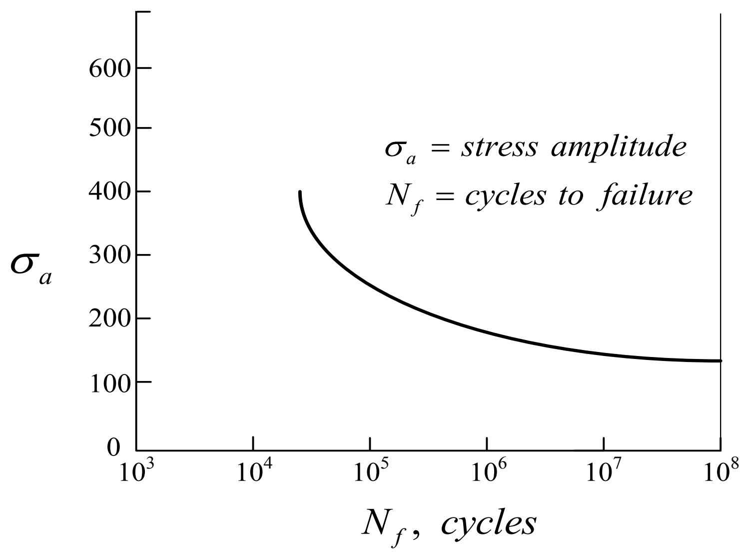

Figure 2.5 *S/N* curve for an aluminum alloy

In such cases, carful inspection and the replacement of fatigue cracked components is necessary to insure continued reliable performance. When repeated stresses are applied such that some of the stresses are above the endurance limit and some below, it is not safe to assume that the stresses applied below the endurance limit do no damage. This is because the stresses that are above the endurance limit may initiate crack, which are then able to propagate at stress amplitudes that lie below the original endurance limit.

2.4 Mechanism of Fatigue

Plastic deformation plays an essential role in the initiation and propagation of fatigue cracks. An important step in understanding the mechanism of fatigue was taken by Ewing and Humphrey (1903), who were among the first to use the metallurgical microscope in marking their observations. In fatigue tests of polished specimens of Swedish iron, they noted that slip bands that developed under cyclic loading differed in appearance from those that formed under tensile loading. Under cyclic loading, the bands formed in uniformly spaced groups within a grain at low stress amplitudes, whereas under tensile loading, the slip bands were more uniformly distributed across the grains. Most importantly, Ewing and Humphrey noted that fatigue cracks originated within the fatigue slip bands. Later work by Gough in the 1920s further demonstrated that plastic deformation was essential to fatigue crack initiation. Fatigue slip bands are favored sites for continuing plastic deformation. If a surface containing these bands is lightly polished and the specimen then recycled, fresh slip bands will appear at the same site as fatigue slip bands were previously observed. Hence the name persistent slip band. In the 1950s, with the advent of the transmission electron microscope (TEM), the fatigue process within fatigue slip bands was observed in greater detail by Forsyth, who found that thin ribbons of material were sometimes extruded from slip bands prior to the development of cracks. Today, the scanning electron microscope (SEM) is a main tool for such observations.

Until the 1960s, the only information available to the design engineer was often an *S/N* curve. However, the *S/N* curve does not distinguish between the crack initiation and crack growth portions of the fatigue process. Interest in the fatigue crack growth increased in the 1950s with the recognition that macroscopic cracks could form and grow in aircraft structures due to cyclic loading. The Comet aircraft disasters in particular emphasized this point. Two other developments also promoted interest in this topic. One was the observation by Forsyth and Ryder (1961) that fatigue cracks advanced and increment in each cycle. The other was the emergence of fracture mechanics as a method for dealing with fatigue cracks in an analytical manner and led to the formulation of Paris's law for the rate of fatigue crack growth.

$$\frac{da}{dN} = C\left(\Delta K\right)^m \tag{2.7}$$

where a is the crack length, ΔK is the range of the stress intensity factor for tension-tension loading, and m and C are constants. Figure 2.6 is plot in log-log coordinates of the rate of fatigue crack growth as a function of ΔK. The overall curve is sigmoidal in shape, bounded at the lower end by the threshold for fatigue crack growth, and at the upper end by the fracture toughness of the material. Region I is known as the near-threshold range, and region II is the region in which Paris's law, Equation (2.7), is applicable. The fractographic makings that are associated with fatigue crack growth are known as striations and they are found in the upper portion of this region. Region III involves both tensile and fatigue modes of fracture.

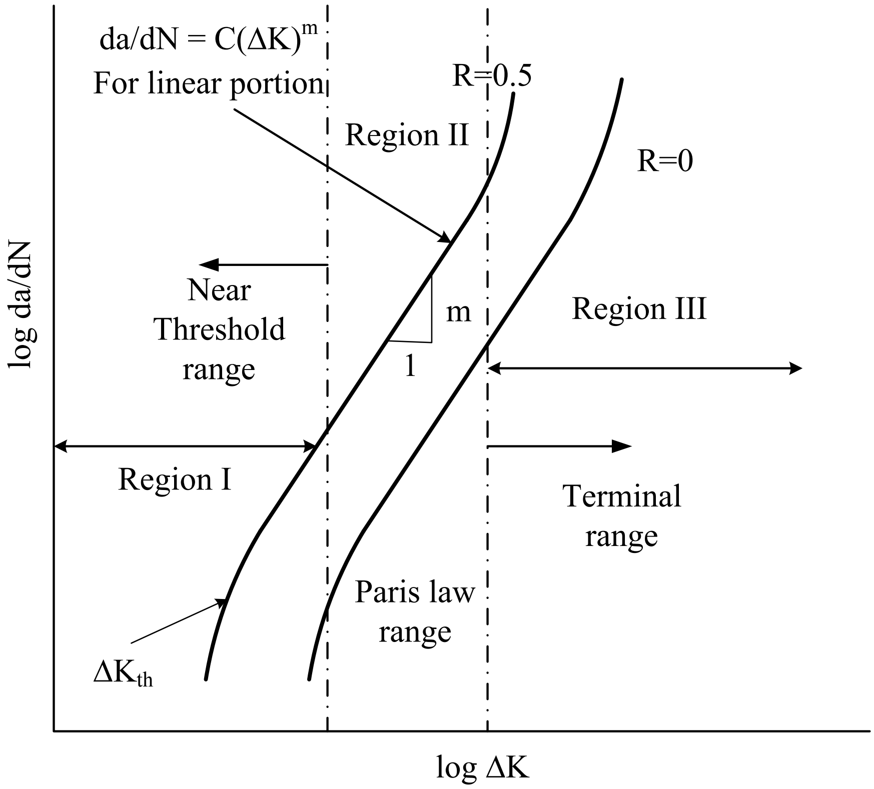

Figure 2.6 The rate of fatigue crack growth as a function of ΔK

Chapter 3

Evaluation of Fatigue Crack Growth Behavior in Materials with Lubricating Oil Holes

In this chapter, the effect of the stress concentration zone on the surface crack is discussed, while the surface crack that is initially developed due to inevitable defects such as the proper defects and manufacturing defects existing in the surface of member parts is propagating. Also, it is presented to estimate the depth profile of the crack using the dates obtained from the experiment.

3.1 Introduction

Fractures in engineering applications occur mostly from surface or internal three-dimensional crack that result from defects already existing in the material, and generally propagate in all directions and often have irregular shapes. (ASM, 1987)
There are not only material metallurgical defects but also discontinuous parts related to fastening, configuration design, lubrication, etc. in the ships and offshore structures. Since these become zones of stress concentration, the fatigue crack initiation and propagation is significantly affected. But as these are inevitable in design, the concept of damage tolerance design has recently been introduced in various fields of industry. This concept of damage tolerance design will be explained simply in the following.

The concept of damage tolerance is widely applied to metallic structures. By understanding and being able to predict the evolution of damages within a material, one can design a structure that can withstand given levels of damage that can be detected through regular inspections. In this manner, both systematic and incidental damages can be detected and repaired before they become critical.

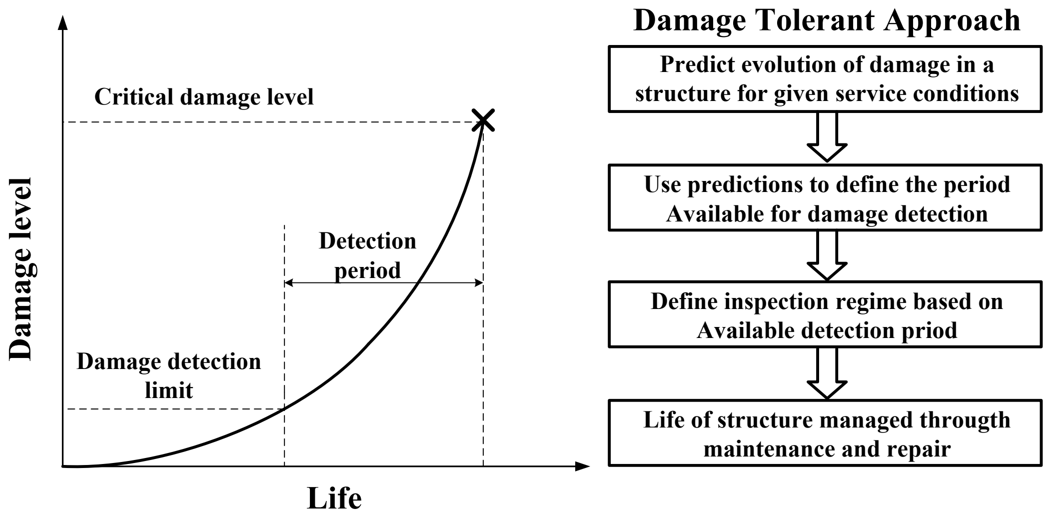

Figure 3.1 Schematic of damage tolerant approach

For the efficient application of such damage tolerant design, research on the fatigue crack growth process is required, in addition to research on the fatigue initiation process, of which there has already been a great deal. In damage tolerance design, it is evaluation and appropriate change time decision of the parts which do not deviate from the economical concept of the persistence strength to be more important than what for maintenance and maintenance. It is very important to evaluate remnant strength for maintenance and to decide an economical and efficient exchange time for members in this concept. As such, it is a significant challenge to accurately grasp the characteristics of fatigue crack growth. For these reasons, there has been a great deal of research on surface cracking. In these studies, the crack shapes may not strictly have an elliptical or circular geometry, although such an approximation in often practiced in research investigation and engineering analyses. This may introduce errors in growth data and the estimated fatigue life, but it also raises several parallel questions. First, what are the factors that can cause three-dimensional cracks to grow in irregular shapes? Second, how can we describe the growth behavior of regular and irregular cracks exhibiting a continuous change in shape, from initiation to failure? Third, how can we predict the growth of these cracks in fatigue leading to unstable fracture? To adequately answer such questions, it is critical to acquire aspects of various fatigue crack growth behavior through the various fatigue experiments. As a result, there has been intensive research on the fatigue crack growth behavior of three-dimensional surface cracks as a fundamental means of improving the safety of machines and structures.

We were able to identify the failure accident of the crankshaft as Figure 3.2 from the investigation on ship failure cases that was carried out before the present study. In the present study, based on such actual failure case, a fatigue crack growth experiment was carried out using an aluminum alloy as experimental material in order to investigate the crack shape and fatigue crack growth characteristics when surface crack initiated from an initial defect grows toward a stress concentration zone such as the lubricating oil hole in Figure 3.2.

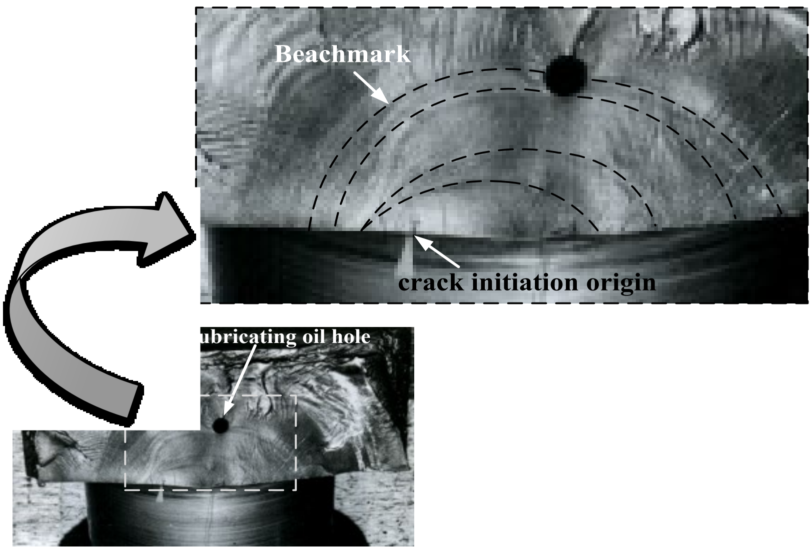

Figure 3.2 Fractograpy of crankshaft in ship

3.2 Experimental Techniques

3.2.1 Specimen and test equipment

The primary purpose of the present study is to investigate the interference effect between the surface crack and the stress concentration zone. As such, the specimens are processed as shown in Figure 3.3.

As Figure 3.3 illustrates, a cylindrical hole 3*mm*in diameter, which is perpendicular to the cross section, in parallel with the electro-discharge, was made by machining and drilling in order to acquire the experimental results that agree with the research purpose. Two terms pertain to the three-dimensional aspects of surface cracks: the crack shape (semicircular, semielliptical, square, triangular, etc) and the crack aspect ratio (a/c, the ratio of half surface length to the distance of maximum depth point in crack front, from surface).In the present study, the semielliptical surface crack, with aspect ratio 0.5, was processed by electro-discharge machining in each specimen's surface in order to promote the fatigue crack growth. The position in the circular hole was used as a variable carried for the more well-informed research. The positions in the circular hole have been defined by the angle made by the circular hole and the surface crack. Therefore, the following three kinds of specimen were used in this study.

(i)	Specimens I:	not circular hole
(ii)	Specimens II:	$0°$ circular hole
(iii)	Specimens III:	$30°$ circular hole

In Figure 3.3, it is possible to confirm the geometry of specimens used in this study.

In the automotive, aeronautic and shipbuilding industries today, there is high demand for low-density materials as part of a drive to lighten end products. Aluminum alloys with a wide range of properties are one example of lightening in engineering structures.

For this reason, aluminum alloy, *A2024-T351*, was employed as experimental material. This is most widely used in various fields of industry. Table 3.1 and Table 3.2 show the chemical compositions and the mechanical properties. Figure 3.5 illustrates the test jig used in this experiment to carry out the fatigue crack growth experiment under pure tensile load. The hydraulic servo pulsar with 10kN total capacity was used as the test equipment, and then the specimen was connected to this test machine using the jig as shown in Figure 3.5.

The waveform of the cyclic loading was set to sine wave, and the frequency was set to15Hz. The experiment was carried out in the load control. Figure 3.6 shows the loading condition. The beach mark method was used in order to observe the aspect of the internal cracks. The beach mark is inserted during 10^4~10^5cycles with the amplitude of *50%* usual load amplitude.

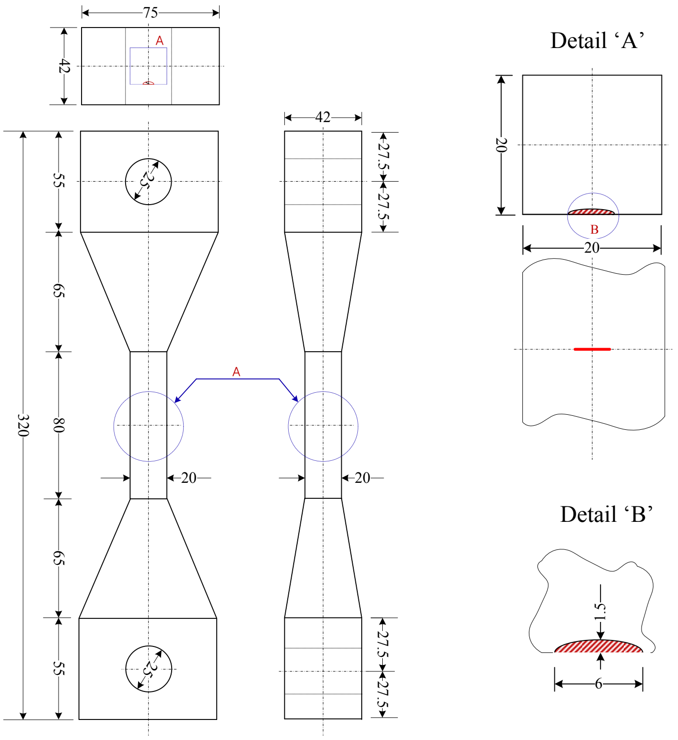

(a) Specimen I (is not circular hole)

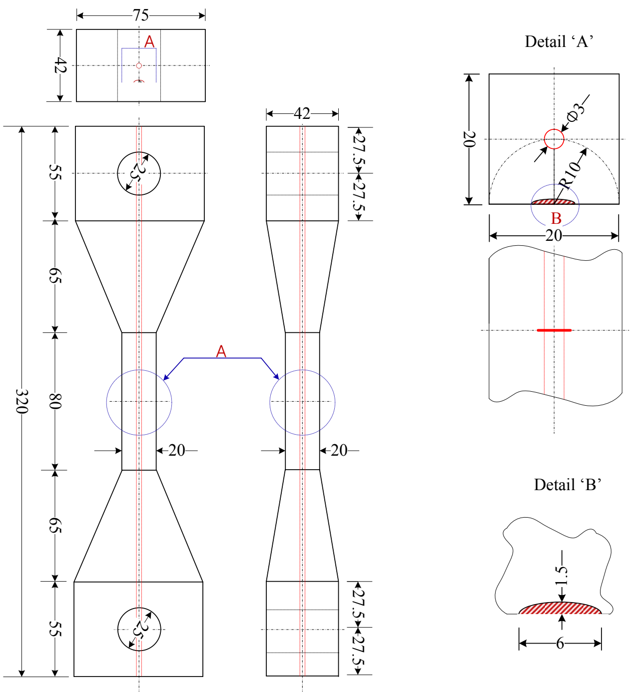

(b) Specimen II (0 ° circular hole)

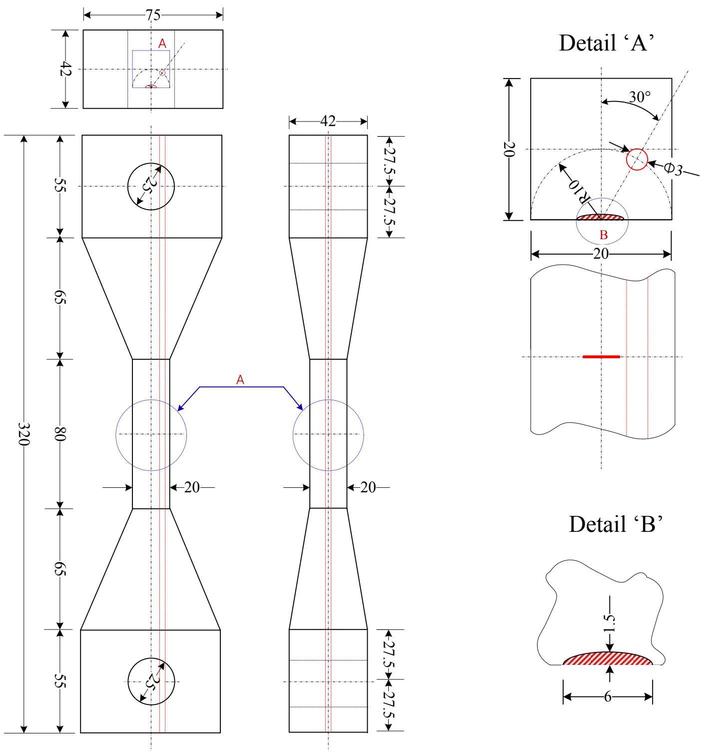

(c) Specimen III (30 ° circular hole)

Figure 3.3 Specimen geometry

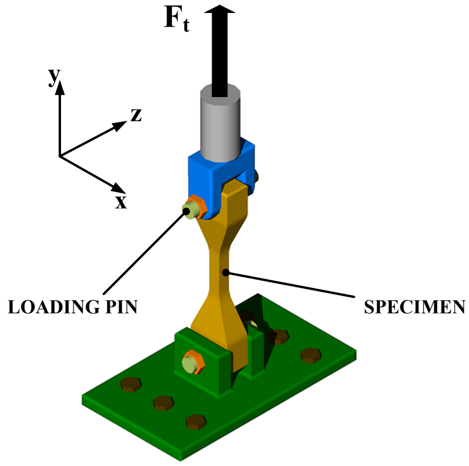

Figure 3.4 Jig for the fatigue crack growth experiment

Product Specifications
- Model: EHF-UB10 1431
- Force capacity:
  - Static Load: 15kN
  - Dynamic Load: 10kN
- Crosshead travel:1000mm
- Test Speed
  - Sine, Triangular, Rectangular wave :0.001~110Hz
  - Ramp wave : 0.001~110F.S/sec

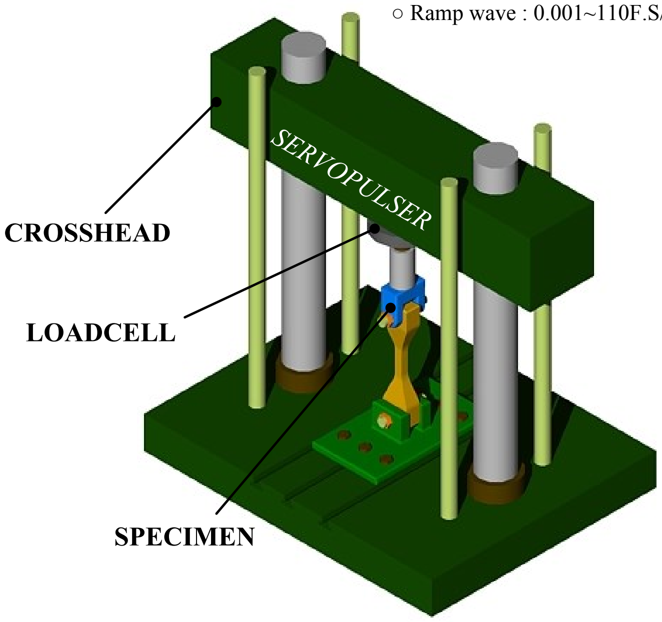

Figure 3.5 Fatigue testing machine

Table 3.1 Mechanical properties of A2024-T351 (wt %)

Silicon	Iron	Copper	Manganese	Magnesium
Max 0.5	Max 0.5	3.8-4.9	0.3-0.9	1.2-1.8
Chromium	Zinc	Titanium	Aluminum	Other
Max 0.1	Max 0.25	Max 0.15	90.7-94.7	≦0.15

Table 3.2 Chemical compositions (wt %)

Ultimate Tensile Strength	469MPa
Tensile Yield Strength	324MPa
Elongation at Break	20%
Modulus of Elasticity	73.1GPa
Poisson’s Ratio	0.330
Fatigue Strength	138MPa
Shear Strength	283MPa
Shear Modulus	28GPa

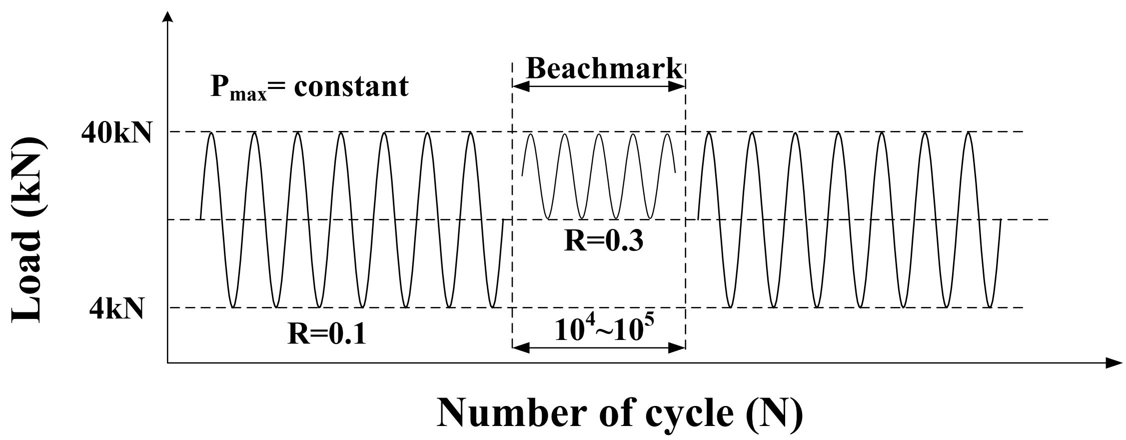

Figure 3.6 Loading condition

3.2.2Experimental data acquisition method

The crack is opened if the uniform tensile stress is acting in finite plate, as illustrated in Figure 3.7. Several studies have obtained various fracture mechanics parameters by measuring the crack opening displacement. In a study by Namba, K. and Torii, T(2004), Mode I stress intensity factors for part-through crack were evaluated from the crack opening displacement distributions measured along the crack on the surface in a finite plate. Based on the crack opening displacement, stress intensity factor range was evaluated and used to estimate fatigue crack propagation. In this way, the investigative effectiveness of the crack opening displacement was verified in several studies.

In the present study, which is focused on observation of the crack opening displacement, an attempt was made to investigate the effect of the stress concentration zone on the fatigue crack growth. Figure 3.7 shows the parameters that are defined for this study.

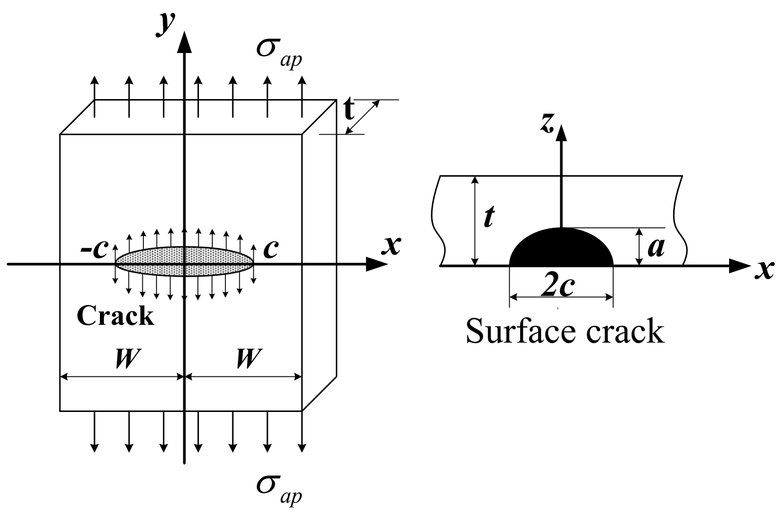

Figure 3.7 Definition of the crack opening displacement and the surface crack

Thus far, various measuring methods, such as the digital image correlation method and measurement based on micro Vickers indentation, have been used by many researchers to obtain more accurate measurements of crack opening displacement.

The CCD camera is used to obtain the images required to measure the surface crack length and the crack opening displacement. The photographing range of CCD camera is $1.65mm \times 1.65mm$, and it is expanded 80 times.

Real-time photographing is impossible to perform with a CCD camera. Therefore, the servo pulsar is stopped during photographing, and then static maximum load (40kN) and minimum load (4kN) identical with the experimental condition were loaded on the specimen in order to take images in the maximum load and in the minimum load. The stopping time is within 20 minutes.

The crack opening displacement was calculated from the images photographed. Crack opening displacements in each load were measured by measuring the interval of fatigue crack top and bottom at intervals of $30\mu m$ as illustrated in Figure 6.8, and then the crack opening displacement was defined as Equation (3.1).

$$\mathrm{COD} = y_i^0 - y_i^1 \tag{3.1}$$

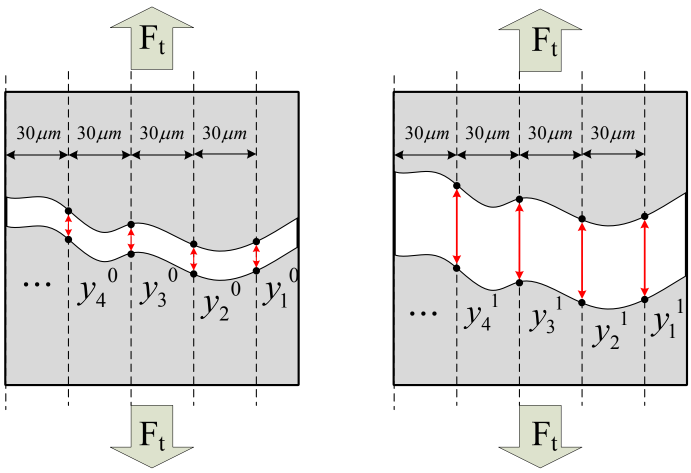

(a) Minimum load (a) Maximum load

Figure 3.8 Measurement method of the crack opening displacement

3.3 The experimental examination

3.3.1 Fatigue crack growth behavior in the surface

In this section, the effect of the stress concentration zone, the cylindrical hole, on the fatigue life and fatigue crack growth behavior in surface are discussed.

Figure 3.9 illustrates the relationship between the fatigue crack length and the number of cycles. The fatigue life is *Specimen I* > *Specimen II* > *Specimen III* as shown in Figure 3.9. Although there is a difference to some extent in the fatigue life of Specimen I and Specimen II, they are almost the same. However, in the case of Specimen III, it was proven that the fatigue life was considerably shorter than for Specimen I and Specimen II. Based on these experimental results, it was proven that the fatigue crack growth is affected more by the position of the circular hole and less by the existence or nonexistence of the circular hole.

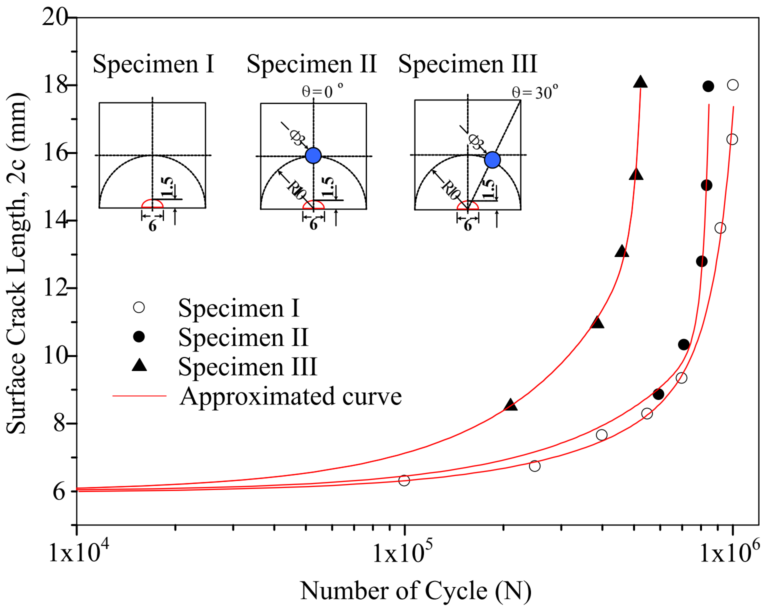

Figure 3.9 Relationship between the surface fatigue crack growth length and number of cycle

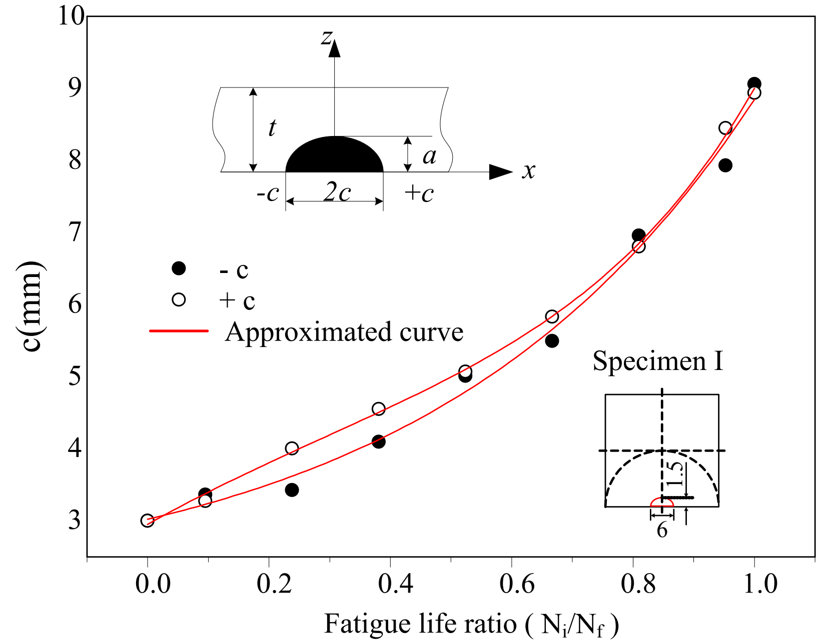

(a) specimen-I

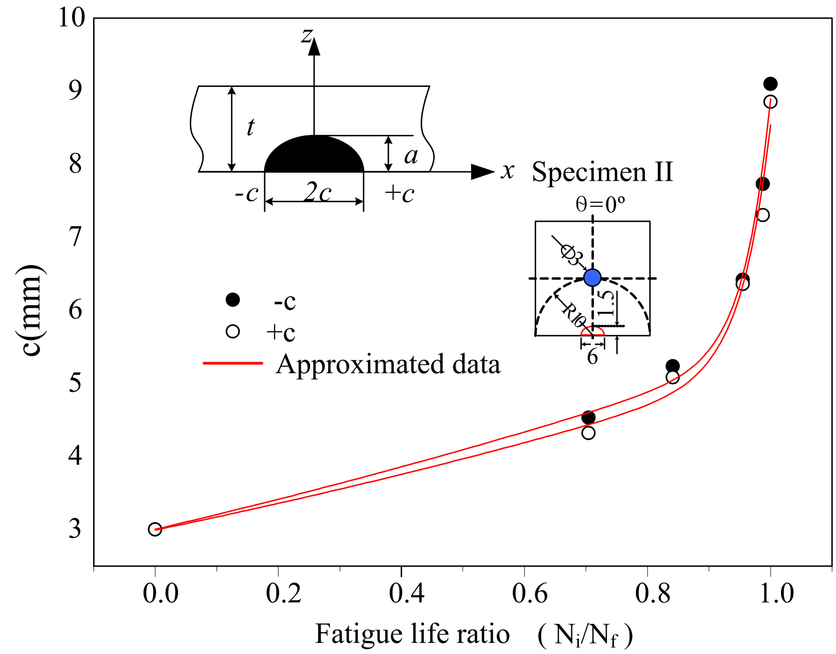

(b) specimen-II

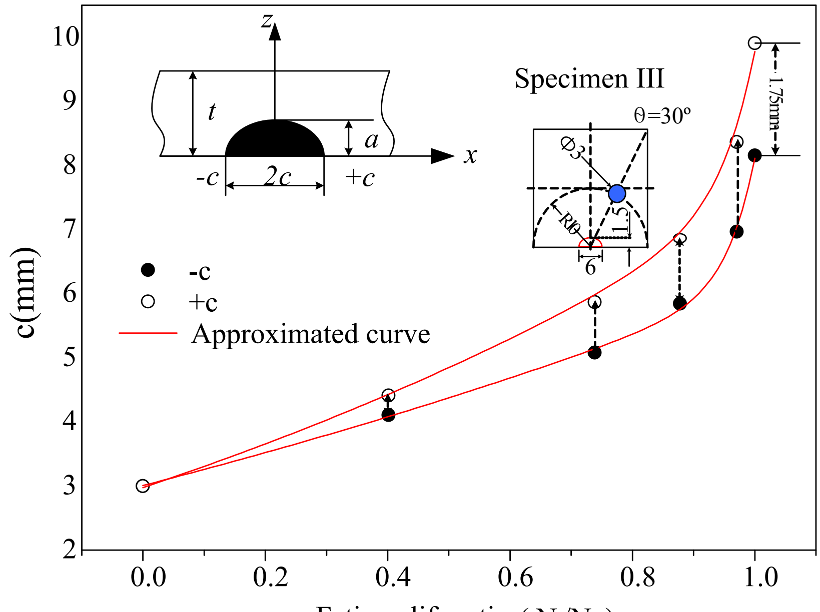

(c) specimen-III

Figure 3.10 Comparison of surface fatigue crack growth length on the left and right side of specimen

Generally, the three-dimensional surface crack is propagated left-right symmetrically toward the interior of the material. Therefore, the crack shape that exists in the three-dimensional structure can be approximated as an elliptical crack. (Shen, G. and Glinka, G., 1991) (Raju, I. S. and Newman, J.C., 1979) However, for Specimen III used in this study, the left (-c) -right (+c) symmetry of the surface fatigue crack growth collapsed as a result of the effect of the stress concentration zone, as depicted in Figure 3.13.

For Specimen I and Specimen II, though there is the range in which the symmetry collapsed a little, this is due to the fatigue crack characteristics that are considerably affected by metallurgical structure. In addition, the fatigue crack velocity is was almost equal on left and right in Specimens I and II. However, on Specimen I, due to the effect of the stress concentration zone, the surface fatigue crack gradually grew more on the right side (+c) than left side(-c) with fatigue crack propagation. The fatigue crack propagation mean velocity was observed as follows: $4.38\times10^{-5}\,mm/cycle$ in right side (+c) and $2.44\times10^{-5}\,mm/cycle$ in left side (-c). Based on these experimental results, it was confirmed that the fatigue crack was extremely affected by the position in the stress concentration zone.

3.3.2 Crack opening displacement and the crack shape

In this section, the crack opening displacement calculated from the images obtained in experiment process will be discussed. Generally, the crack opening displacement under the pure tensile load is symmetrical, and is largest at the center of the surface crack. However, the crack opening displacements in specimens used for this study have each been observed to have a slightly different aspect.

Figures 3.11, 3.12, 3.13 show experimental data, and Figure 3.14 illustrates approximated data. To begin with, the change in the crack opening displacement of Specimen I will be discussed. According to previous research, the crack opening displacement is more significantly affected by crack growth in the depth direction than crack growth on the surface. In addition, the crack opening quantity depends on the crack depth.

In Figure 3.11 and Figure 3.14 (a), the crack opening displacement of Specimen I, without a circular hole where cross section is vertical, stably grows in both surface of specimen and the depth direction until the surface crack length (2c) is approximately 12mm (c/W=0.6). However, the crack opening displacement shows no further increase with subsequent crack growth, as shown in Figure 3.11 and 3.14(a). As mentioned above, the crack opening displacement is deeply influenced by the crack depth. In other words, it can be said that the crack growth in the depth direction was slowed.

On the other hand, for Specimens II and III with a circular hole, the crack opening displacement is increased at an accelerated rate until the specimen is ruptured. It is considered that this is the effect of the circular hole at the stress concentration zone. Based on these results, it was proven that the discontinuity that exists in the member subject affected the surface crack growth behavior significantly, even under pure tensile load condition. In the cases of Specimen I (no circular hole) and Specimen II ($\theta = 0°$),while there is some data spread due to the metallurgical structure and experimental error, the maximum point of crack opening displacement is near the center of the crack. However, for Specimen III ($\theta = 30°$) the maximum point is continually changing while the crack is growing. This is shown in Figure 3.13 and 3.14(c). As can be seen in the figures, a maximum point is located for the direction with the circular hole in the effect of the circular hole. As such results, the crack opening displacement is confirmed to be extremely affected not only by the position of the stress concentration zone but also by the existence of the stress concentration zone.

The Beachmark was introduced to confirm the propagation history from fractography after the experiment was finished. It was illustrated graphically in Figure 3. 15. As was proven previously by observation of the crack opening displacement, it is proven again that the surface crack growth distance is larger than the crack propagation distance toward the inside of specimen after c/W exceeded 0.6, as shown in Figure 3.15. Also, its left-right symmetry was maintained while the fatigue crack is propagating toward the inside of the specimen because there are no circular holes in Specimen I.

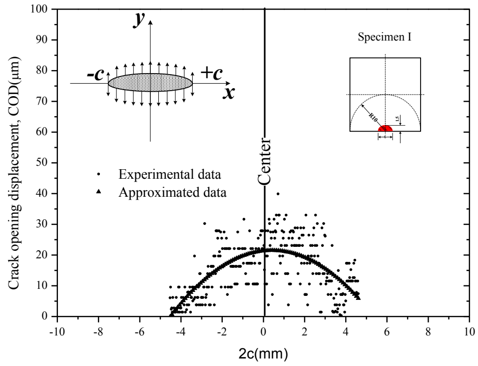

(a) N_i/N_f=0.381

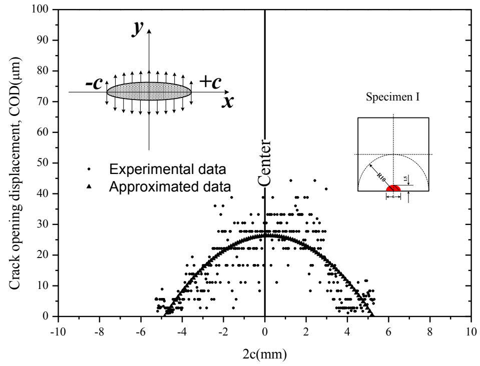

(b) N_i/N_f=0.524

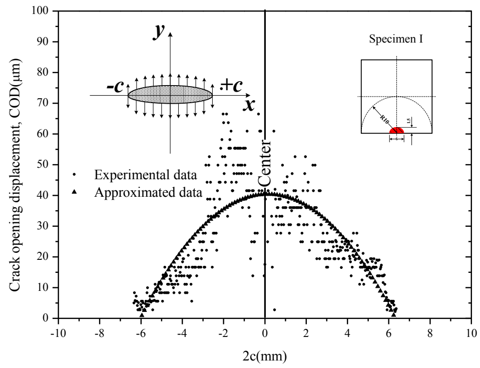

(c) N_i/N_f=0.666

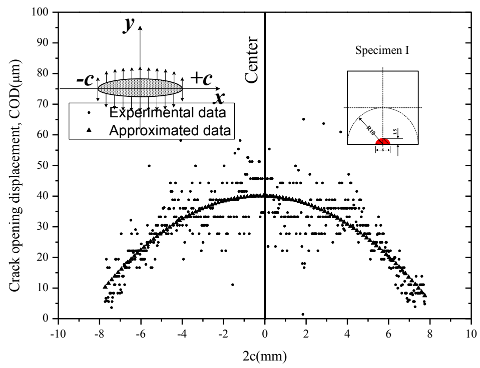

(d) N_i/N_f=0.809

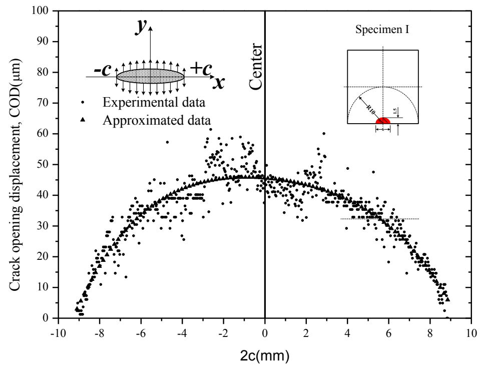

(e) N_i/N_f=1

Figure 3.11 Crack opening displacement in Specimen I

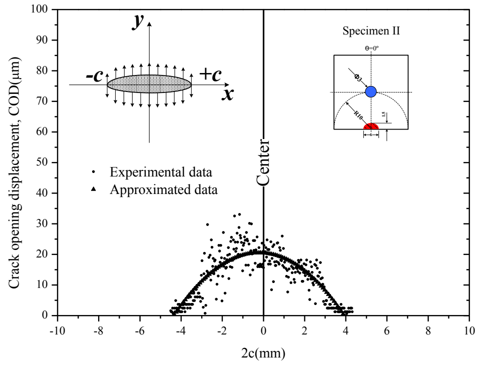

(a) N_i/N_f=0.704

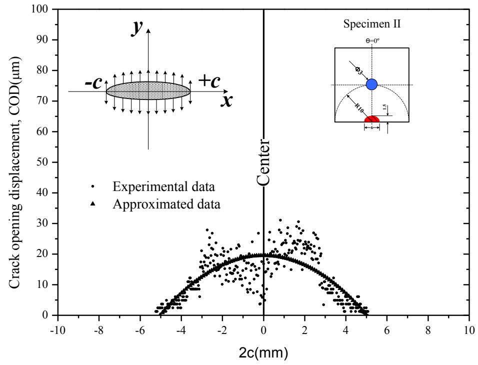

(b) N_i/N_f=0.841

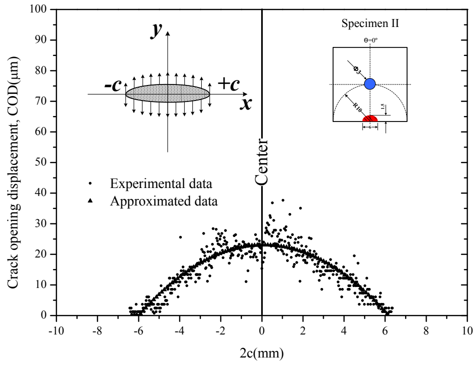

(c) N_i/N_f=0.954

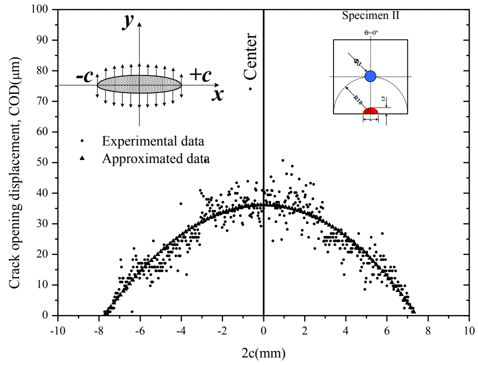

(d) N_i/N_f=0.988

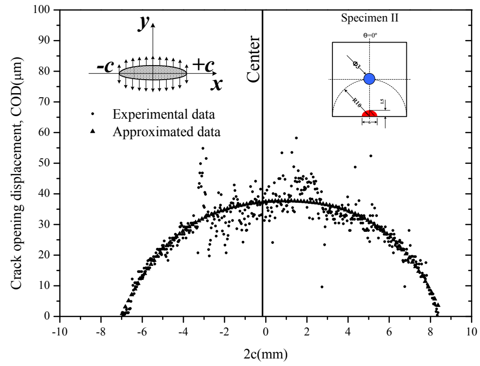

(e) N_i/N_f=1

Figure 3.12 Crack opening displacement in Specimen II

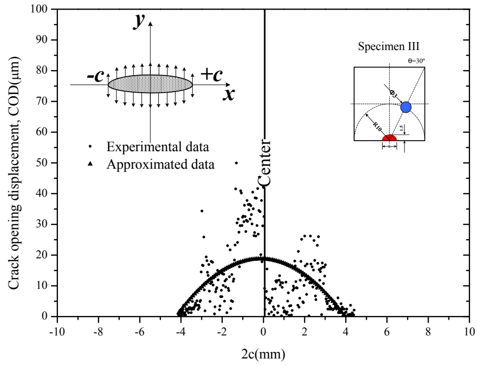

(a) N_i/N_f=0.401

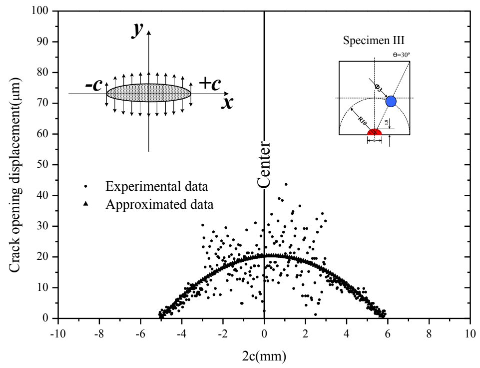

(b) N_i/N_f=0.738

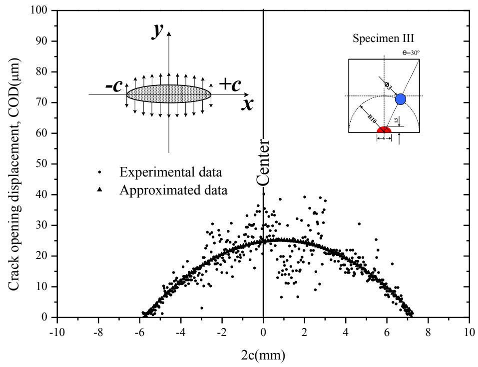

(c) N_i/N_f=0.878

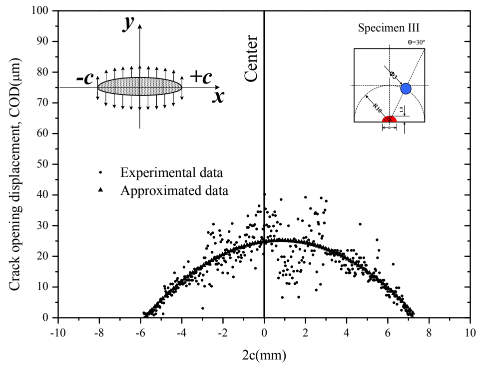

(d) N_i/N_f=0.971

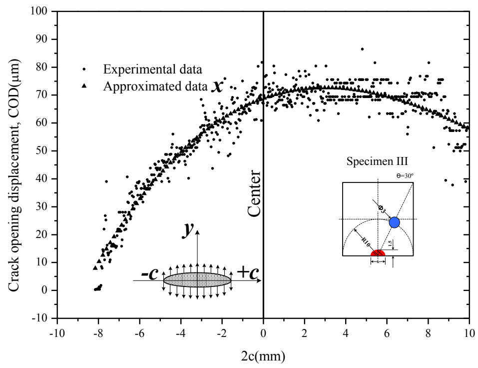

(e) N_i/N_f=1

Figure 3.13 Crack opening displacement in Specimen III

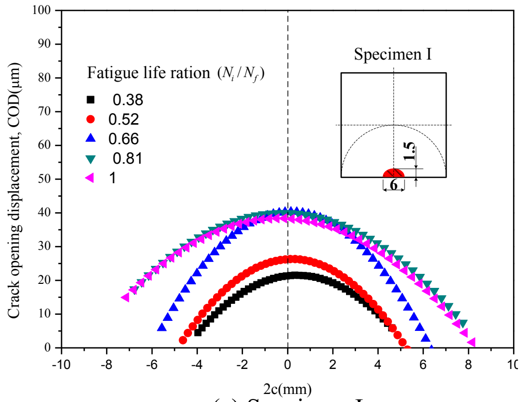

(a) Specimen I

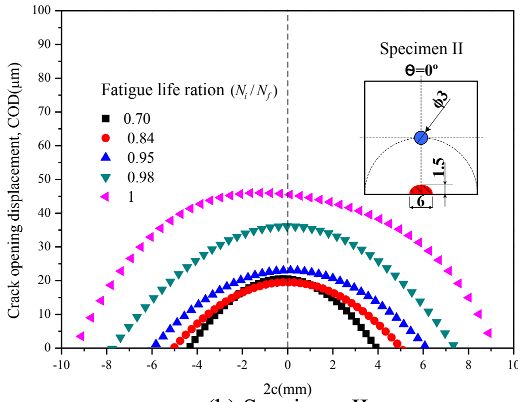

(b) Specimen II

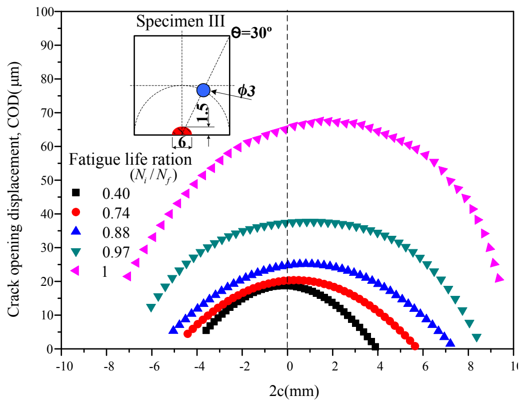

(c) Specimen III

Figure 3.14 Approximated curves of crack opening displacements

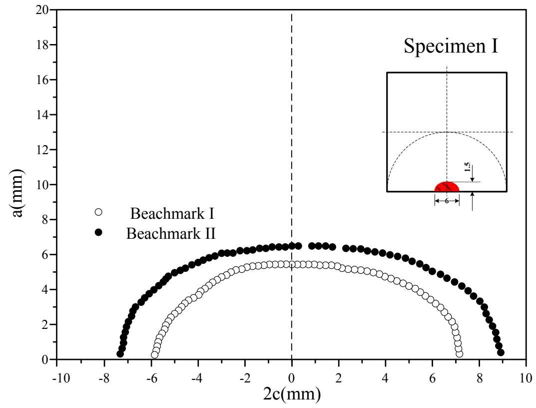

(a) Specimen I

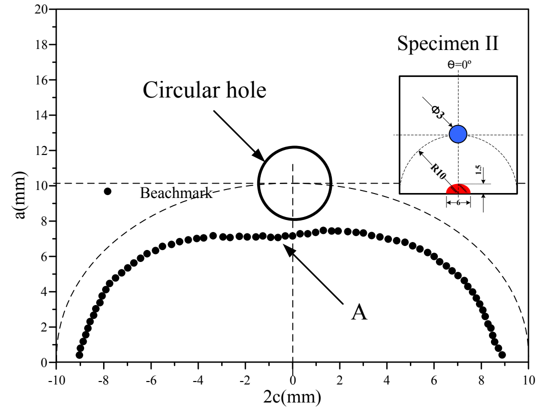

(b) Specimen II

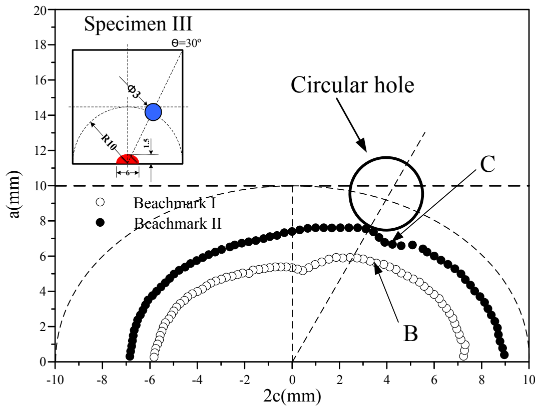

(c) Specimen III

Figure 3.15 Crack shape in interior of specimen

3.1 Conclusion

In this study, based on an actual failure case, the fatigue crack growth experiment was carried out using aluminum alloy as experimental material in order to investigate the crack shape and fatigue crack growth characteristics when surface crack initiated from the initial defect is grown toward the stress concentration zone.

As result, the main findings were as follows: (a) it was proven that the fatigue life is affected more by the position of the circular hole than by the existence or nonexistence of the circular hole. (b) The crack opening displacement is confirmed to be extremely affected not only by the position of the stress concentration zone but also by the existence of the stress concentration zone.(c) It was proven that the discontinuity that exists in the member affected the surface crack growth behavior significantly, even under pure tensile load condition.

Chapter 4

A Study on Fatigue Crack Growth Characteristics for Mutual Interaction Effect on 3-D Surface Crack

4.1 Introduction

Three-dimensional surface crack is one of the most common defects that exist in the physical structure. In order to assess the strength of structures in which the defect exists, introduction of fracture mechanics has brought great strides to use the materials safer and prevent the fracture in advance.

The initial studies on cracks from the point of view of fracture mechanics assumed that most defects existing in structure were through crack and mostly required two-dimensional interpretation. It has recently been known that fatigue crack propagation in actual structure with load has begun in form of crack with three-dimensional feature such as surface crack or part-through crack. Thus, the three-dimensional crack interpretation is essential for fracture mechanics assessment for actual structures. However, these three-dimensional cracks and defects may exist independently and multiple cases may be dense and occur. For example, as shown in Figure 1, a number of little surface cracks occur in engines used in the industrial field or ships, or actual machine and structure such as aircraft or pressure vessels. As adjacent surface cracks are incorporated, it grows as a main crack. Thus, multiple cracks and defects give many effects on other cracks or crack growth behavior due to mutual interaction effect.

When adjacent cracks exist independently due to mutual interaction, ΔK value of stress intensity factor which is the fracture mechanistic parameter is very high. Since the increase of stress intensity factor adversely affects crack propagation and fracture behavior, it is very important to consider the effect of crack interaction in terms of safety. However, experiments and numerical studies on mutual interaction effect of adjacent cracks and defects have been conducted by many researchers and research institutions, many of them did not derive the safety based on quantitative assessment due to complexity and diversity, but it represented only structural conservation biased to excessive safety. Thus, this study conducted fatigue crack growth test for single crack and multiple cracks in order to quantitatively and precisely investigate the interaction effect of cracks, and it observed mutual interaction effect between cracks by identifying surface crack and internal crack growth behavior with the beach mark method.

Figure 4.1 Surface cracks of engine block

4.2 Fatigue crack growth experiment

4.2.1 Specimen and test equipment

Test sample used in fatigue crack growth experiments was chrome molybdenum steel SCM440. SCM440 has been standardized according to JIS G 4053. Mechanical and chemical properties of this material were shown in tables 1 and 2. Single and adjacent two three-dimensional semi-elliptical surface cracks were processed in order to quantitatively and precisely investigate the mutual interaction effect of cracks. For appearance of cracks, 4 kinds of test samples were processed by changing the mutual distance of single and cracks with gaps of 1 mm, 2 mm and 4 mm, and aspect ratio of 1. In addition, electric discharge machining was made on surface cracks to purse the precision. The dimension and appearance of specimens used in this study were shown in Figure 4.2, 3.

In addition, abrasive paper was used on surface of test sample in order to more precisely observe growth behavior of surface crack in each test sample. Aluminum oxide was used for secondary abrasion after using the abrasive papers from #500 to #2000.

4.2.2Experimental condition and experimental process

Fatigue experiment is conducted in the constant amplitude load according to provisions of ASTM E647-93 by using a hydraulic fatigue experimental device for 10kN at room temperature. As shown figure 4.4, the specimen is attached on experimental device and repeated load is given in vertical directions. The fatigue experiment is carried out with load control. And the waveform of the cyclic loading was set to sine wave, and the frequency was set to 10Hz. Figure 4.5 shows the loading condition.

The beach mark method was used in order to observe the aspect of the internal cracks. A beach mark is the crack mark left on fatigue fracture surface based on rapid change of load or environment. Invisible internal crack growth pattern can be identified by using this beach mark. In addition, the minimum load is changed to insert a beach mark like a red dotted line in figure 4.5 in order to investigate the pattern of internal fatigue crack growth.

Length of crack is measured by using a CCD camera. The experimental device is paused and recorded surface crack of the specimen every 10,000 cycles. In addition, time to pause the experimental device is up to 5 minutes upon measurement.

Table 4.1 Mechanical properties of SCM440 (wt %)

C	Si	Mn	P	S	Cr	Mo
0.38~0.43	0.15~0.35	0.6~0.9	0.03	0.03	0.9~1.2	0.15~0.3

Table 4.2 Chemical compositions of SCM440 (wt %)

Tensile Strength Ultimate	1071Mpa
Tensile Strength Yield	980Mpa
Modulus of Elasticity	205Gpa
Poisson's Ratio	0.29
Shear Modulus	80Gpa

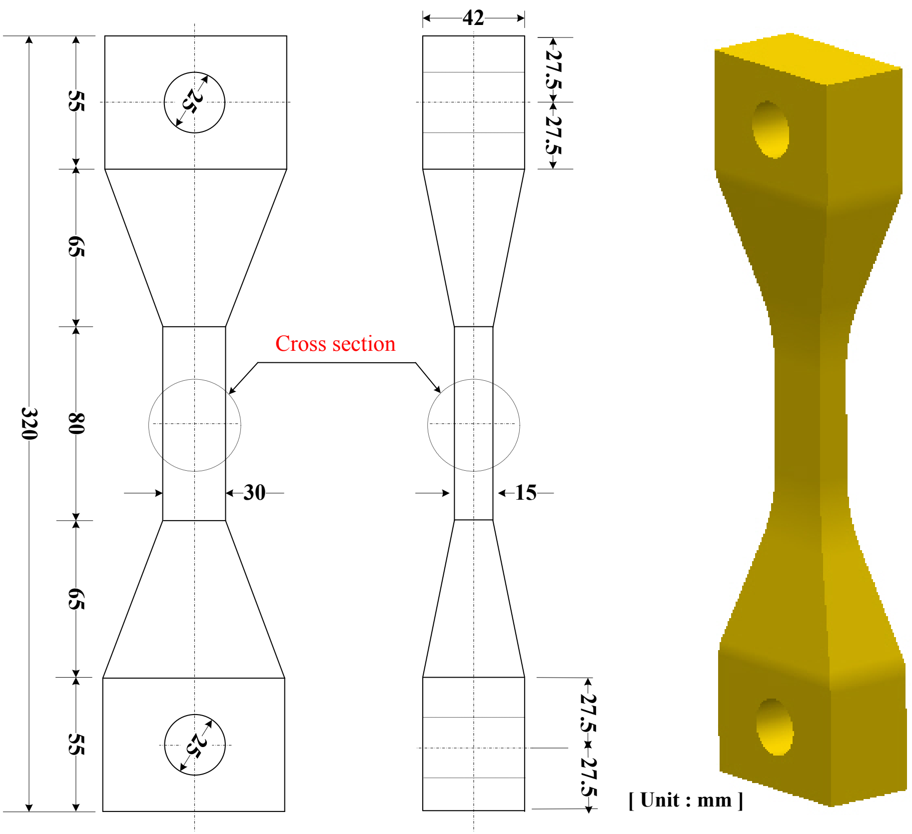

Figure 4.2 Geometry of specimen for fatigue crack growth experiment

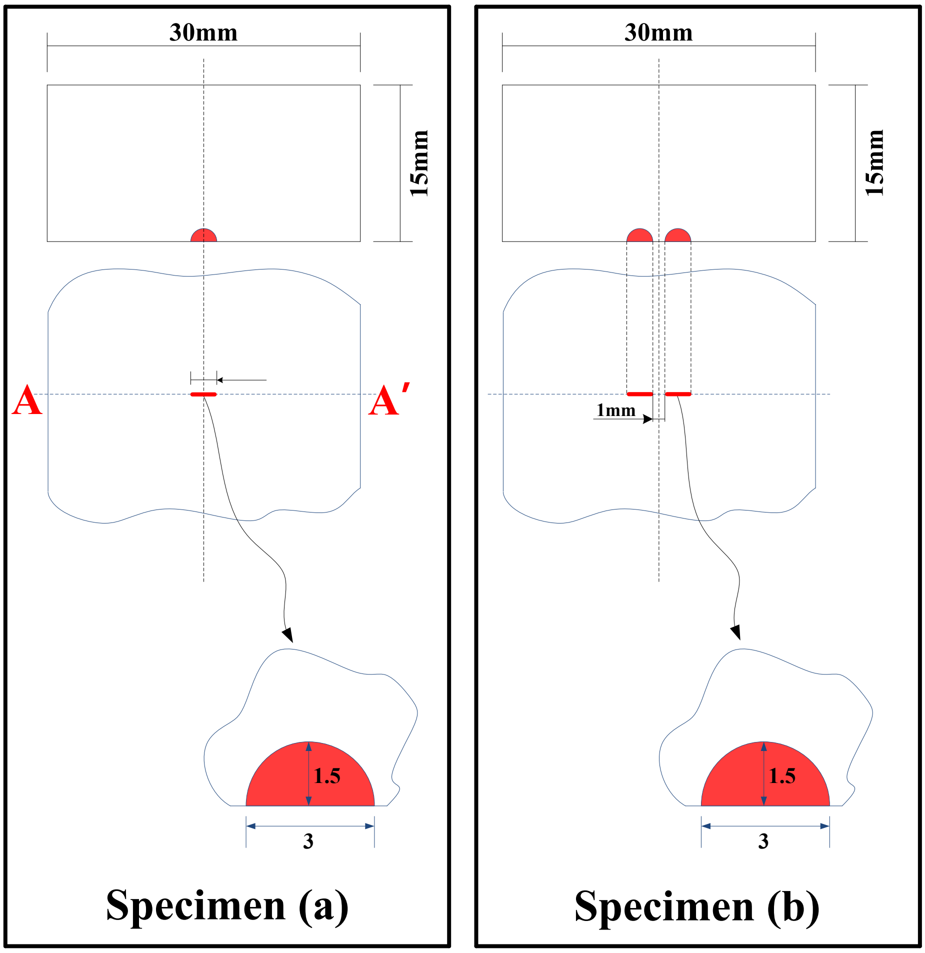
30mm
15mm
A
A′
1.5
3
Specimen (a)
30mm
15mm
1mm
1.5
3
Specimen (b)

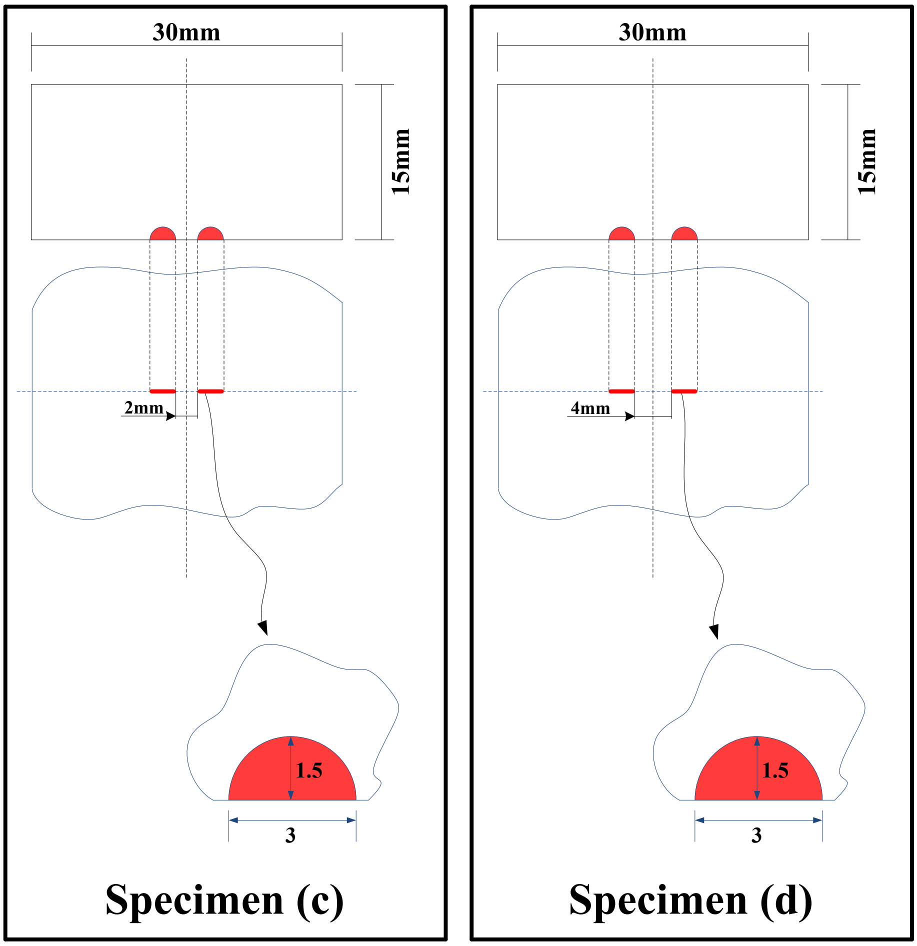

Figure 4.3 Geometry of initial crack

Product Specifications

- Model: EHF-UB10 1432
- Force capacity
    - Static Load:15kN
    - Dynamic Load: 10kN
- Crosshead travel: 1000mm
- Test speed
    - Sine, Triangular, Rectangular wave: 0.001~110Hz
    - Ramp wave: 0.001~100F.S/sec

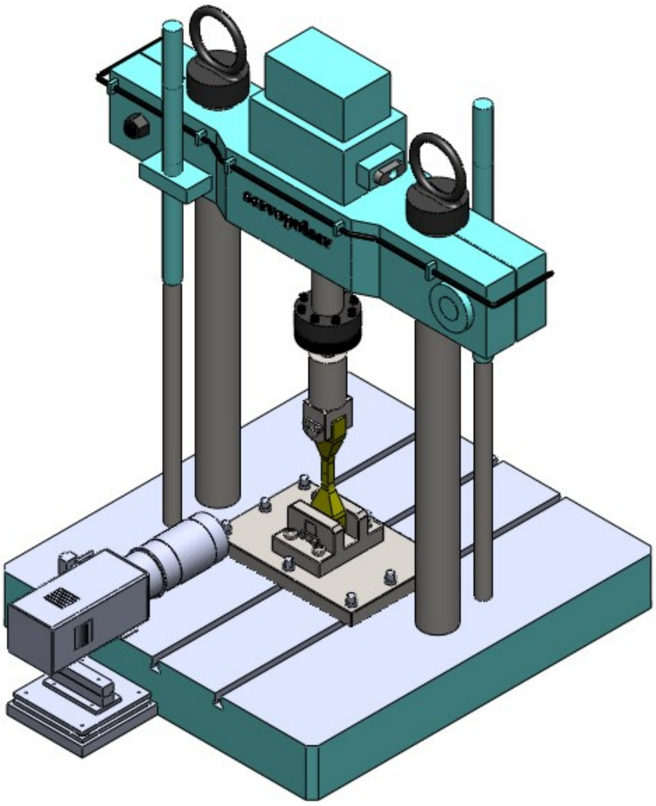

Figure 4.4 Fatigue testing machine

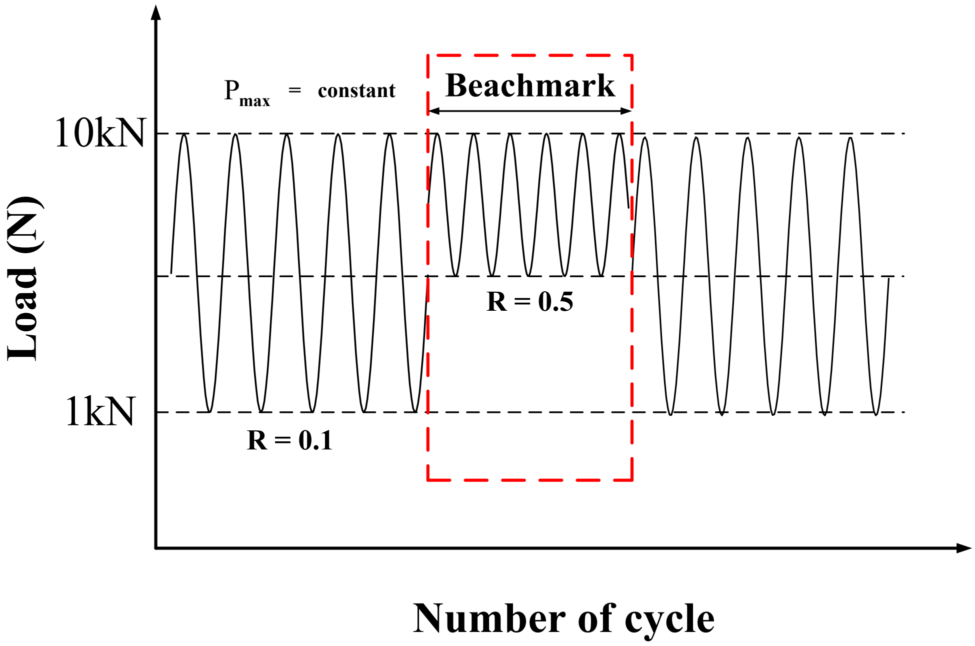

Figure 4.5 Loading condition

4.3 Experimental investigation

4.3.1Fatigue crack growth behavior in the surface

In this section, it is discussed that effect of mutual interaction on 3-D surface crack, on the fatigue life and fatigue crack growth behavior in surface. And, for appearance of cracks, 4 kinds of specimens ware processed by changing the mutual distance of single and cracks with gaps of 1mm(specimen b), 2mm(specimen c), 4mm(specimen d), and same aspect ratio (1) of initial crack.

Figure 4.6 illustrated the relationship between the fatigue crack length (2C) and the number of cycle. The fatigue life is Specimen (d) > Specimen (c) > Specimen (b) > Specimen (a). As it is shown in figure 4.6 the fatigue life appears to be decrease as the distance of cracks was small, and so that the distance of two cracks became near, when the distance of two cracks is 1mm(specimen b), 2mm(specimen c), and 4mm(specimen d). And it is the cycle that it is coalesced cracks of each specimen b, c, and d is the specimen b(1mm) 200000cycle, the specimen c (2mm) 380000 cycle, and the specimen d (4mm) 480000cycle. According to such experimental results, it was proven that the fatigue life is decreased as the coalescence of crack became a lot faster.

In cases of the two crack length 2mm(specimen c), 4mm(specimen d), these shows the similar crack progress situation before the crack is coalesced. However, the case where the distance between cracks was the 4 mm (specimen d) showed the tendency for crack progress speed to decrease. And we can confirm that fatigue cracks shows similarly crack progress characteristic from 9mm surface crack to a fracture by comparing the surface crack length of each specimen in figure 4.6.

According to such experimental results, it was proven that the fatigue life appears to be decrease since interaction effect acted greatly as the distance of cracks was small on the two surface cracks. And it was confirmed that it was shown the same fatigue crack growth characteristic with single crack after cracks were coalesced a lot late.

4.3.2 Characteristics of the fatigue fracture surface

In this section, it will be discussed that the beach mark which is calculate from the images obtained in experiment process. The beach mark was introduced to confirm the propagation history form fractograpy after the experiment has been finished. It was illustrated graphically in Figure 4.10~4.13.

Figure 4.7~4.9 shows the crack progress length of the horizontal axis and vertical axis to each number of cycle through a beach mark. In order to compare with the case of a beach mark with a single crack, in the case of approach two cracks was observed the crack progress characteristic of anti-elliptical shape after cracks were coalesced. As the figure 4.11~4.13 shows, the surface crack (2c) have ever increasing after cracks were coalesced in the case of specimen (b), (c), and (d). On the other hand, it can confirm that anti-elliptical shape is to break down as fatigue crack velocity of the inside is decreased.

However, the specimen (a) of single crack is increased on the same velocity of the inside and surface. And a surface crack shows the tendency to be fast a little over time. Such results can confirm in figure 4.7, 4.8, and 4.9. In the case of the specimen a, the length of a surface crack approach about 8.5 on aspect ratio as a number of cycle increases, but in the case of the specimen b, c, and d, it has shown aspect ratio increases.

In this experiment, since it was a specimen of a limited plate, an exact data value was not able to be acquired. And as shown in figure 4.10~4.13, the deepest points b, c, d of the crack show a flat state without progress on the coalescence immediately.

The crack progress velocity of the deepest point is accelerated changing in the form of the anti-elliptical crack as a single crack. Acceding to such experimental results, it can have confirmed that internal crack velocity decrease as the interaction effect of the two cracks during cracks are coalesced, and the fatigue life becomes short that the distance of crack was more small on the two surface cracks.

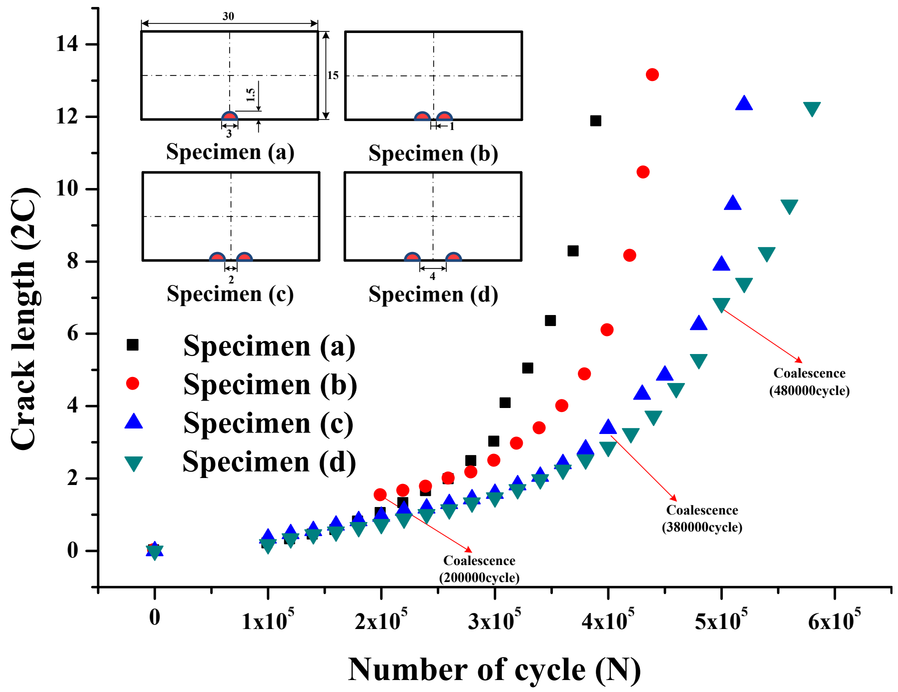

Figure 4.6 Relationship between the surface fatigue crack growth length and number of cycle

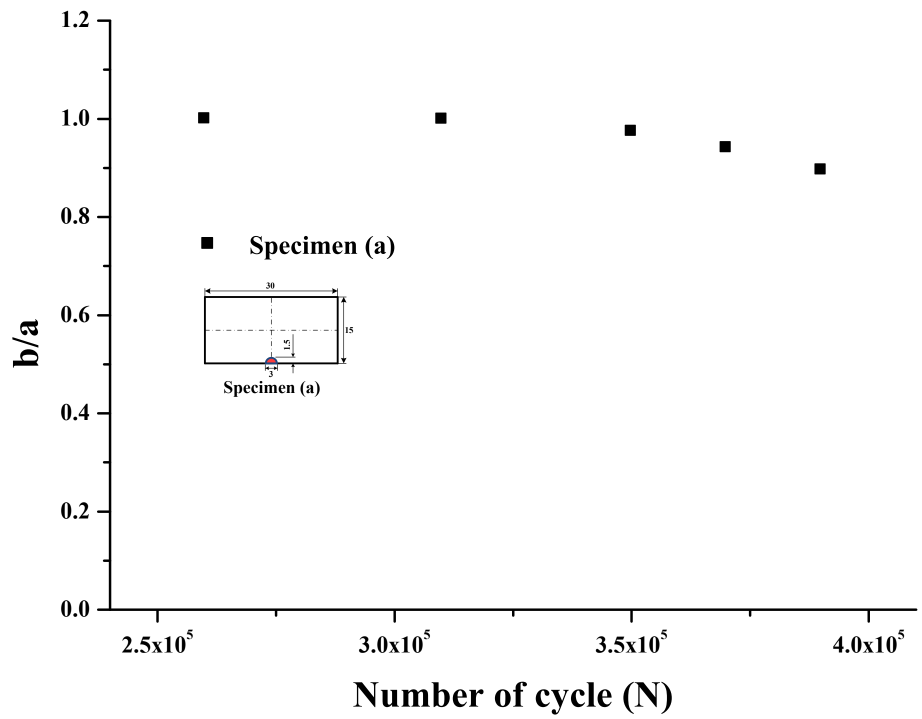

Figure 4.7 Relationship between the aspect ratio and number of cycle in specimen (a)

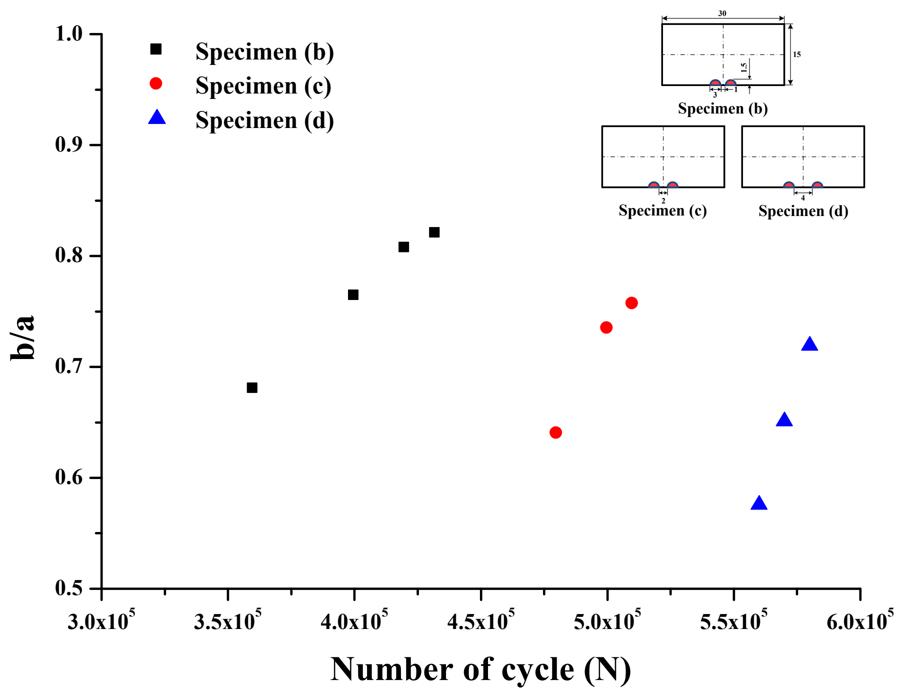

Figure 4.8 Relationship between the aspect ratio and number of cycle in specimen (b), (c), (d)

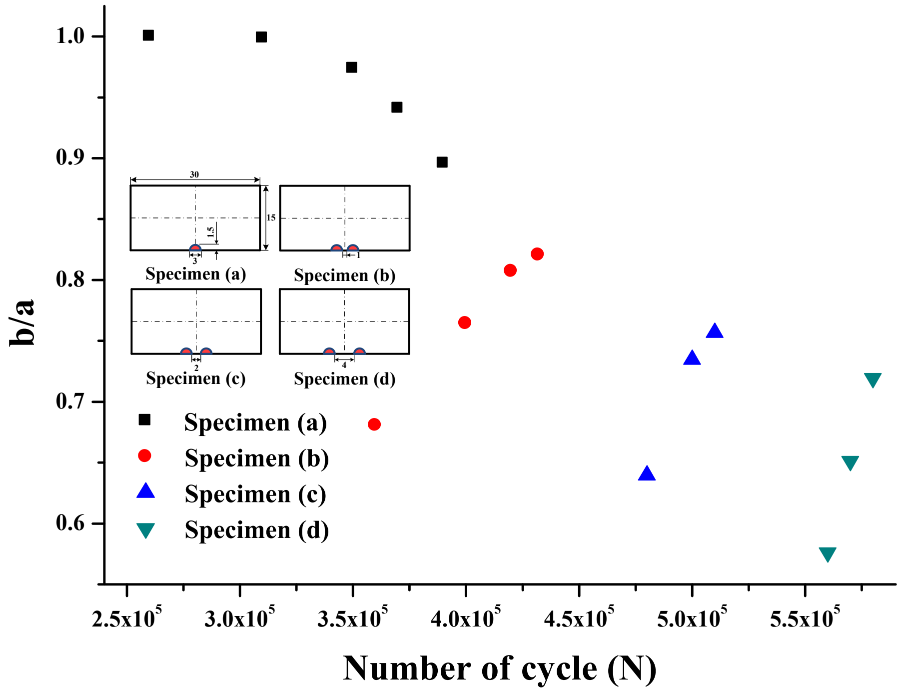

Figure 4.9 Relationship between the aspect ratio and number of cycle in specimen (a), (b), (c), (d)

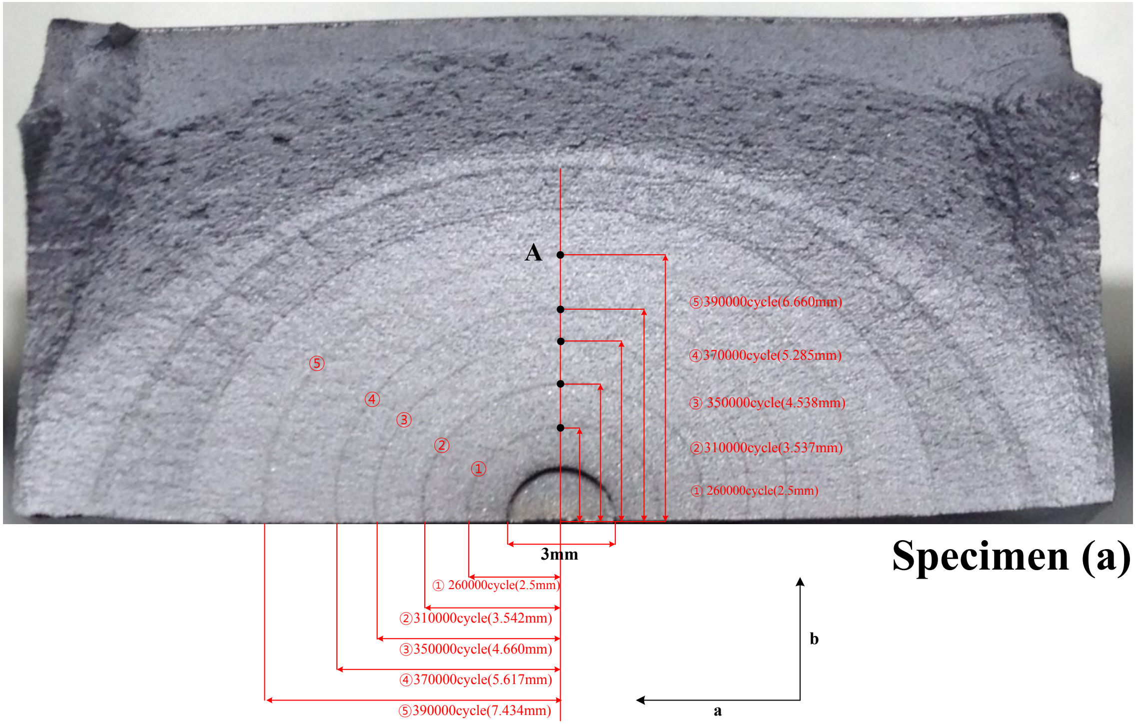

Figure 4.10 The beach mark phenomenon of specimen (a)

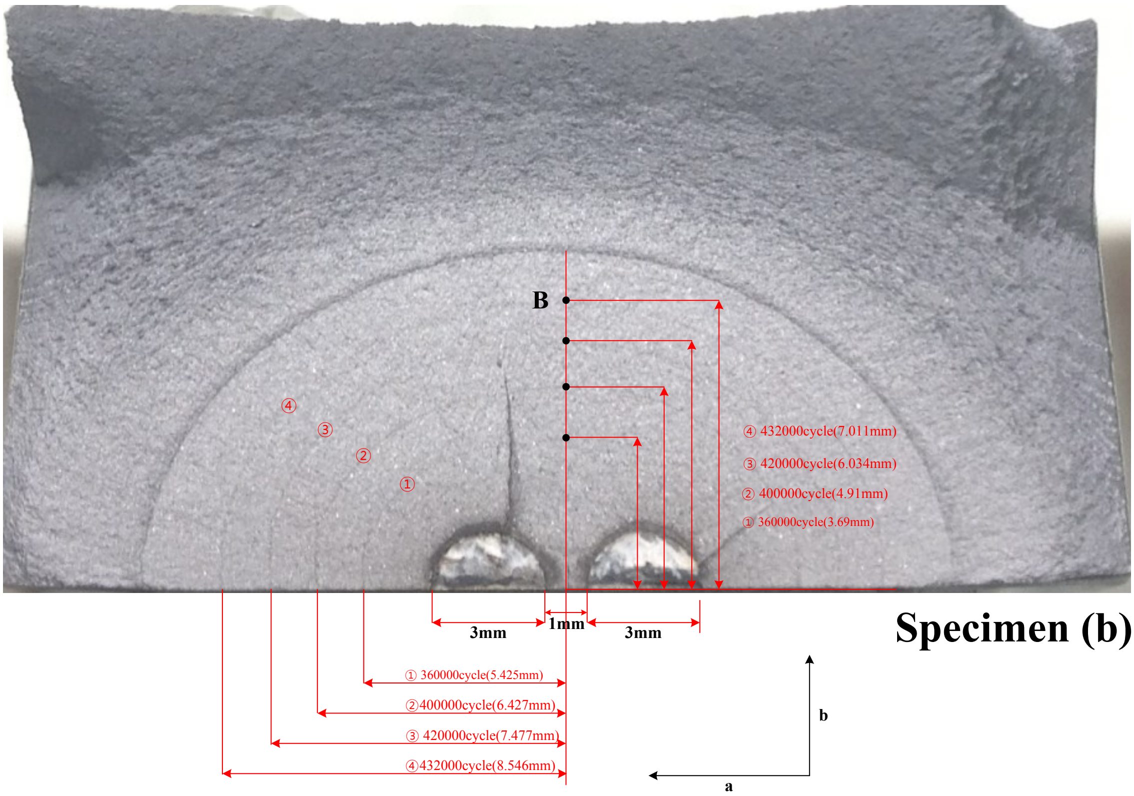

Figure 4.11 The beach mark phenomenon of specimen (b)

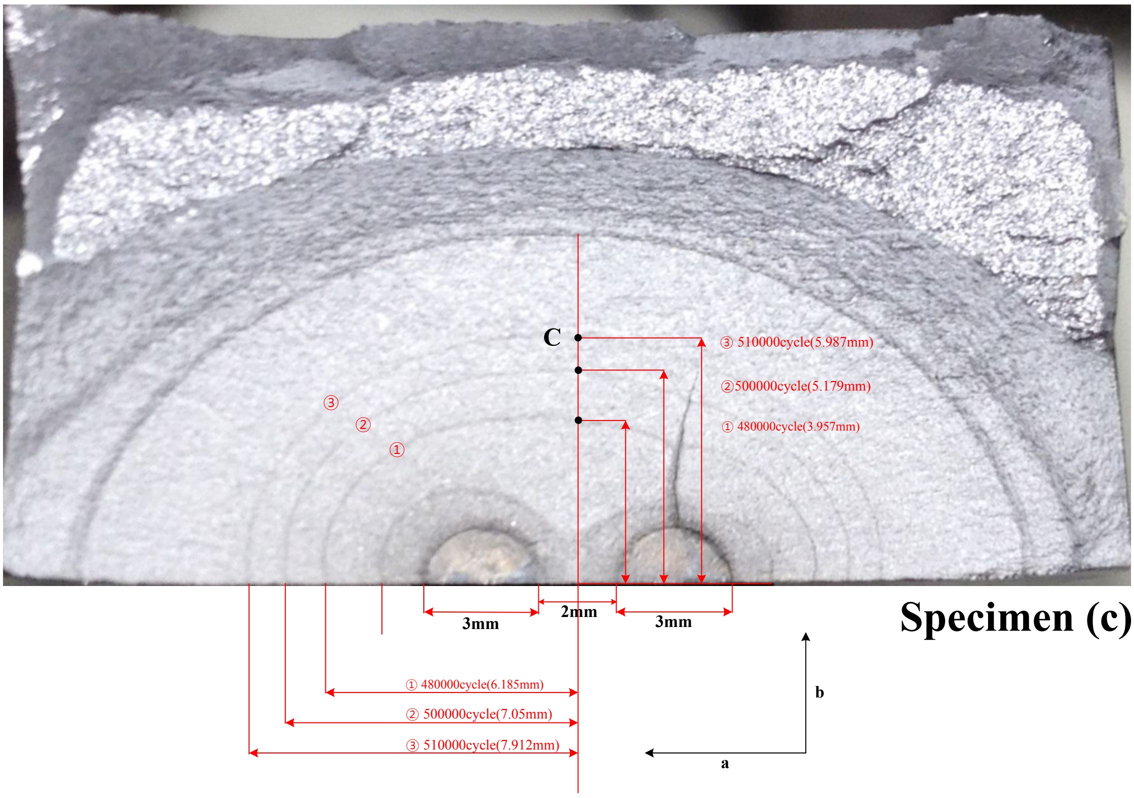

Figure 4.12 The beach mark phenomenon of specimen (c)

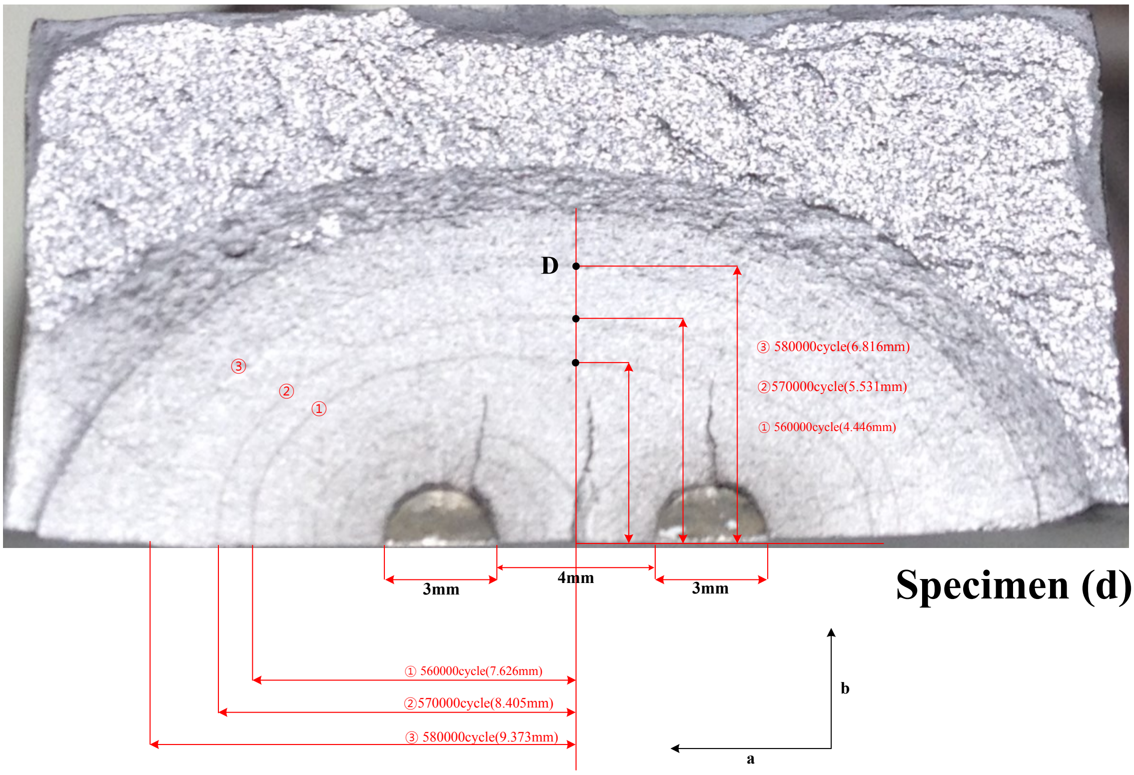

Figure 4.13 The beach mark phenomenon of specimen (d)

4.4 Conclusion

In this study, it was carried out the fatigue crack growth experiment using the 4 kinds of specimens (single and two cracks) in order to investigate the effect of mutual interaction on 3-D surface crack.

As result, the main findings were as follows: a) it was proven that the fatigue life is decreased as the coalescence of crack became a lot faster on the specimen of the mutual different distance. b) it can have confirmed that internal crack velocity decrease as the interaction effect of the two cracks during cracks are coalesced, and the fatigue life becomes short that the distance of crack was more small on the two surface cracks.

Chapter 5

3D Observation of Distorting Crack Growth in Three-Point Bending Specimen

5.1 Introduction

Without exception, all machines or structures have defects or cracks caused by inclusions in the material, non-wilding spot zones, corrosion, fatigue, or other sources. As a representative example of the defect, the proper defects of material and the manufacturing defects occurring at the time of manufacture. Since such defects and inclusion may be become an allowable defect without a problem on safety, it may not do so. However, if such defects and inclusion will be placed on corrosion, fatigue and other several environments, a possibility of growing up to be a crack is high.

Under these circumstances, the crack surface generated when a load is applied to a structure or material is hardly in the direction perpendicular to the load. A good example is the failure of the Mianus River Bridge in Greenwich, Connecticut, US on June 28 1983. This bridge consisted of normal pin and hanger assemblies. The collapse was caused by the fracture of two pin and hanger assemblies that held the deck in place on the outer side of the bridge. The hanger on the inside part of the expansion joint at the southeast corner was forced from the pin that was holding it, and the load was shifted to the only other pin in the joint. The extra load on the remaining pin caused the initiation of a fatigue crack at a sharp corner on the pin. The crack caused a catastrophic outcome, owing to the propagation in the load direction as the pin could not support the heavy load. As such, if the load direction is not normal, the crack propagates through the structure while being distorted. Nonetheless, fracture behavior has not yet been elucidated clearly. Thus, it is essential to establish a theory to estimate the crack propagation route against several distorting propagation phenomena to prevent fractures and fracture accidents.

In this study, we performed three-point bending tests under a static load to acquire basic knowledge of such phenomena, and the propagation features of the distortion were observed by changing the degree of the initial crack. From the results, the differences between the fracture routes were examined, showing that the extent and velocity of crack propagation, the stress intensity factor, and the relationship between load and displacement varied according to the degree of initial crack in the specimen. Input energy to the specimen are estimated from the relationship between load and displacement. Surface area on crack propagation zone is measured from fractured specimens. Based on these data for the input energy and surface area, energy release rate is approximately evaluated for each specimen.

Figure 5.1 The collapse accident of Mianus River Bridge

5.2 Experimental Procedures

5.2.1Experimental specimen

Figure 5.2 shows the geometry and dimensions of specimen PMMA used for this test. PMMA is a type of acrylic resin and poly methyl methacrylate; Table 5.1 summarizes its mechanical properties. As shown in Figure 5.2, the specimen is of length L = 320 mm, height H = 70 mm, and thickness W = 10 mm. The 25mm of notch is inserted by a rotary saw cutting machine of thickness 1mm and the remaining 10mm is inserted with a pop-in on the center of the specimen by pure mode I using the hammer. Finally thorough straight initial crack 35mm can be obtained. Four types of specimens the initial angles of 0°, 15°, 30°, and 45° were processed by such a method.

Four types of specimens were used for the test to investigate the crack propagation type according to the initial crack, and the angle of the initial crack was set at θ = 0˚–45˚ in steps of 15˚. The specimens were subjected to a three-point bending test under static load to evaluate the crack propagation, stress intensity factor, and energy release rate.

5.2.2Experimental Methods

Figure 5.3 illustrates the test device installed to show the crack propagation under a three-point bending test. The load was applied to the specimen using a hydraulic servo-type fatigue testing machine. The load was obtained to the specimen using displacement control, and the displacement velocity was set as 0.025 mm/s.

As shown in Figure 5.3, the specimen was connected to a hydraulic servo load control device. The change in displacement and load was recorded as the relation between the load cell and crosshead on the test device using an x-y recorder. To investigate the crack propagation, a digital camera in front of the specimen, and a CCD camera on the side were installed to record images of the crack propagation.

Table 5.1 Mechanical Properties

Material	**PMMA**
Poisson`s Ratio	0.329
Young`s Modulus E $[GPa]$	2.95
Mass Density ρ $[kg/m^3]$	1190
Optical constant C_0 $[m^2/N]$	1.05
Dilatational wave velocity C_d $[m/s]$	1666.7
Shear wave velocity C_s $[m/s]$	965.4

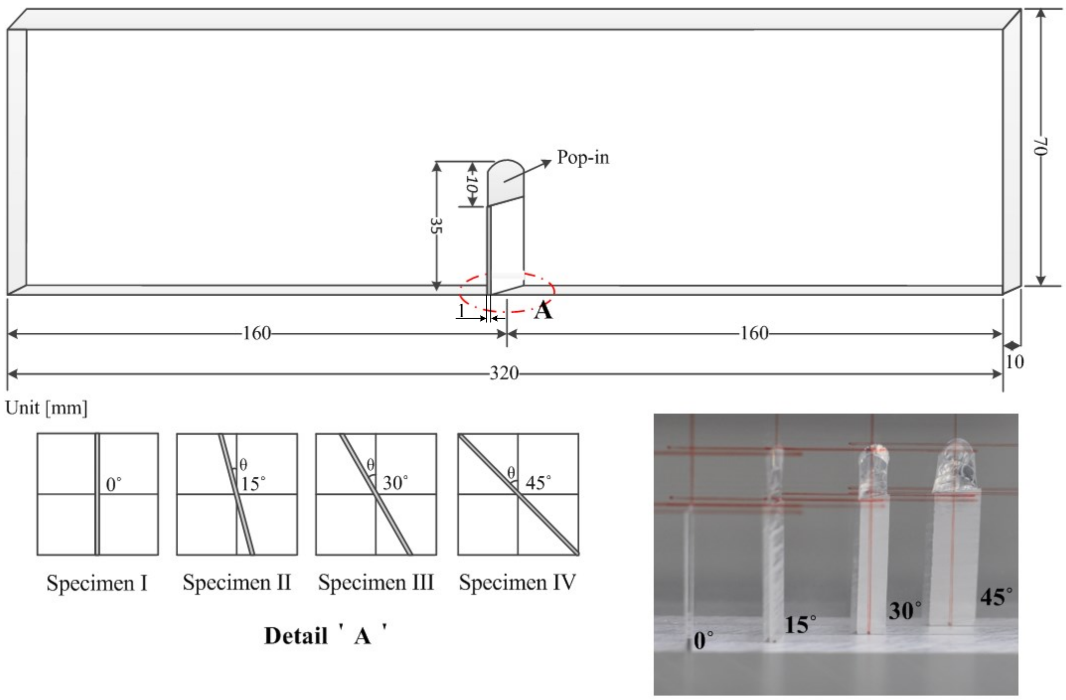

Figure 5.2 Specimen geometry

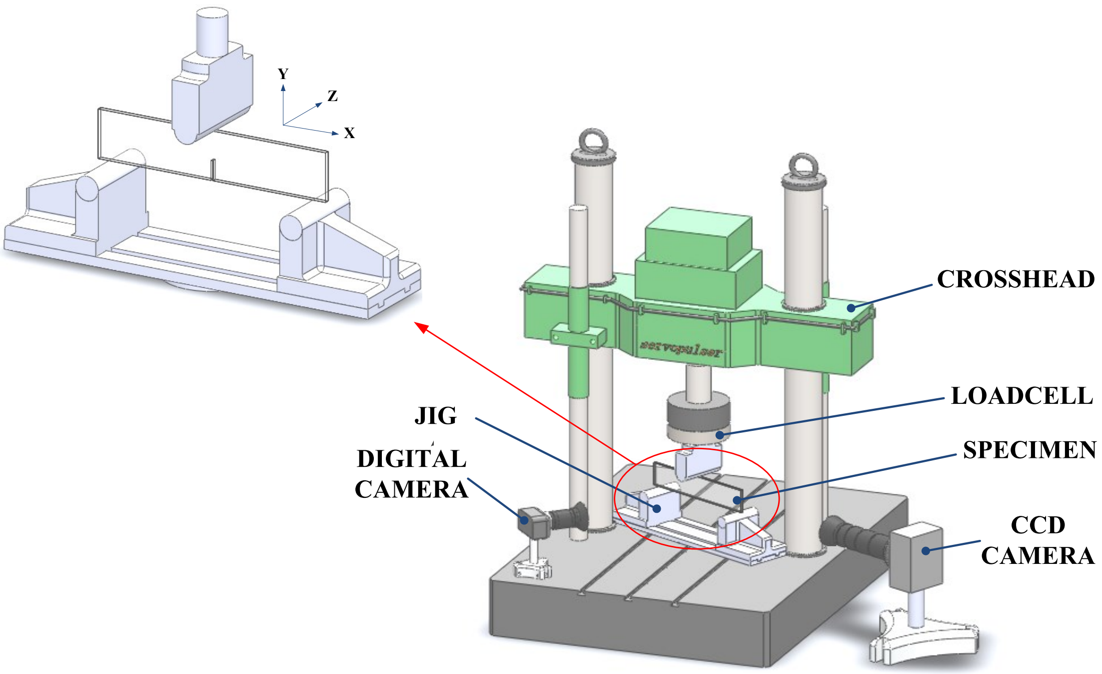

Figure 5.3 Testing machine

5.3 Experimental Results

5.3.1Fracture route observation

Figures 5.4 (a) and (b) are pictures of the front of the specimen and the crack surfaces acquired after the static fracture test using different specimens with different angles of the initial crack. The fracture route of the specimen shows that the pattern changes with the degree of initial crack. Upon examining the effect of the initial crack on the fracture route we see that when θ = 0˚ the crack propagated directly to the load point.

In the case of θ = 15˚– 45˚, the crack propagated to the load point but with a distortion and when the angle of initial crack was large, the distortion became large. Figure 5.5 shows the change of load given to the specimens with an initial crack degree of θ = 0˚– 45˚. For θ = 0˚, 15˚, 30˚, and 45˚, the maximum load is about 283.8 N, 415.5 N, 409.1 N, and 414.5 N, respectively. When the degree of the specimen is θ = 15˚– 45˚, the maximum load becomes about 400N – 420N.

When this is compared with the load of 280 N for θ = 0˚, the load value of θ = 15˚– 45˚ is proven much higher. This result for maximum load might be due to the fact that while θ = 0˚ is a pure mode I, θ = 15˚– 45˚ becomes a mixed mode that requires more energy. The initial point of fracture was confirmed to start near the maximum load. Figure 5.6 shows the crack propagation length and velocity. According to the graph, in the case of θ = 0˚, the crack progressed at a constant velocity while θ = 15˚ and 45˚ initially demonstrated high crack propagation velocity, which later became constant, similar to the crack propagation velocity at θ = 0˚. In the initial crack propagation stages of our experiments, highest crack velocity can be observed in the case of θ = 15˚ and it can be confirmed to become a constant velocity from crack length 33mm.

5.3.2Relation between fracture toughness and angle of initial crack

The fracture toughness K_{IC} is derived from the value of the applied load just before the starting of the crack in each specimen with θ = 0˚– 45˚. Figure 5.7 is a graph showing the relation between fracture toughness K_{IC} and degree according to the degree of initial crack. It shows that for the initial crack angles of θ = 0˚, 30˚, and 45˚ the fracture toughness had a constant distribution, but for θ = 15˚ the value of fracture toughness had an irregular distribution.

5.3.3Energy release rate from the surface area of the crack

This test used a three-dimensional laser focus displacement meter to evaluate the energy release rate using the crack surface area. The laser focus displacement meter is a device which evaluates the reflection of the laser beam against a measuring object. Each specimen's crack surface area according to the x, y, and z axis coordinate value is obtained.

The crack length was calculated from the images photographed using the CCD camera during the experiment was carried out. We were able to obtain crack progress length per second from the images photographed. And, the area of each static fracture test load-time graph (Figure 5.5) is regarded as the energy absorbed by the fracture. Therefore, energy required for fracture was calculated from integrating the area of each static fracture test load-time.

According to the data obtained, the average energy release rate can be calculated by dividing the energy obtained from the load-time graph by the surface area of the crack. The energy release rate for θ = 0˚– 45˚ is shown in Figure 5.8. The average energy release rate of each specimen increases if the degree of initial crack increases. It is thought that the rate of mixed mode in each specimen gets bigger as the initial crack angle of the specimen increases.

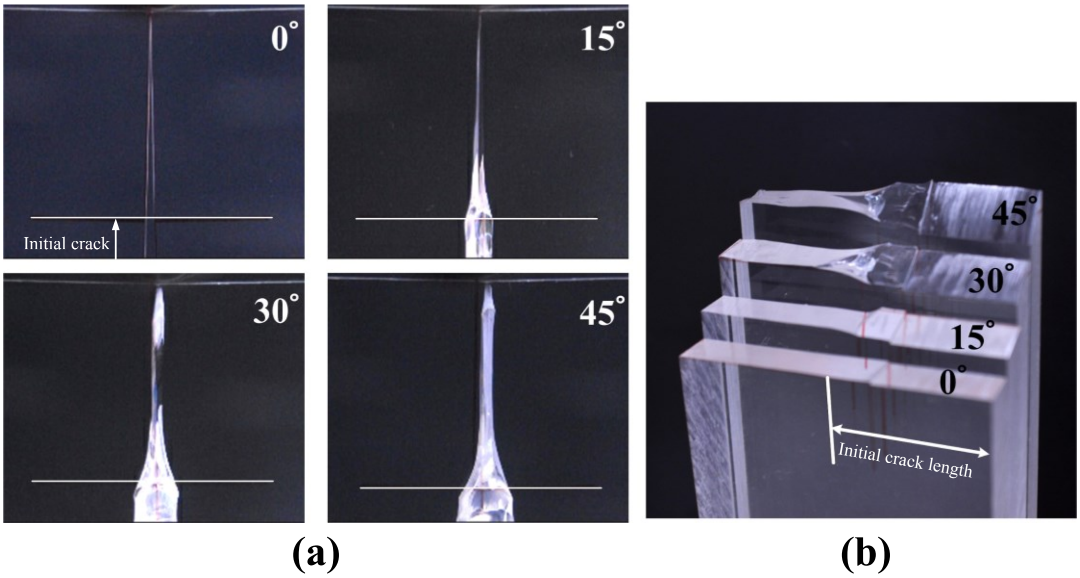

Figure 5.4 Images of the crack growth and crack surface

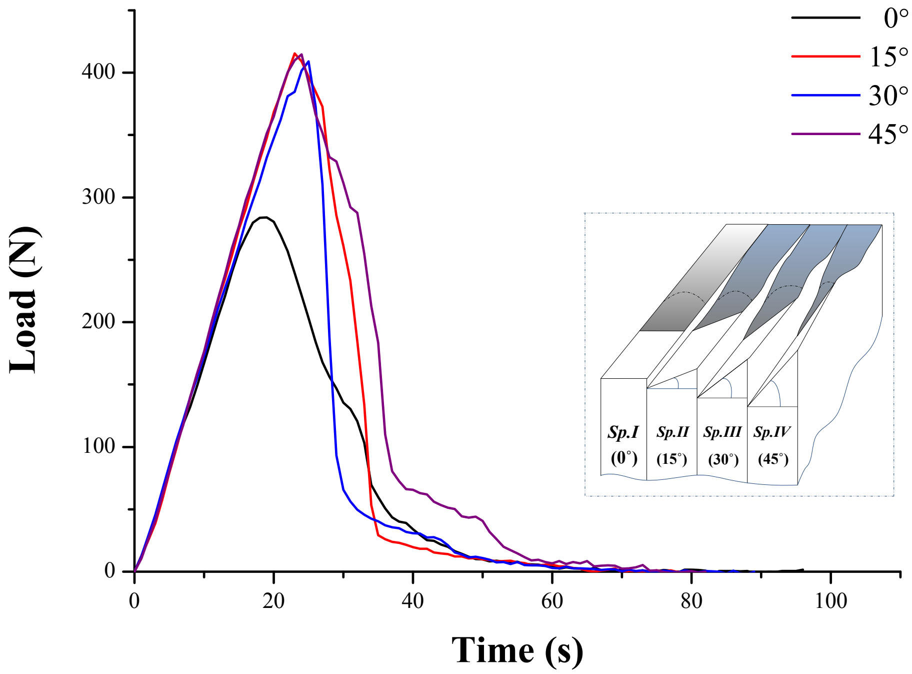

Figure 5.5 The relationship between the load and time

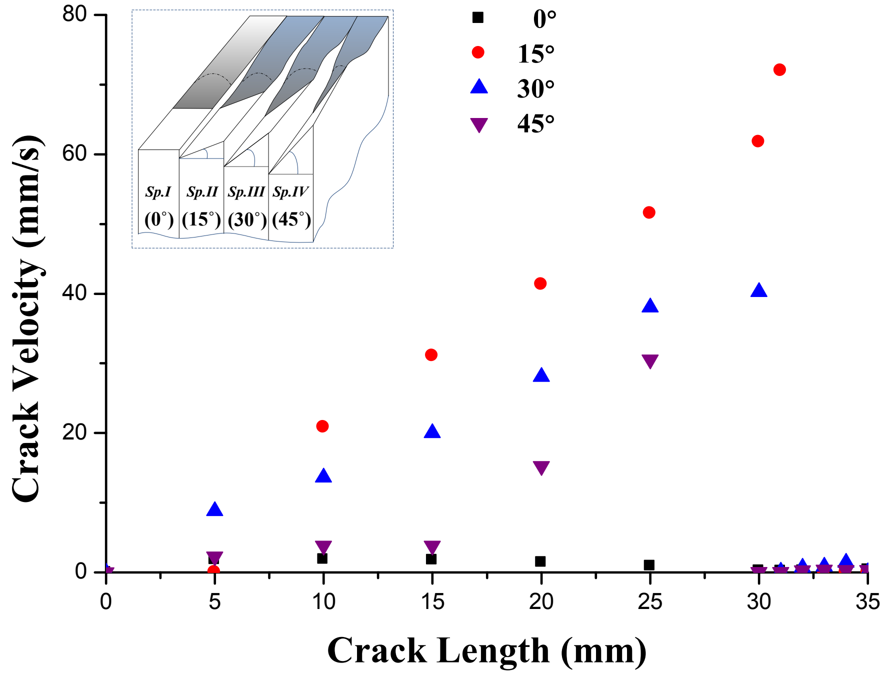

Figure 5.6 Crack progress velocity

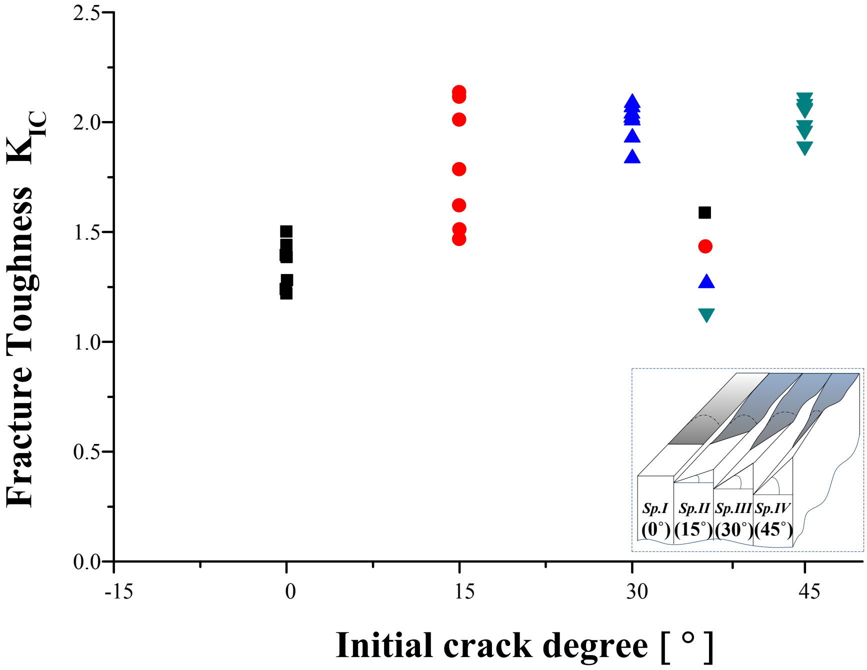

Figure 5.7 Relationship between the fracture toughness and initial crack angle

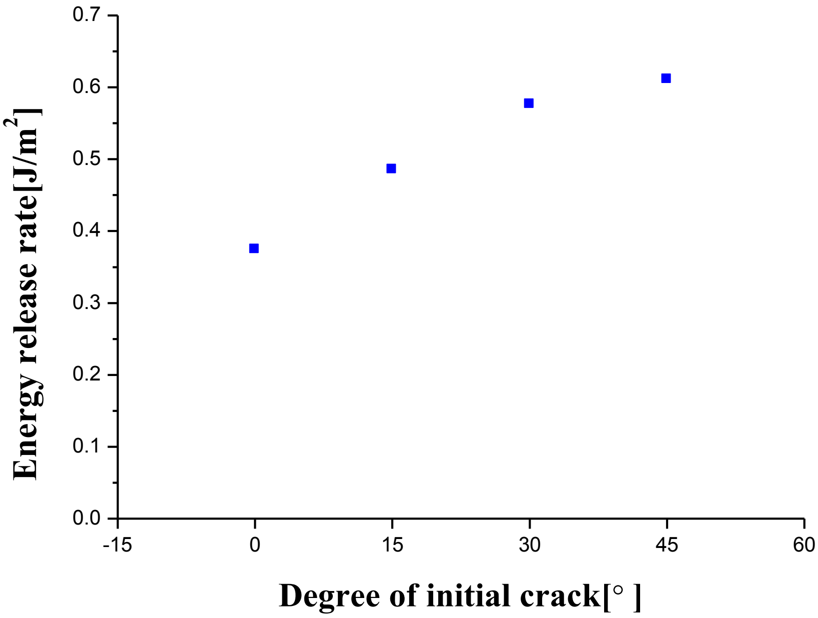

Figure 5.8 Energy release rate from surface area of crack surface

5.4 Conclusion

A three-point bending test which involved changing the initial crack angle of each PMMA specimen was carried out to investigate the crack propagation characteristics. The relation between the crack propagation and fracture dynamics parameter was investigated. The following results were obtained from observations of the crack surface according to the degree of initial crack.

1) The fracture route varied according to each degree of initial crack, propagating with added distortion as the degree of initial crack increased.

2) In the case of θ =15˚– 45˚ unstable crack propagation appeared due to the influence of the mixed mode.

3) The energy release rate according to the degree of initial rate in each crack surface increased when the degree of initial crack was large.

4) The crack propagation velocity was fastest for θ = 15˚. Comparing the crack pr opagation velocity according to each degree of initial crack, there might exist a degree between θ = 0˚ and θ = 30˚ which has faster crack progress velocity.

Chapter 6

Evaluation of Fatigue Crack Growth Characteristics about Mixed Mode Influence and Thickness Dependence Using the Three-point Bending Specimens

6.1 Introduction

Fracture of machinery and structures is mostly caused by cracks being initiated and propagated from the defects in the inside and outside. However, there are some cases in which slight defects occur on the surface or the inside during molding of materials, member manufacturing or assembly process. Thus, since the thoughts to perform the inspection and maintenance to manufacture ideal machinery and structures are not realistic, safety of structures should be considered while a certain degree of defects or cracks is included.

The use of high strength steel has recently been increased in order to promote the high strength of structures or part of machinery. Since chrome molybdenum steel (SCM steel), which is one kind of high strength steel, has very strong resistance and mechanical properties through heat treatment, it is used for various mechanical parts such as car's crankshaft and gear compared to other metals. These mechanical parts or members have very different load weights depending on place, environment and state. In addition, its use direction can be changed. Likewise, if repeated load occurs for a long period of time, surface crack may occur due to metal fatigue.

It has been known that final propagation direction of fatigue crack has the load direction as the normal direction, and most of them become mode I dominance pattern. However, crack which occurs due to unexpected causes such as collision of device to the surface of machinery or structures is not the case. Likewise, it is said that fatigue crack growing from defect or crack grows by changing the shape to become mode I dominance pattern, but the detailed theory and process has not been established yet.

Recently many studies on fatigue crack growth behavior in a mixed mode state have been conducted. However, there are some concerns in which the unexpected risk place may exist in structures where it is difficult to detect crack position through study on fatigue crack growth. In addition, because ASME section which is the indicator of mutual interaction of fatigue crack and safety evaluation does not introduce the surface crack which does not follow fatigue caused by unexpected cause, it cannot be said that it should be safe as the safety indicator of this problem. Therefore, this study observed the fatigue crack growth behavior in a mixed mode state considering load working direction and correlation in initial crack direction and it investigates its fatigue crack growth mechanism.

6.2 Experimental apparatus and methods

6.2.1 Experimental specimen

The experimental species used in the fatigue crack growth experiments used SCM440 which was chrome molybdenum steel. SCM440 has been standardized in JIS G 4053 and used as a member of various machines and structures in order to pursue the latest lightweight high strength. In particular, it has been used as the parts of engine in aircraft, automotive and ship or a major part of members such as gear and crankshaft. The mechanical properties and chemical composition of this SCM440 experimental species are shown in tables 6.1 and 6.2. Figure 6.1 shows the dimension and shape of specimens used in this study. The purpose of specimens is to observe the effect of change in thickness on fatigue fracture growth by using chrome molybdenum steel being used as the important part which is highly versatile and requires high strength. The thickness of specimens is made in three patterns such as 10 mm, 20 mm and 30 mm. In order to conduct fatigue fracture growth experiment in a mixed mode, inclination angle of initial crack is made in four patterns such as 0°, 15°, 30° and 45° and then experiments are conducted.

Table 6.1 Mechanical properties of SCM440 (wt %)

C	Si	Mn	P	S	Cr	Mo
0.38~0.43	0.15~0.35	0.6~0.9	0.03	0.03	0.9~1.2	0.15~0.3

Table 6.2 Chemical compositions (wt %)

Tensile Strength Ultimate	1071Mpa
Tensile Strength Yield	980Mpa
Modulus of Elasticity	205Gpa
Poisson's Ratio	0.29
Shear Modulus	80Gpa

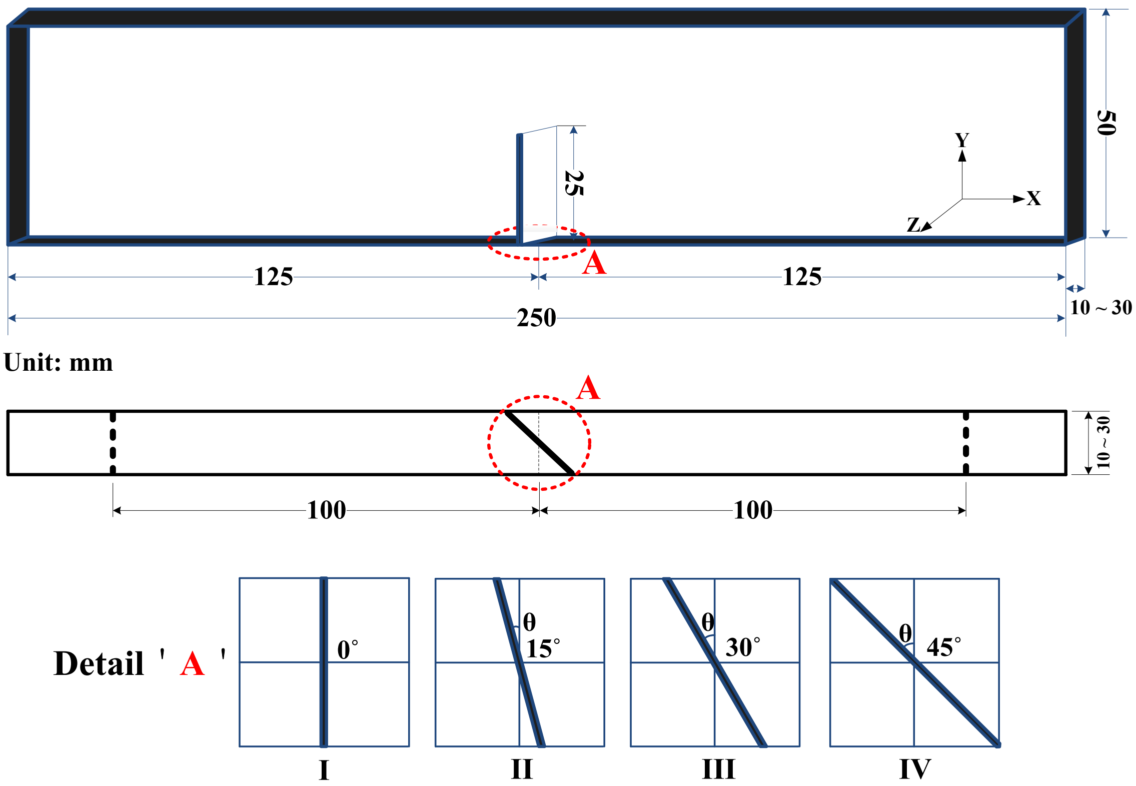

Figure 6.1 Specimen geometry

6.2.2Experimental apparatus and test method

Fatigue experiment is conducted in the constant amplitude load according to provisions of ASTM E647-93 by using a hydraulic fatigue experimental device for 100kN at room temperature. As shown in figure 6.3, the specimens is attached on experimental device and repeated load is given in vertical directions. The fatigue experiment is carried out with load control, repeated rate of 10 Hz and repeated waveform of the sin wave. As shown in table 6.3, load working on unit thickness is set as the same in all experimental species. In addition, the minimal load is changed to insert a beach mark like a red dotted line in figure 6.2 in order to investigate the pattern of internal fatigue crack growth. A beach mark is the crack mark left on fatigue fracture surface based on rapid change of load or environment. Invisible internal crack growth pattern can be identified by using this beach mark. Length of crack is measured by using a CCD camera. The experimental device is paused and recorded every 10,000 cycles. In addition, time to pause the experimental device is up to 5 minutes upon measurement.

The range of the stress expansion factors for three-point bending experimental species is calculated using the equation (1). Crack growth rate is calculated by using the second method using equation (2) organized by paris-erodogan.

$$\Delta \mathbf{K} = \frac{\mathbf{3SP}}{\mathbf{2tW^2}}\sqrt{\boldsymbol{\pi}\mathbf{a}}(1.09-1.735\alpha+8.20\alpha^2-14.18\alpha^3+14.57\alpha^4) \quad (1)$$

(W is the height of a specimen, S is the distance of support point, a is crack length, P is load working on unit thickness, α=a/W)

$$da/dN = C(\Delta K)^m \quad \text{(C, m is Material constant)} \quad (2)$$

Table 6.3 Loading condition

Thickness, B(mm)	10				20				30			
The initial angle, (°)	0°	15°	30°	45°	0°	15°	30°	45°	0°	15°	30°	45°
Maximum load, P_{max}(kN)	3.43kN				6.86kN				10.29kN			
Stress ration, R	0.1											
Frequency, f(Hz)	10											
Wave form	Sin											

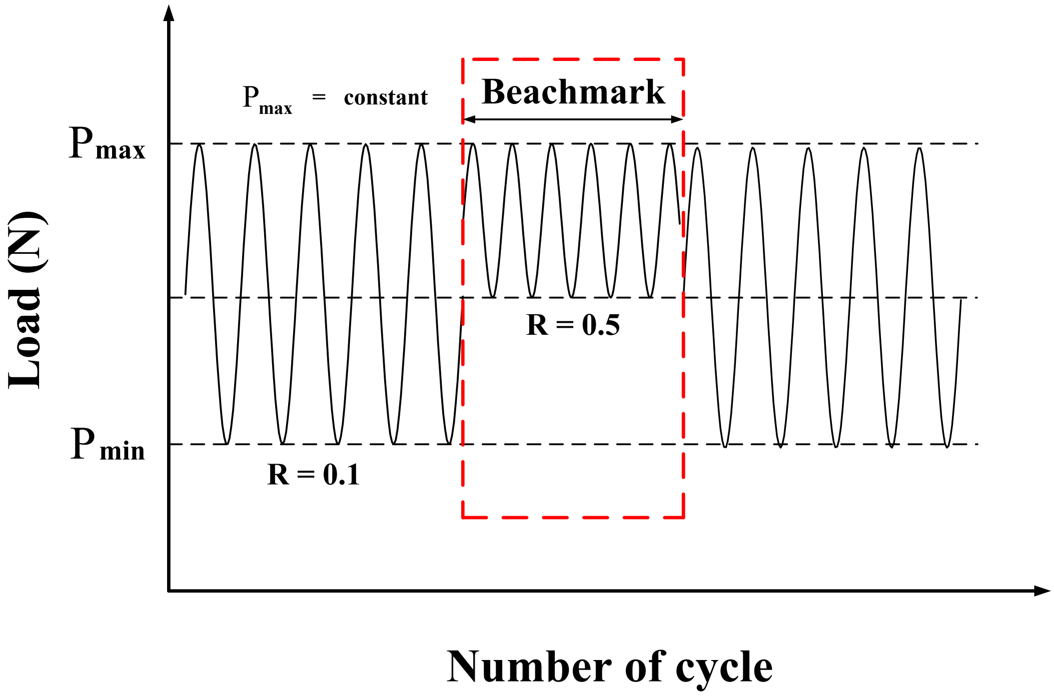

Figure 6.2 Loading condition for the beach mark

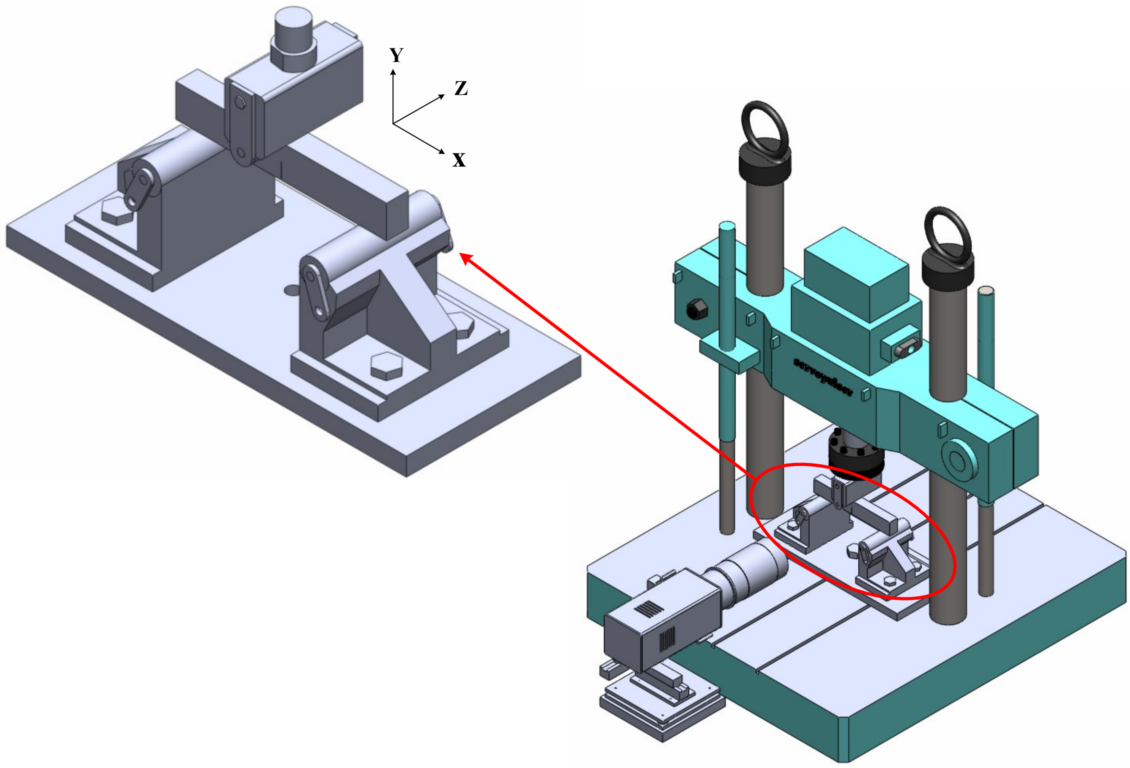

Figure 6.3 Testing machine

6.3 Results and Discussion

6.3.1Observation of fatigue crack growth behavior in mode I

Three point bending fatigue crack growth experiment was carried out using specimens (thickness of 20 mm, load of three patterns such as 3.42 kN, 6.86 kN and 10.29 kN) at initial crack inclination angle of 0°on which mode I was working at stress ratio of R=0.1. Figure 6.4 showed the result obtained from the experiment and a-N curve representing the relationship between number of cycle and length of crack. The graph of da/dN - ΔK representing the relationship between stress expansion factor and fatigue crack growth rate which was calculated by using data of Figure 6.4. It was shown in Figure 6.5. As shown in Figure 6.5, it passed through zone I around initial stress expansion factor of 14MPa and it grew up to stress expansion factor of approximately 32MPa in zone II. In addition, it was confirmed that it entered zone III. Table 6.4 showed c and m values of three patterns of load calculated by using equation (2) organized by Paris. Average fatigue crack growth rate in zone II of normal state of 3 patterns from calculated results was $da/dN = 3.3339\times10^{-13}(\Delta K)^{3.8659}$.

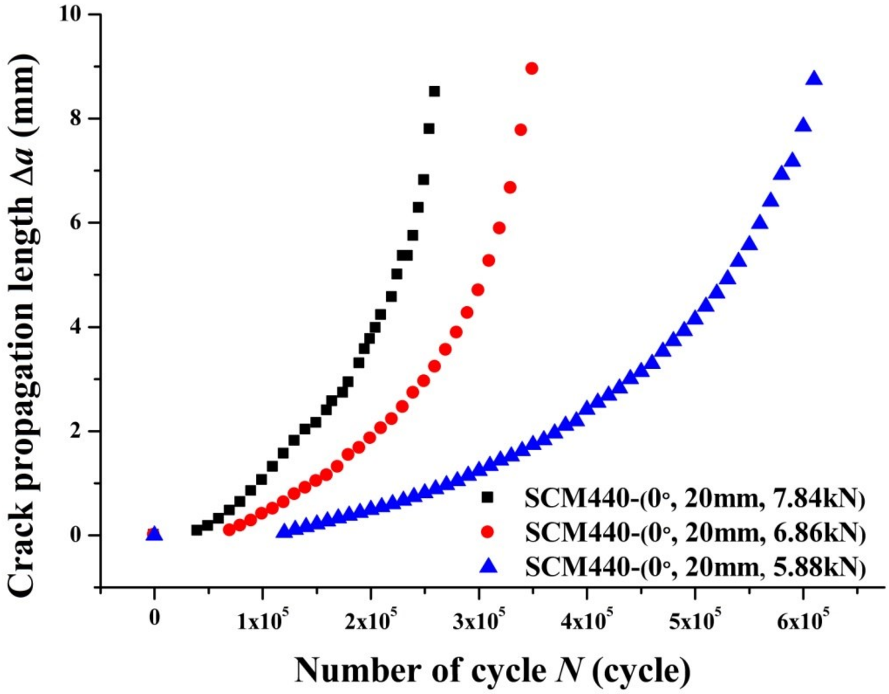

Figure 6.4 Relationship between crack length and loading cycle

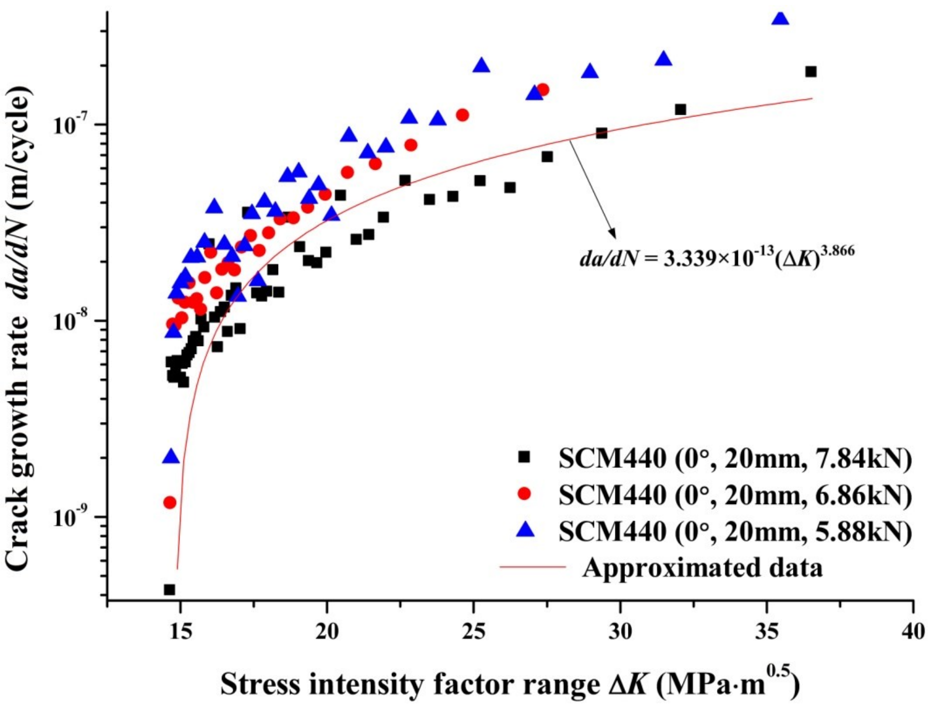

Figure 6.5 Fatigue crack growth rate for SCM440 steel

Table 6.4 Material constants in paris-erdogan equation

Maxim Load (kN)	Paris-Erdogan eq.	
	m	C
3.42(600kg_f× 9.8)	4.0249	2.2929×10^{-13}
6.86(700kg_f × 9.8)	3.7166	4.9751×10^{-13}
10.29(800kgf ×9.8)	3.8562	2.7491×10^{-13}
Average	3.8659	3.3339×10^{-13}

6.3.2Observation of fatigue crack growth behavior in a mixed mode

Fatigue crack growth behavior was observed in a mixed mode considering the correlation between load working direction and initial crack direction. Figures 6.6 and 6.7 were the results through fatigue experiments in the state of same load per each thickness including 10 mm, 20 mm and 30 mm for initial crack inclination angles of four patterns such as 0°, 15°, 30° and 45°. Figure 6.6 showed the results of the fatigue experiments by changing the initial crack inclination angles by every 15° for the same load and thickness. Upon looking at a graph in figure 6.6, there was not much difference in crack growth rate in 0° and 15° in case of thickness of 10 mm. It implied that mixed mode did not give the impact much. However, it was shown that crack growth rate was reduced in 30° and 45° as crack inclination angle got bigger. It was thought that as fatigue crack inclination angle got bigger, shearing force which was the influence of mode II was increased and crack surface was interfered so that crack growth life was increased and crack growth rate was reduced. In addition, case of 20 mm and 30 mm showed the same pattern of thickness of 10 mm, but it was thought that the effect of a mixed mode got increased from 15°.

In the next, crack growth rate of thickness of 10 mm, 20 mm and 30 mm with the same inclination angle was investigated. First, upon looking at graph of 0° to 45° in figure 6.7, crack growth rate of 10 mm and 20 mm showed a slight difference. However, upon comparing graph of 10 mm and 20 mm with that of 30 mm, case of 30 mm showed a big difference of fatigue life. The cause of this result was that displacement rate of plate thickness direction inhibited Poisson effect in center part of specimens when thickness was 30 mm. In this zone, stress began to work in direction of contact to crack surface and the stress components values contributing to modes II and III became large. Thus above results were thought to be caused.

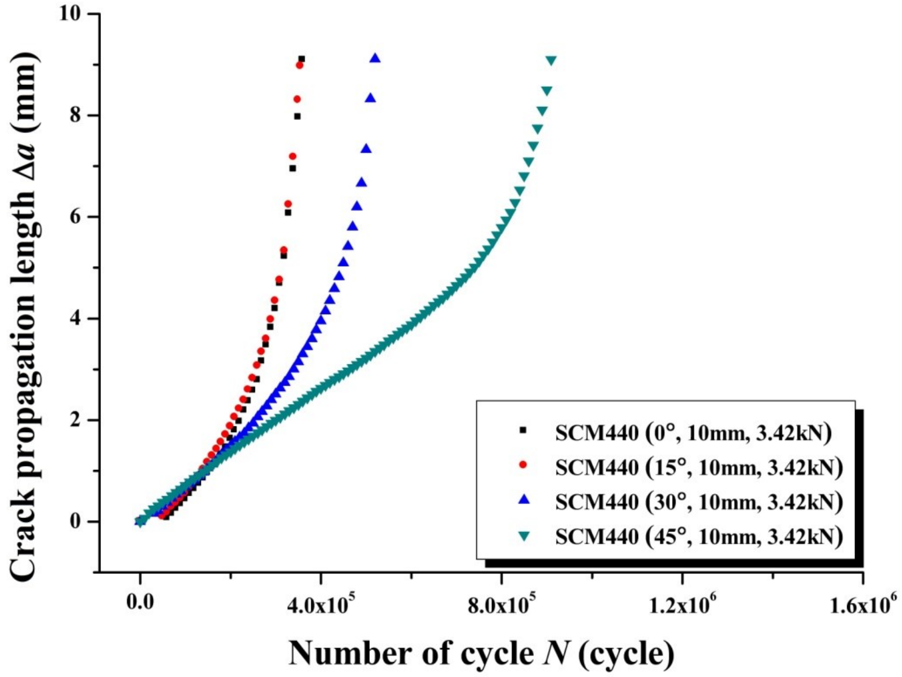
Crack propagation length Δa (mm)
Number of cycle N (cycle)
SCM440 (0°, 10mm, 3.42kN)
SCM440 (15°, 10mm, 3.42kN)
SCM440 (30°, 10mm, 3.42kN)
SCM440 (45°, 10mm, 3.42kN)
0.0
4.0x10^5
8.0x10^5
1.2x10^6
1.6x10^6
0
2
4
6
8
10

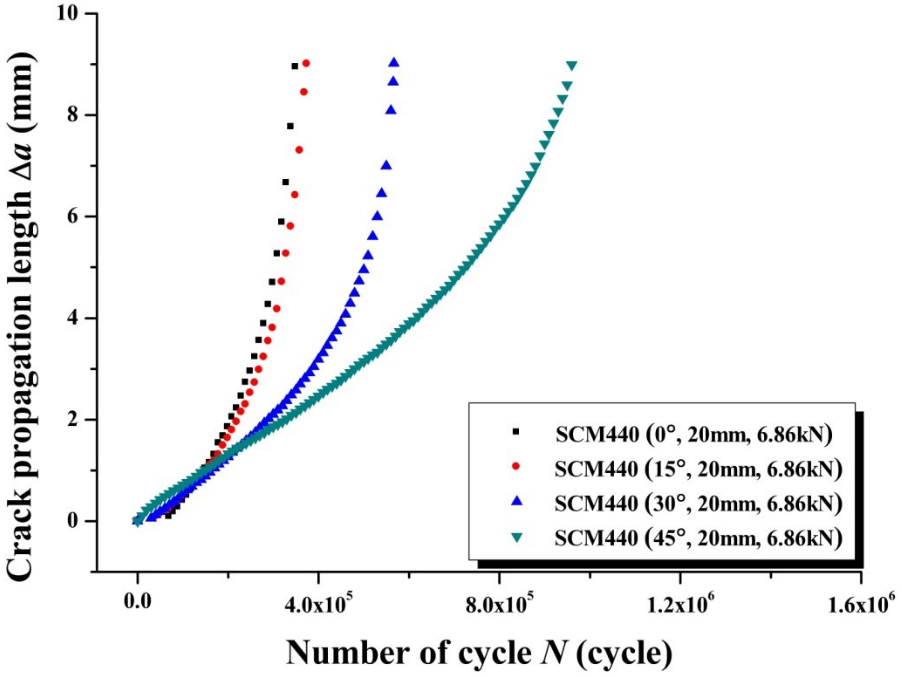
Crack propagation length Δa (mm)
Number of cycle N (cycle)
SCM440 (0°, 20mm, 6.86kN)
SCM440 (15°, 20mm, 6.86kN)
SCM440 (30°, 20mm, 6.86kN)
SCM440 (45°, 20mm, 6.86kN)
0.0
4.0x10^5
8.0x10^5
1.2x10^6
1.6x10^6
0
2
4
6
8
10

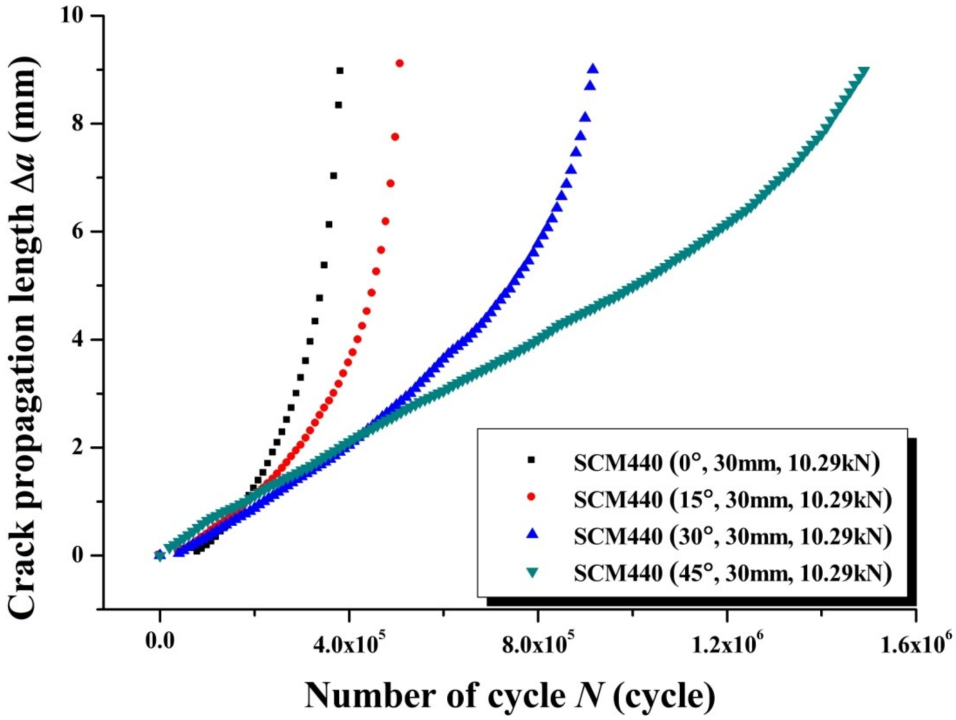

Figure 6.6 Relationship between crack and loading cycle for each thickness

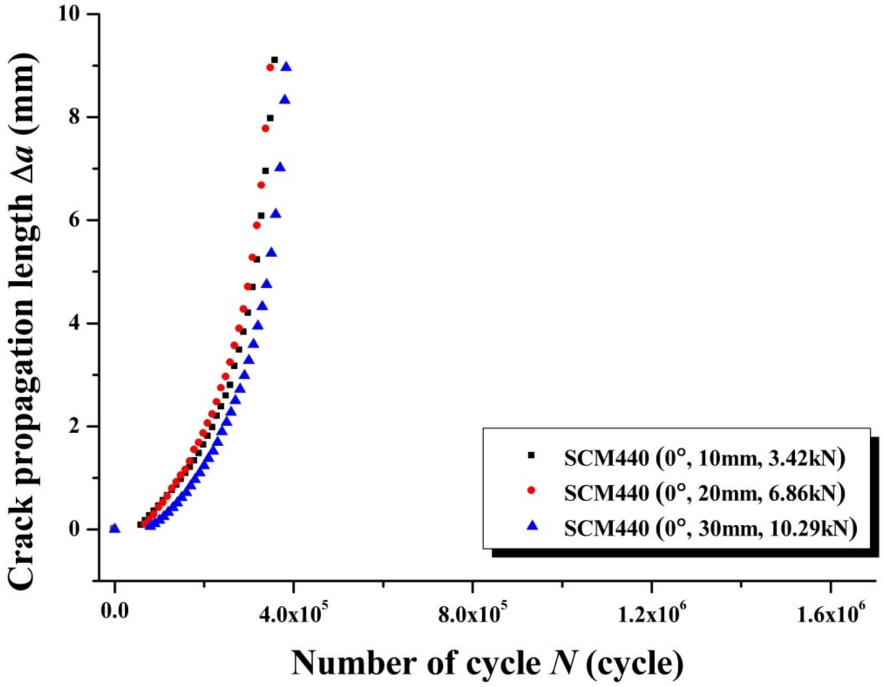
Crack propagation length Δa (mm)
Number of cycle N (cycle)
SCM440 (0°, 10mm, 3.42kN)
SCM440 (0°, 20mm, 6.86kN)
SCM440 (0°, 30mm, 10.29kN)

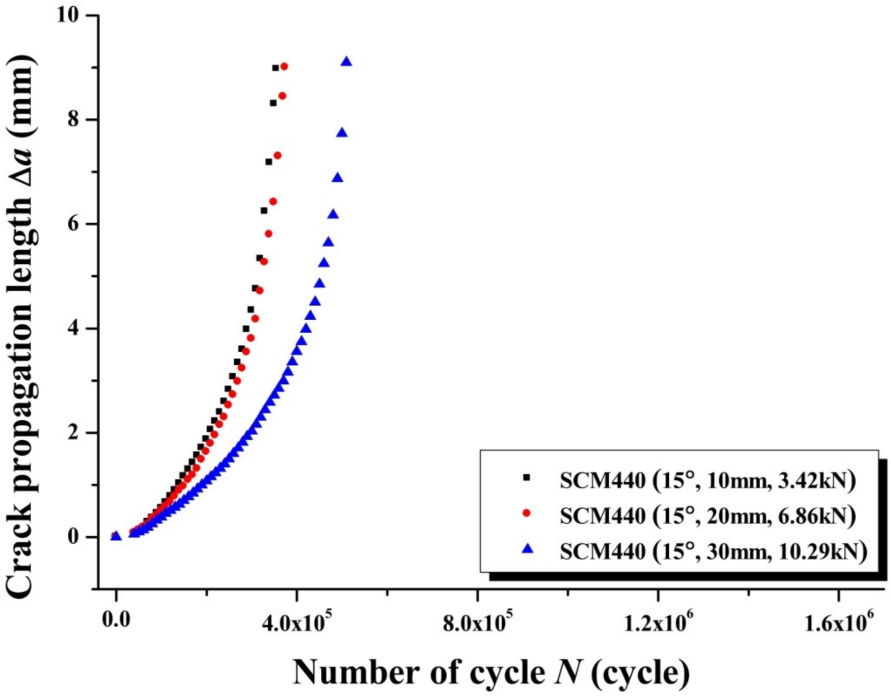
Crack propagation length Δa (mm)
Number of cycle N (cycle)
SCM440 (15°, 10mm, 3.42kN)
SCM440 (15°, 20mm, 6.86kN)
SCM440 (15°, 30mm, 10.29kN)

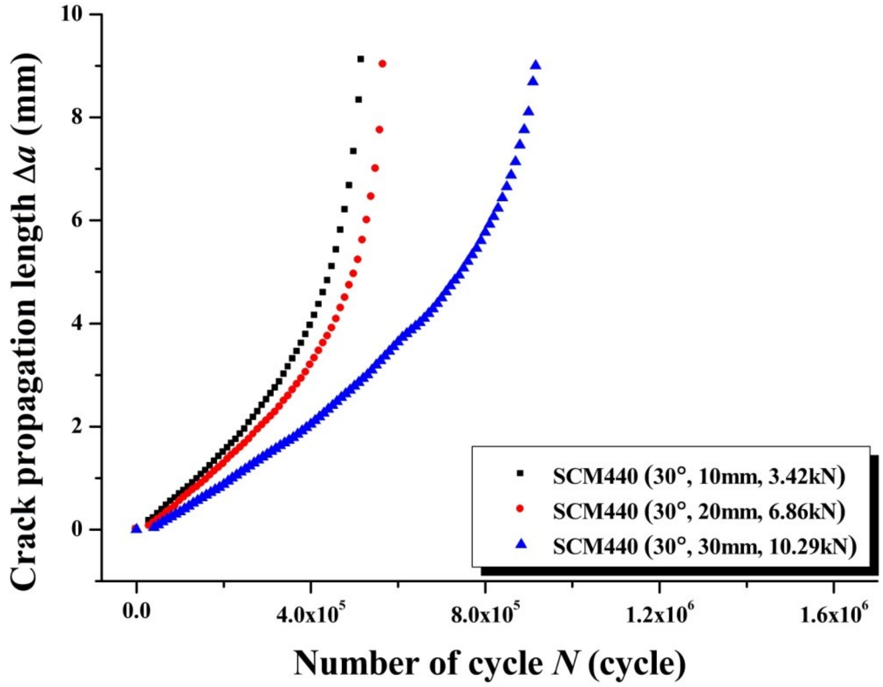

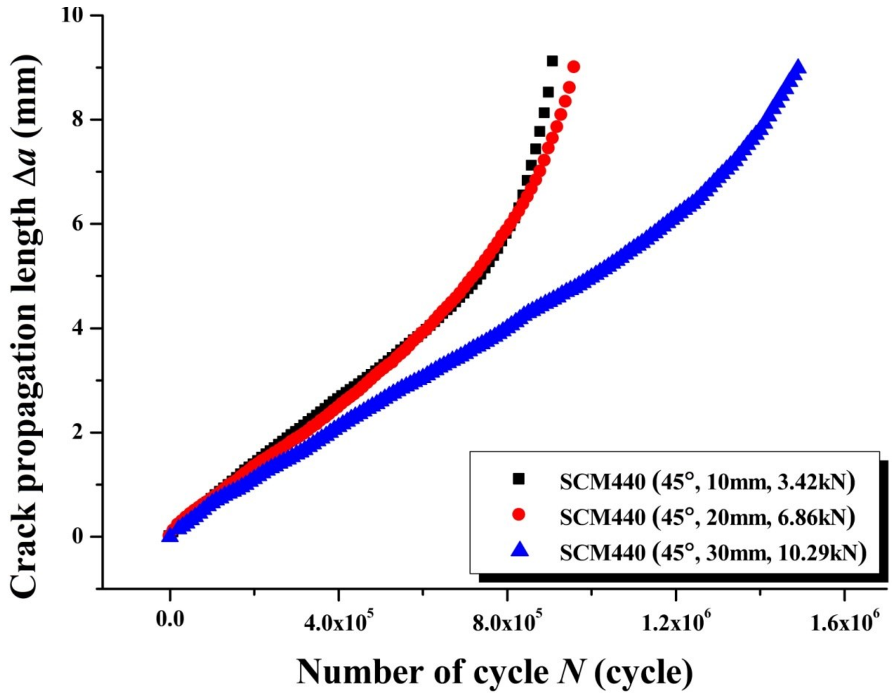

Figure 6.7 Relationship between crack length and loading cycle for each initial slant crack angle

6.3.3Discussion of fracture surface

Figure 6.8 shows the fracture surface at 0°, 15°, 30° and 45° in 30 mm after the fatigue experiments. As shown in a photo of fracture surface, it is observed that several cracks (disconnected line) occur at start point of crack growth and fatigue cracks grow in the step type between cracks (disconnected line). If this crack (disconnected line) returns to a certain degree of mode I, it disappears. Fatigue crack in each section relatively easily grows, but a diagonal crack which does not follow cracks (disconnected line) shows relative high fracture resistance to contribute to the fracture resistance. Finally, the fatigue crack growth rate is reduced. The trends in which cracks (disconnected line) occur show that it easily occurs as thickness of specimens gets more and crack inclination angle gets bigger.

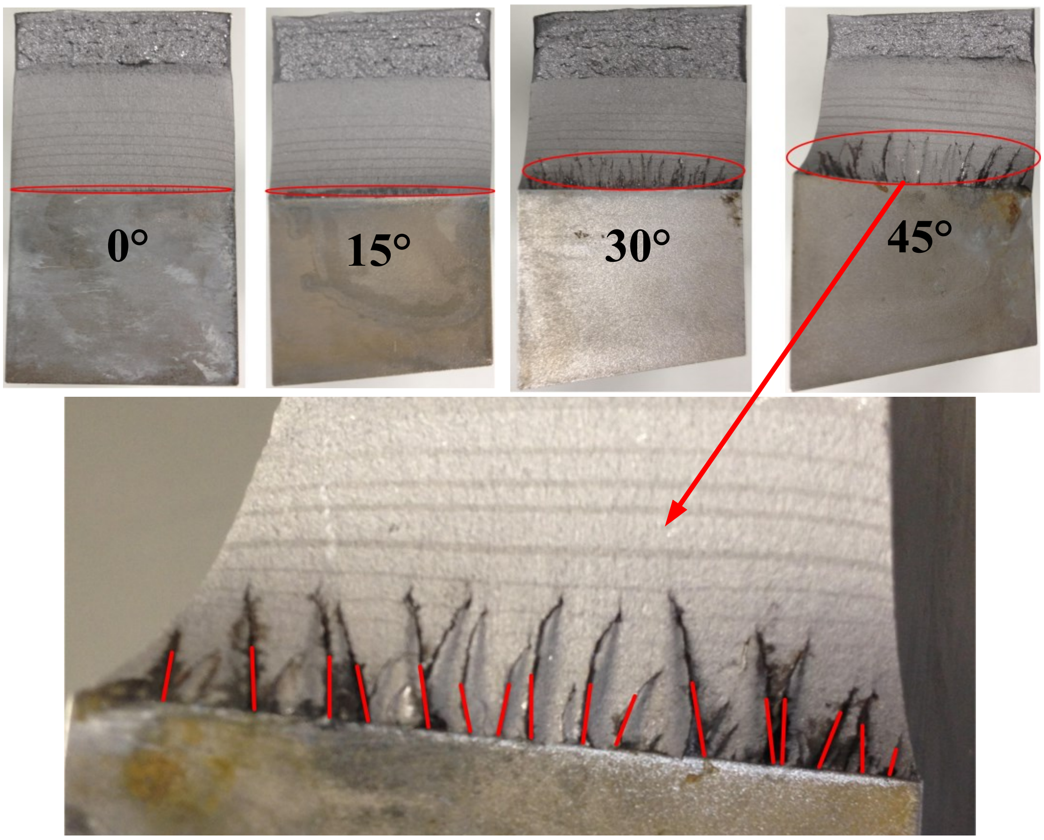

Figure 6.8 Images of fracture surface

6.4 Conclusion

SCM440 which is chrome molybdenum steel widely used in various structures or major parts of machine is used as the specimens to conduct the fatigue crack growth experiment in this study. We observed the fatigue crack growth behaviors in mode I and mixed mode conditions considering correlation between initial inclination angle and thickness.

Observed results are as follows.

i) The fatigue crack which arises from a crack growth being twisted, and the crack slant angle decreases. It checked from the beach mark that there was no big change in the crack edge shape at that time. Moreover, when the initial crack slant angle was large, the crack arose at the time of initial crack growth, and it was suggested that the crack growth behavior is unstable.

ii) The difference of the crack growth history appeared greatly, as the initial crack slant angle and a specimen thickness increased. Since the dynamic condition at the tip of a crack changed with the influence of the mixed mode, or the influences of a modification restraint near the specimen thickness center, it thinks.

iii) If the initial crack growth continues to some extent, a crack slant angle will decrease and the dynamic condition at the tip of a crack moves a mode I dominated. Even if it saw the overall crack growth history, it has checked that the crack growth rate of the crack growth last stage was a state practically equal and pure mode I crack growth.

Chapter 7

Strength Evaluation of Marine Hooks by Static-load and Fatigue Experiments

7.1 Introduction

Recently, many types of crane hooks are widely used in construction sites and industrial sites. Moreover, crane hooks are being used for not only freight transportation and loading but also performing internal repairs on ships. Figure 7.1 shows a crane hook that is used for repairs on a ship. While crane hooks are widely used, they are also prone to frequent damage and fracture.

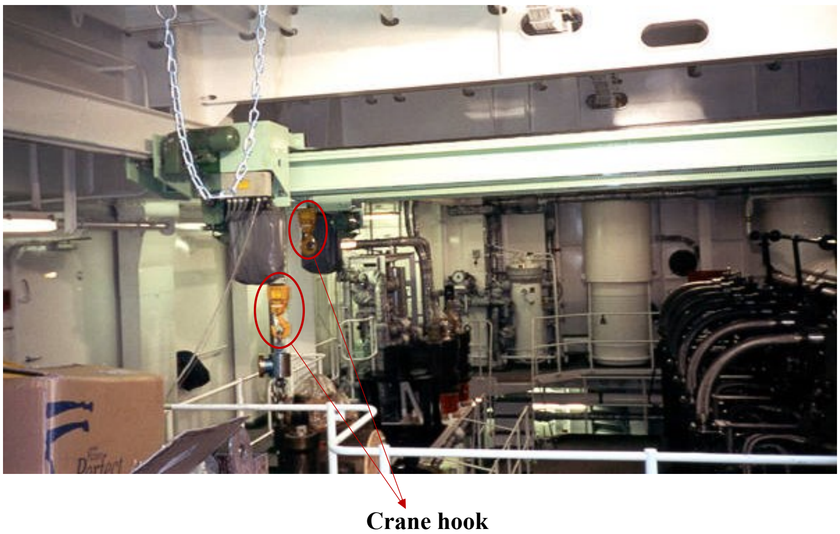

Figure 7.1 Engine room crane hook in the ship

Though it is appropriate to consider the safe working load of a crane hook, it is not possible to do this on site. That is to say, crane hooks are often operated with loads that exceed its safe working load, because operators at sites assume that the crane hook can handle these loads on the basis of previous experience. A crane hook experiences transformation in such working environments and ideally, it should be replaced immediately as soon as small transformation and damage become apparent. The crane hook is indispensable for the protection safety, and repair of articles on ships. However, violation of safety requirements while handling crane hooks can cause a catastrophic loss of life and property. Therefore, both the hook operators and the manufacturers have to pay careful attention to the condition of the crane hooks in order to ensure safety of workers. As the crane hook has come into wide use, and the regulation control for the crane user has been eased in Japan. The use of the hook up to the safe working load became possible even by the person who did not have a special license. Therefore, the person who does not especially have the knowledge and experience of the structure strength will use the crane hook, and the case that the crane hook was not used according to the rules within the safe working load happened frequently. Already the accidents are arising. Therefore, more detailed knowledge is requested about the safety use, the strength evaluation, and the enhanced safety of the crane hook. With this background, in this study, static-load and fatigue experiments were carried out for a crane hook, which was widely used at construction sites, industrial sites, and on ships. Moreover the level of observable transformation at varying loads was investigated.

These observations can be used to prevent the falling of loads during service and to minimize the risk to those people working in the dangerous conditions. Further, the database prepared on the basis this experiment can offer beneficial product information to the developer and the operator.

7.2 Experimental Procedures

7.2.1 Material and Experiment equipment

The specimens that were used for experiments were shown in Figure 7.2, 7.3 Specimen (1) was previously used on site. The brachial region was often damaged when it was used. The diameter and rounding of the brachial region on Specimen (2) were altered in order to carry out a test of the difference of the crane hook strength. Test equipment is shown in figure 7.5, 7.6. We identified points on Specimen (1), as show in Figure 7.6(b), and the difference between the point-to-point distance before and after the experiments for all the points was measured. And, we examined the characteristics of fracture and damage due to the load change on the hook. The material of the specimen in the ball-bearing region (SCM420) was different from the material in the brachial region (SCM435). The material used in the specimen corresponded well with the strength required for each part. The safe working load of the crane hook is 2.9 tons, and the safety rating is 5. Therefore, the maximum safe working load is 14.5 tons.

The main experimental device-④ was used for the experiment on a hydraulic servo-type testing machine as figure 7.4 shows. The specimen was connected to the test machine using the jig-①, as shown in Figure 7.5. The reflector-② is installed at the bottom to allow direct photography from different angles. A CCD-camera-③ and a VIDEO-camera-⑤ were used for taking photographs of the experimental conditions and the crack growth behavior while the experiment is performed. Static loads of 15 tons and dynamic loads 10 tons could be applied for both tension loading and compressive loading during the experiment. Therefore, as described later on, because the maximum safe working load of the crane hook is 14.5 tons, we could use the experiment machine for the safety evaluation of the crane hook.

7.2.2 Experimental methods

The loading modes are tension-tension and tension-compression. Figure 7.5(a) shows that Specimen (1) was installed in the jig horizontally and connected with the main experiment machine using a link. Specimen (2) was installed the main experiment machine in a similar manner as shown in Figure 7.5(b). We carried out the strength experiments for the specimens under increasing static load and crack growth behavior experiments under cyclic loading. The static load experiment was performed using the displacement control method under the following conditions; displacement speed 0.05 mm/s, maximum displacement 25 mm, and experiment rate 500 s. The experiment was carried out three times each for Specimen (1) and Specimen (2) under the same conditions.

Further, the cyclic-loading fatigue experiment was performed using the load control method at 2 Hz frequency and 0.1 stress ratio; the end time was determined as the time at which the specimen could no longer hold the maximum load. The test was carried out to examine the effect of the existence of grease in the lubrication part of the crane hook as well as the effect of different loads on the fatigue life of the crane hook. In addition, the influence of varying the diameter and rounding of the crane hook on the crane hook strength was examined. Figure 7.6(a) shows that Specimen (1) was installed in the jig vertically for the other static load test; this position was implemented because crane hooks at construction sites generally operate on the load in the vertically position, as shown in Figure 7.6(a). The Specimen marked with points A, B, C, D, and E, as shown in Figure 7.6(b). The non-deformation lengths are as follows: AB = 65 mm, BC = 30 mm, CE = 64 mm, EA = 65 mm. A displacement rate control of 0.05 mm/s was employed, and a tensile load was taken from upper part. The tensile load was taken, until the load value reached the maximum safe working load (14.5 ton) of the hook. Thereafter, it was removed the tensile load that was added, until the original load value (0 ton) was reached. The point-to-point displacement of the hook was observed for all the experiment processes.

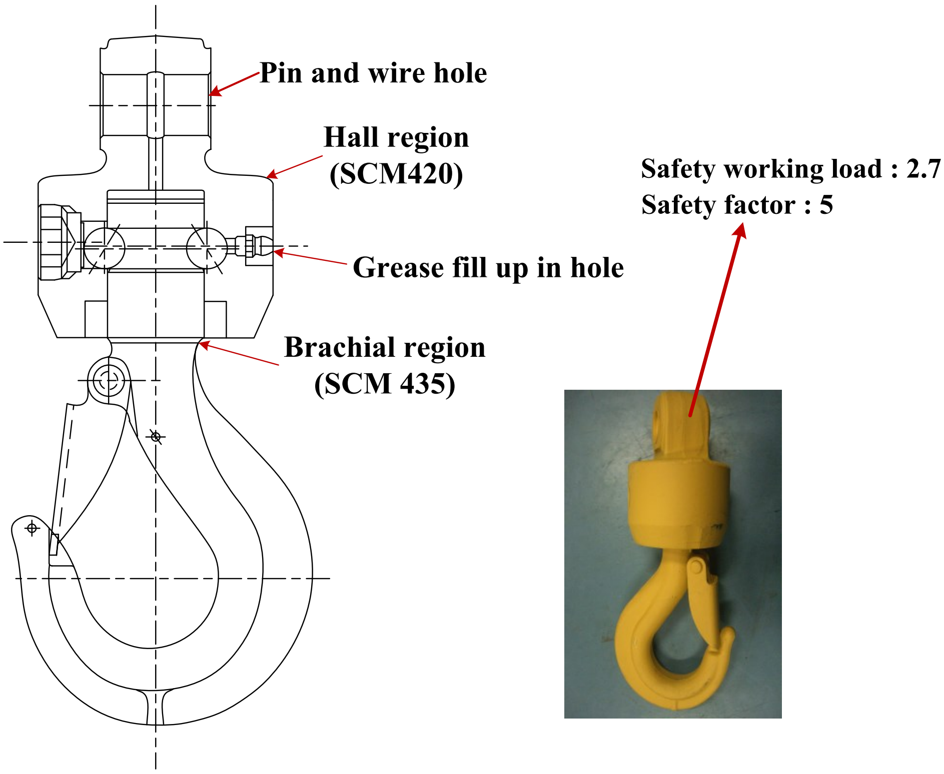

Figure 7.2 Specimen (1)

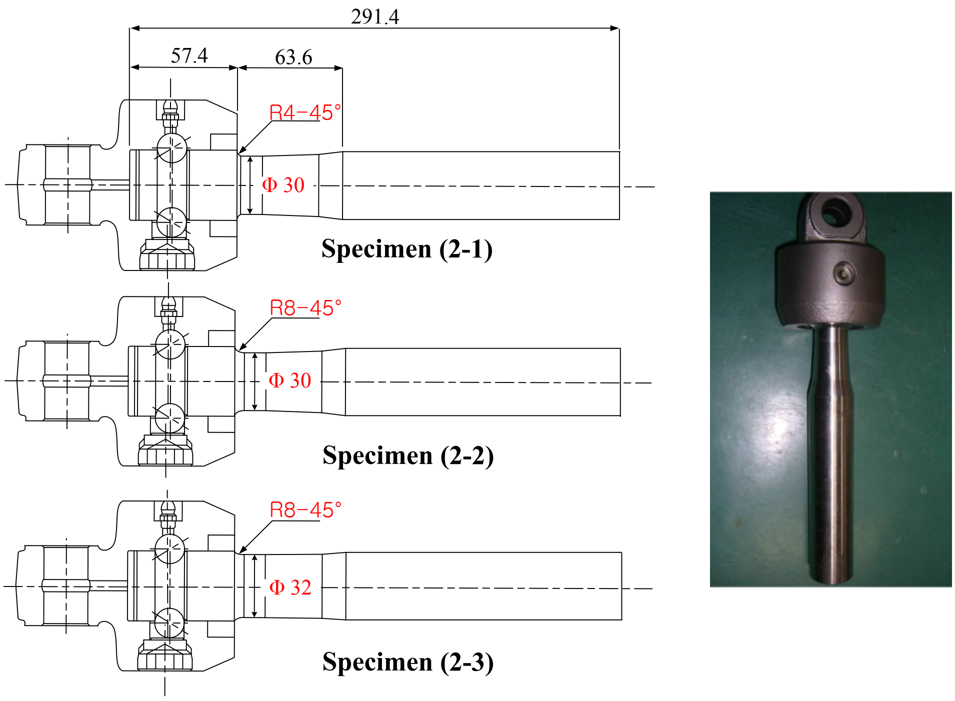

Figure 7.3 Specimen (2)

Product Specifications

- Model: EHF-UB10 1431
- Force capacity:
  - Static Load: 150kN
  - Dynamic Load: 100kN
- Crosshead travel:1000mm
- Test Speed
  - Sine, Triangular, Rectangular wave :0.001~110Hz
  - Ramp wave : 0.001~110F.S/sec

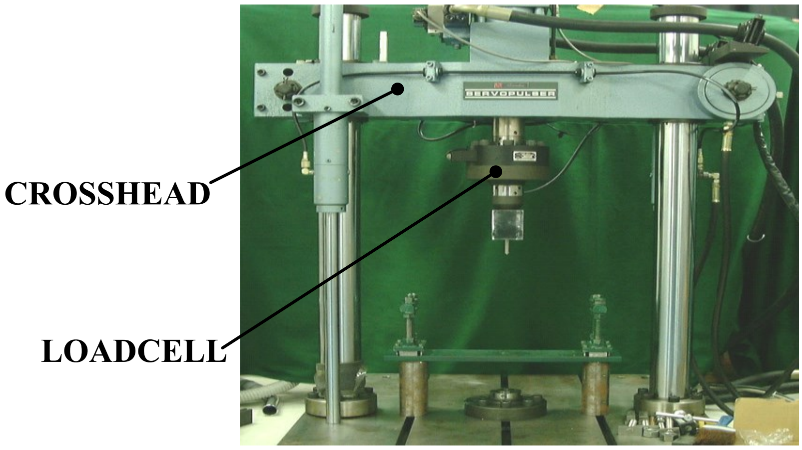

Figure 7.4 Fatigue testing machine

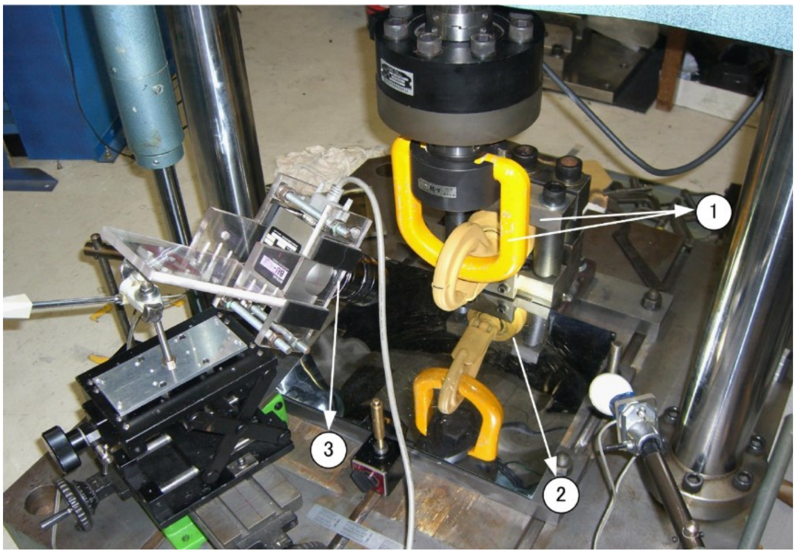

(a)

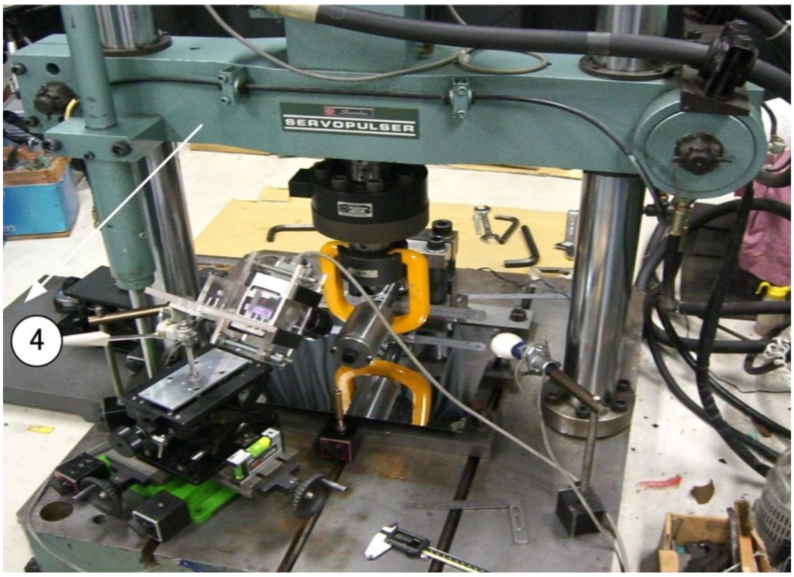

(b)

Figure 7.5 Test equipments

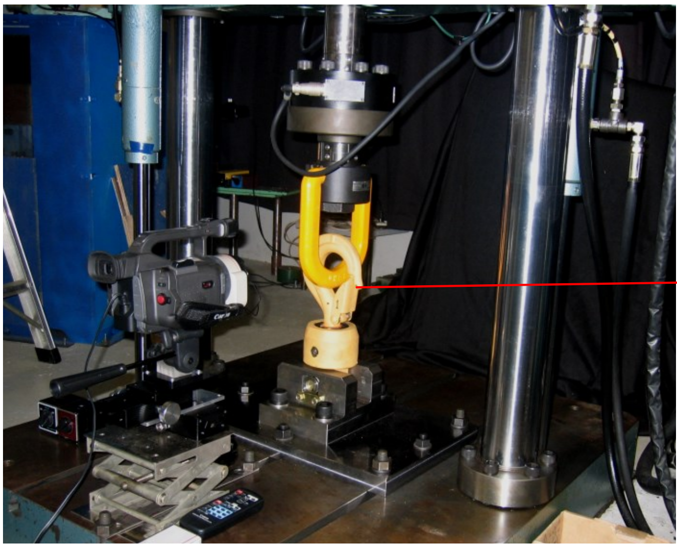

(a)

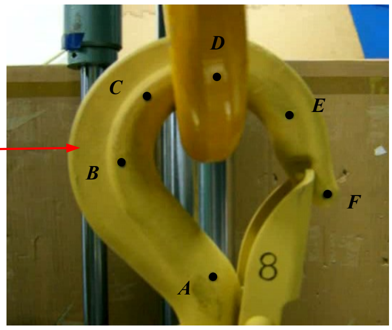

(b)

Figure 7.6 Test equipments

7.3 Results and Discussion

7.3.1 Results of static load

Figure 7.7, 7.8 shows the relationship between the load and displacement. As shown in Figure 7.7, 7.8, the change of rounding did not affect the crane hook strength. From the comparison of the result of Specimen (2-2) and Specimen (2-3), on the other hand, it was confirmed that the diameter of crane hook affected its strength. From these results, we can conclude that the strength of the crane hook was more sensitive to a change in the diameter than to a change in the rounding. The initial crack occurred at 10.66, 17.14, and 19.61 mm from the starting point of displacement as Figure 7.7. The starting point initial crack appeared at difference of the displacement. This difference might probably be attributed to the fact that the difference was evaluated using the data from the picture obtained by using the reflector.

Figure 7.9 shows the shape of the specimen after the completion of the experiment. As shown in Figure 7.9, in Specimens (1), the crack originated in the brachial region, which is quite a dangerous development, and propagated from this initial position. On the other hand, no cracks were observed for Specimen (2). In the Specimen (2), we could only confirm the change in displacement.

Figure 7.10 shows the relationship between the load and time for static load. As shown in Figure 7.10, the linear relation between time and load deviates at the 12 ton load. This fact suggests that a plastic deformation occurs in the hook at the 12 ton load. In addition, Figure 7.11, 7.12 indicates that the increment of the distance FA increases remarkably for the near 12 ton load, where the plastic deformation first occurred. In the unloading process, the increment of distance FA decreases. The removal of the load causes a reduction in the elastic strain of the hook; this reduction is due to the diminution of the elasto-plasticity deformation that occurred in the hook. As a result, the increment of distance decreases with the reduction in load.

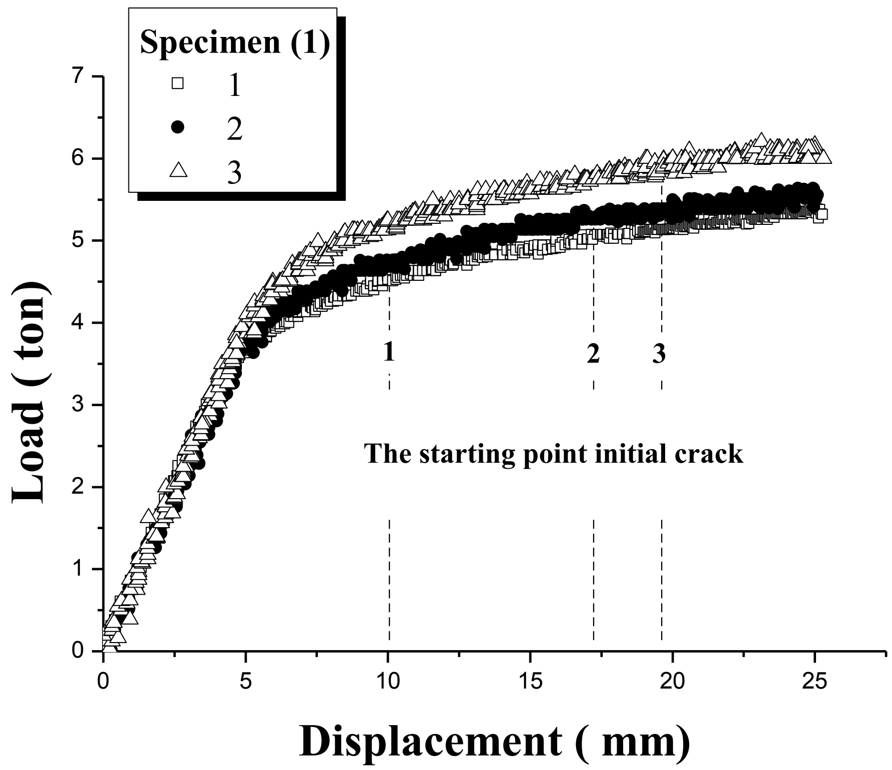

Figure 7.7 Relationship between load and displacement for static load (Specimen 1)

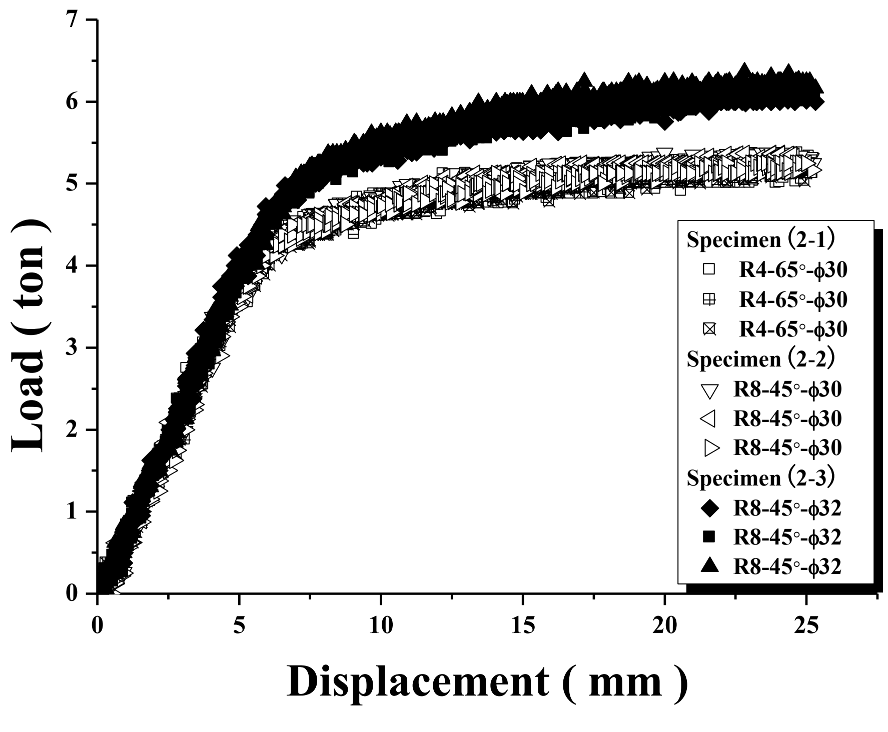

Figure 7.8 Relationship between load and displacement for static load (Specimen 2)

Specimen (1)

Specimen (2)

Figure 7.9 Shape of specimen after end of experiment

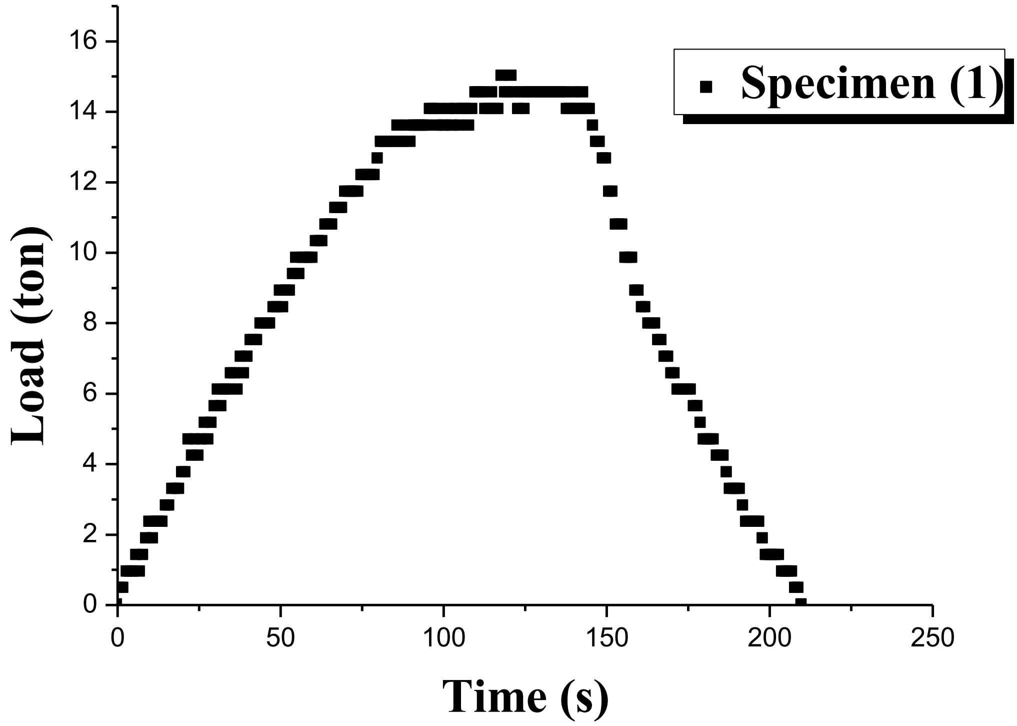

Figure 7.10 Relationship between and time for static load

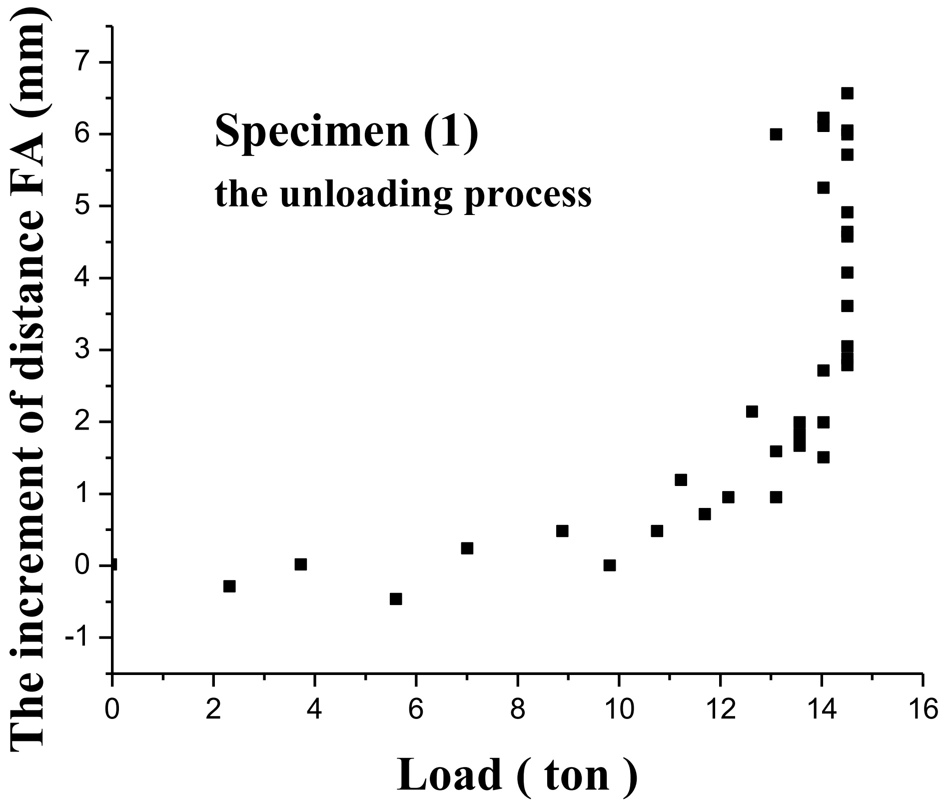

Figure 7.11 Relationship between increment of distance FA and load for static load (load process)

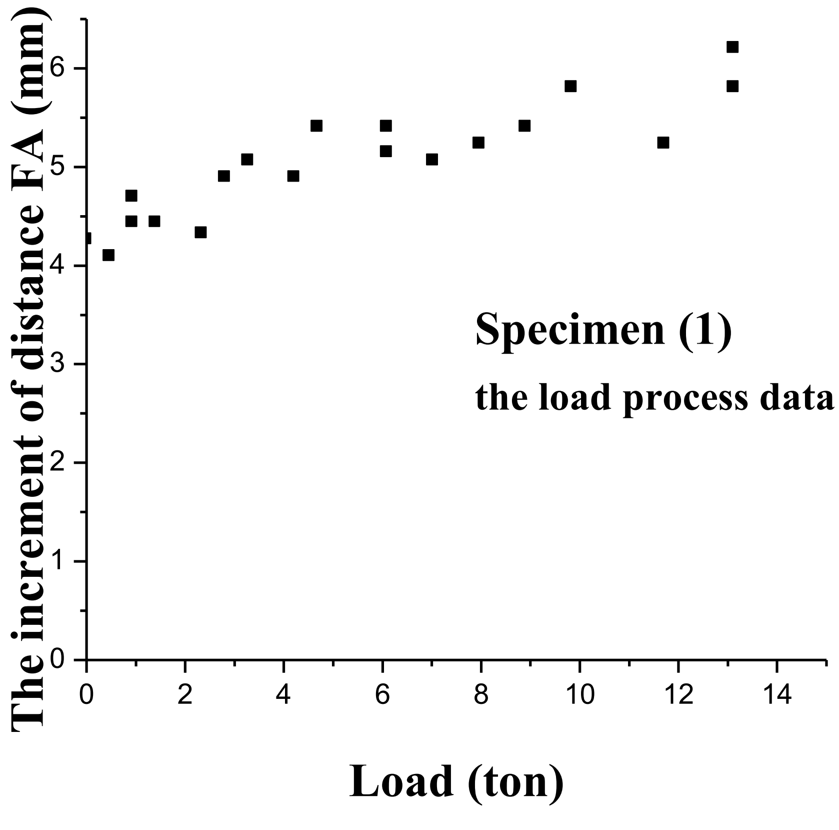

Figure 7.12 Relationship between increment of distance FA and load for static load (unload process)

7.3.2Results of cyclic load on Specimen (1)

We carried out fatigue experiments on Specimen (1) to observe how the existence of grease affects the crane hook strength and the fatigue life. Figure 7.13, 7.14 shows the fatigue experiment results; in this figure, it is possible to confirm the relationship between existence of grease and fatigue life. As shown in Figure 7.13, 7.14, the initial crack started later in the specimen without grease, and the fatigue life was slightly longer. It was confirmed that the existence of grease does not affect the fatigue life. However, the longer fatigue life for the specimen without grease can be attributed to the fact that during the course of the experiment, the stress on the specimen with grease was more than the specimen without grease. Further, Figure 7.13, 7.14 shows the fatigue life as a function of the load difference. Fatigue life reduced with increasing load. Moreover, the crane hook had roughly the same fatigue life in the cases of similar load. When comparing the difference in the fatigue life of specimens with loads of 3.6 tons and 2.9 tons, we found that the 2.9 tons specimen had an approximately 2.36 times longer fatigue life. Further, the initial crack in the 3.6 tons specimen was approximately 2.48 times larger than that of the 2.9 ton specimen. Figure 7.15 shows fatigue fracture shape in the crane hook. Table 7.1 shows the crack length of cyclic load on specimen (1). Consequently, we can conclude that the fatigue strength of crane hook was affected more by the load than by the existence of grease.

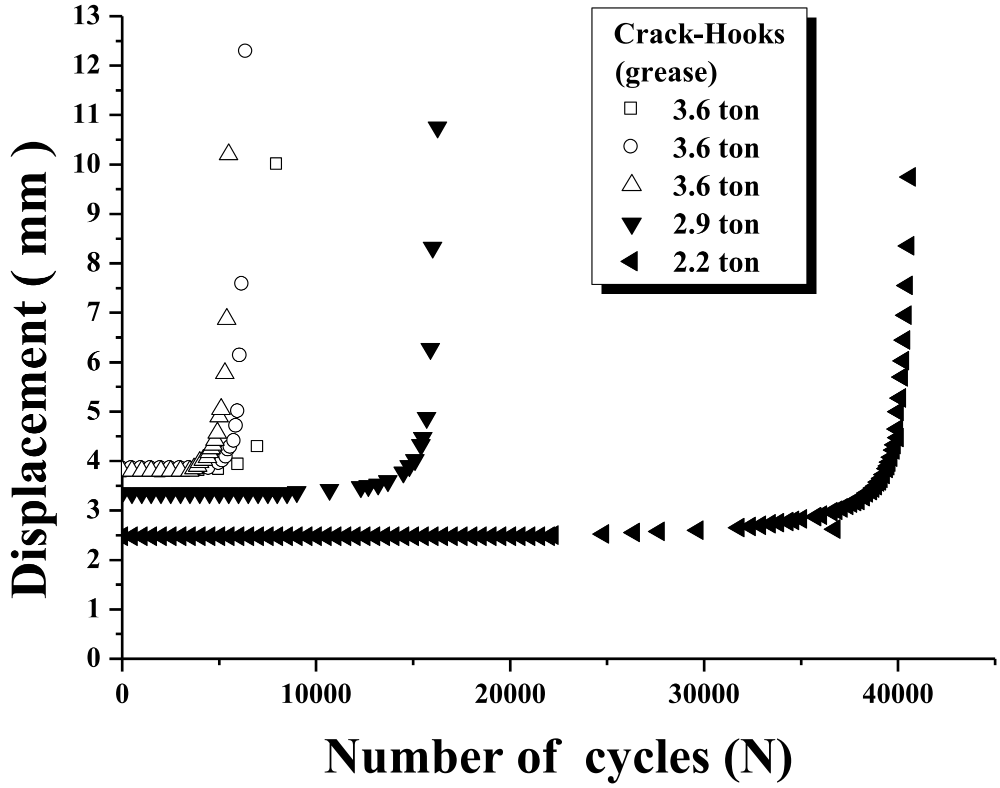

Figure 7.13 Relationship between existence of grease and fatigue life in the crane-hook (grease)

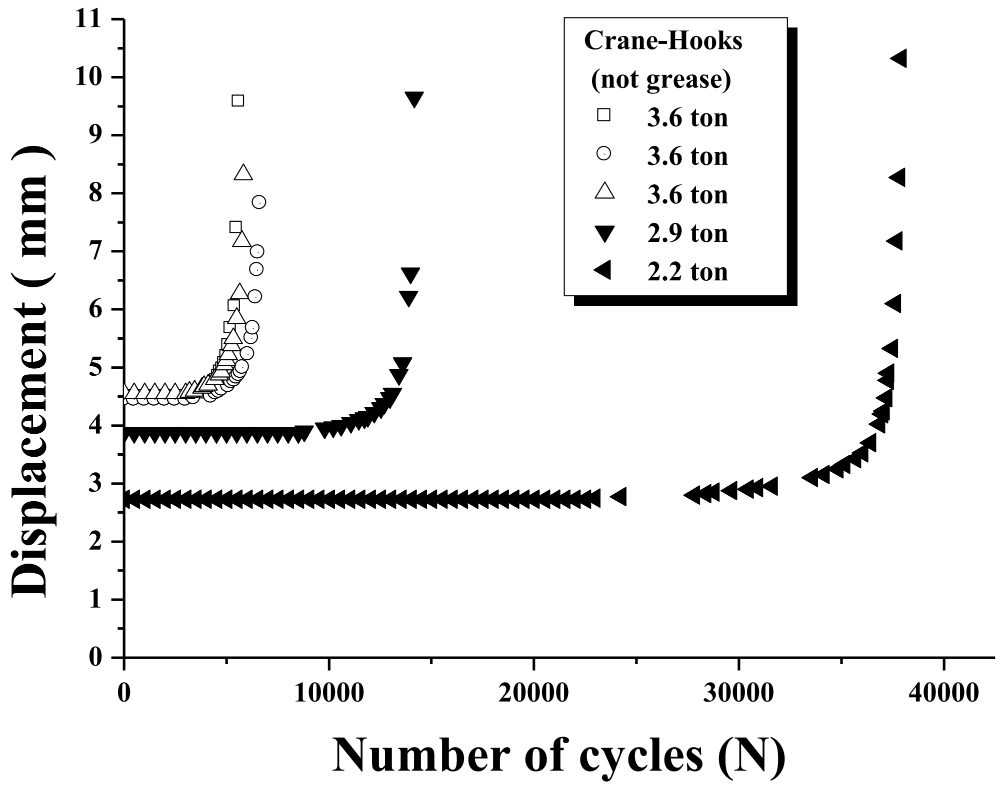

Figure 7.14 Relationship between existence of grease and fatigue life
in the crane hook(not grease)

1) with grease (3.6 ton)

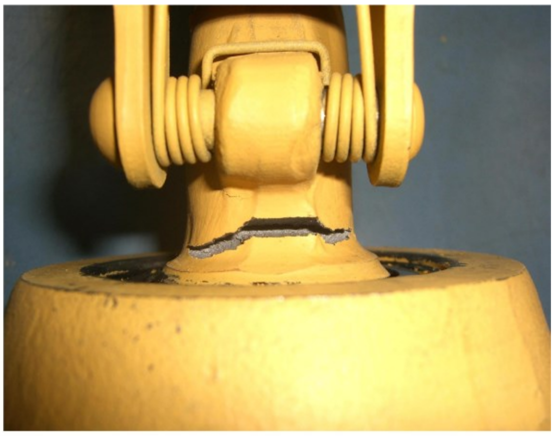

2) without grease (3.6 ton)

Figure 7.15 Fatigue fracture shape in the crane hook

Table 7.1 Crack length of specimen (1)

SPECIMEN (1)	
Load and Grease existence	Crack length (mm)
3.6ton (grease supply)	15
3.6ton (grease supply)	12
3.6ton (grease supply)	13
2.9ton (grease supply)	18
2.2ton (grease supply)	10
3.6ton (without grease)	11
3.6ton (without grease)	5
3.6ton (without grease)	7
2.9ton (without grease)	12
2.4ton (without grease)	7

7.3.3Results of cyclic load on Specimen (2)

We carried out fatigue experiments on Specimen (2). Specimen (2) was modified by changing the rounding and diameter of the brachial region, where damage and fracture are frequent are frequent. Figure 7.16 shows the S-N curve based on the result of a fatigue test. Specimen (2-1) and Specimen (2-2) had modified rounding. As shown, the fatigue life for Specimen (2-2) was approximately 1.69 times longer than that for Specimen (2-1). Specimen (2-2) and Specimen (2-3) were also modified by changing their diameter. The fatigue life for Specimen (2-3), which had the larger diameter, was about 2.25 times longer. Table 7.2 shows the crack length of cyclic load on specimen (2). Consequently, we can conclude that the fatigue life of the crane hook is more sensitive to a diameter change than a rounding change.

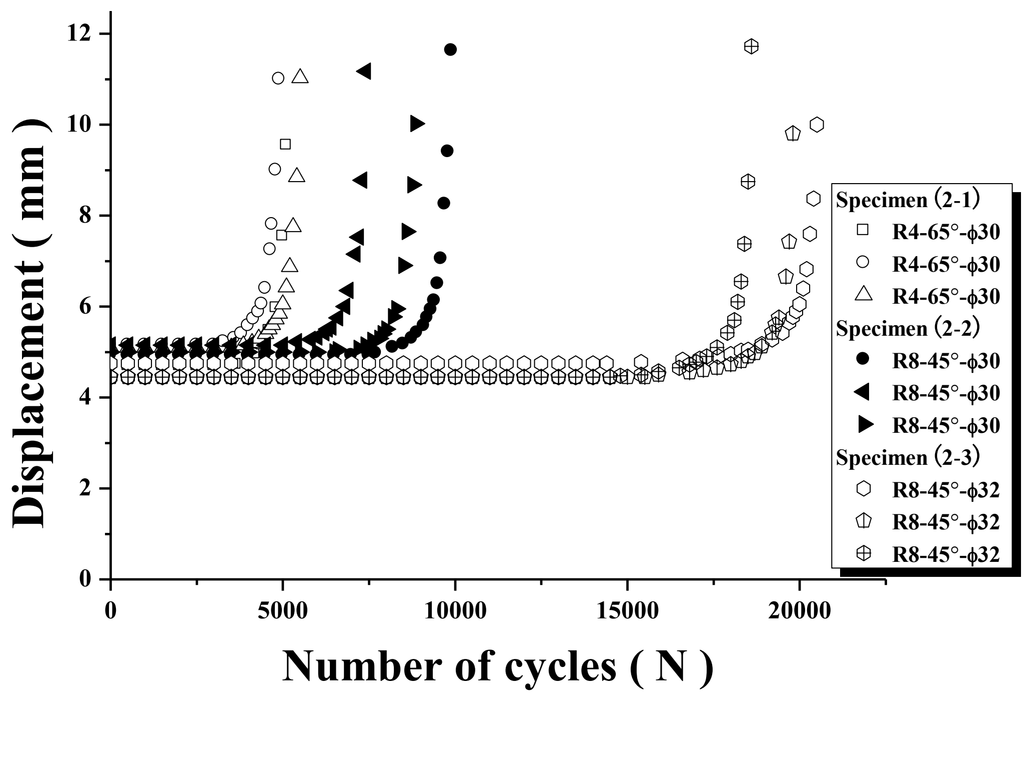

Figure 7.16 D-N curve in the specimen (2)-(3.6ton)

Table 7.2 Crack length of specimen (2)

SPECIMEN (2)	
Specimen number	Crack length (mm)
$R4-65°-\phi30$	8
$R4-65°-\phi30$	7
$R4-65°-\phi30$	8
$R8-45°-\phi30$	12
$R8-45°-\phi30$	9
$R8-45°-\phi30$	10
$R8-45°-\phi32$	12
$R8-45°-\phi32$	13
$R8-45°-\phi32$	13

7.4 Results and Discussion

The damage and fracture at the brachial region, which is a critical section of the crane hook, is closely connected to the diameter and the working load. Therefore, an accurate database will enable the user to avoid accidents as well as to gain further information pertaining to crane hooks. With this in view, in this study, we carried out static-load and fatigue experiments with crane hooks that are used at construction sites and industrial sites.

The following are the results of our experiment

(1) From the results of static load, it was clarified that the strength of crane hook was more sensitive to a change in the diameter than the rounding.

(2) From the results of cyclic load, it was confirmed that the fatigue strength of crane hook was affected by the load, and the existence of grease in the lubrication part of crane hook did not affect the fatigue strength.

(3) It was confirmed that fatigue life of crane hook was more sensitive to a diameter change than a rounding change.

(4) When an operator uses the crane hook at loads that are less than the safe working load, the crane hook can be used safely for a long period of time.

Chapter 8

Conclusions

The works carried out in this dissertation can be concluded following part.

1. Evaluation of fatigue crack growth behavior in materials with lubricating oil holes

In this study, based on such actual failure case, the fatigue crack growth experiment was carried out using aluminum alloy as experimental material in order to investigate the crack shape and fatigue crack growth characteristics when surface crack initiated from initial defect is grown toward the stress concentration zone As result, the following were the main finding: (a) it was proven that the fatigue life is affected by position of the circular hole more and on existence or nonexistence of the circular hole less. (b) the crack opening displacement is confirmed extremely affected by not only the position of stress concentration zone but also existence of the stress concentration zone.(c) It was proven that the discontinuity which exists in the member subject affected the surface crack growth behavior very much even under pure tensile load condition.

2. A study on fatigue crack growth characteristics for mutual interaction effect on 3-Dsurface crack

In this study, it was carried out the fatigue crack growth experiment using the 4 kinds of specimens (single and two cracks) in order to investigate the effect of mutual interaction on 3-D surface crack.

As result, the main findings were as follows: (a) it was proven that the fatigue life is decreased as the coalescence of crack became a lot faster on the specimen of the mutual different distance.(b) it can have confirmed that internal crack velocity decrease as the interaction effect of the two cracks during cracks are coalesced, and the fatigue life becomes short that the distance of crack was more small on the two surface cracks.

3. 3D observation of distorting crack growth in three-point bending specimen

A three-point bending test which involved changing the initial crack angle of each PMMA specimen was carried out to investigate the crack propagation characteristics. The relation between the crack propagation and fracture dynamics parameter was investigated. The following results were obtained from observations of the crack surface according to the degree of initial crack.

(a) The fracture route varied according to each degree of initial crack, propagating with added distortion as the degree of initial crack increased. (b) In the case of θ =15˚– 45˚ unstable crack propagation appeared due to the influence of the mixed mode. (c) The energy release rate according to the degree of initial rate in each crack surface increased when the degree of initial crack was large. (d) The crack propagation velocity was fastest for θ = 15˚. Comparing the crack propagation velocity according to each degree of initial crack, there might exist a degree between θ = 0˚ and θ = 30˚ which has faster crack progress velocity.

3-1 Evaluation of Fatigue Crack Growth Characteristics about Mixed Mode Influence and Thickness Dependence Using the Three-point Bending Specimens

SCM440 which is chrome molybdenum steel widely used in various structures or major parts of machine is used as the specimens to conduct the fatigue crack growth experiment in this study. We observed the fatigue crack growth behaviors in mode I and mixed mode conditions considering correlation between initial inclination angle and thickness.

Observed results are as follows.

(a) The fatigue crack which arises from a crack growth being twisted, and the crack slant angle decreases. It checked from the beach mark that there was no big change in the crack edge shape at that time. Moreover, when the initial crack slant angle was large, the crack arose at the time of initial crack growth, and it was suggested that the crack growth behavior is unstable. (b) The difference of the crack growth history appeared greatly, as the initial crack slant angle and a specimen thickness increased. Since the dynamic condition at the tip of a crack changed with the influence of the mixed mode, or the influences of a modification restraint near the specimen thickness center, it thinks. (c) If the initial crack growth continues to some extent, a crack slant angle will decrease and the dynamic condition at the tip of a crack moves a mode I dominated. Even if it saw the overall crack growth history, it has checked that the crack growth rate of the crack growth last stage was a state practically equal and pure mode I crack growth.

4. Strength evaluation of marine hooks by static-load and fatigue experiments

The damage and fracture at the brachial region, which is a critical section of the crane hook, is closely connected to the diameter and the working load. Therefore, an accurate database will enable the user to avoid accidents as well as to gain further information pertaining to crane hooks. With this in view, in this study, we carried out static-load and fatigue experiments with crane hooks that are used at construction sites and industrial sites. The following are the results of our experiment

(a) From the results of static load, it was clarified that the strength of crane hook was more sensitive to a change in the diameter than the rounding. (b) From the results of cyclic load, it was confirmed that the fatigue strength of crane hook was affected by the load, and the existence of grease in the lubrication part of crane hook did not affect the fatigue strength. (c) It was confirmed that fatigue life of crane hook was more sensitive to a diameter change than a rounding change. (d) When an operator uses the crane hook at loads that are less than the safe working load, the crane hook can be used safely for a long period of time.

References

Hertzbeg R.W. and Richard Roberts, 1979, Crack Initiation in a High-Strength Low-Alloy Steel, Fracture Mechanics, ASTM STP 677 Smith, ED., American Society for Testing and Materials, pp. 290-302.

Clark, W. G. Jr., 1979, Effect of spherical discontinuities on fatigue crack growth rate performance, Fracture Mechanics, ASTM STP 677, Smith, C. W. ED., American Society for Testing and Materials, pp.303-319.

Crew, J. H., 1970, Crack initiation at stress concentration as influenced by prior local plasticity, Achievement of high fatigue resistance in metals and alloys, ASTM STP 467, Philadelphia, pp. 37-52.

Erdogan, F. and Sih, G. C., 1963, On the crack extension in plates under plane loading and transverse shear, J. Basic Eng., 85, pp.519-525.

Forsyth, P. J. E., Acta Met., 11, 1963, pp 703.

Forsyth, P.J.E., and Ryder, D., 1961, Metallurgia, Vol. 63, pp. 117-124.

Heath, B.J., Grandt. Jr., A. F., 1984, Stress intensity factors for coalescing and single corner flaw along a hole bore in a plate, Engineering Fracture Mechanics, Vol.40, No.4, pp. 665-673.

Iida, K. and Kawahara, M., 1975, Change in fatigue crack shape during growth, Naut Report No.9011, Department of Naval Architecture, University of Tokyo.

Irwin, G. R., 1957, Analysis of stresses and strains near the end of a crack traversing a plate., Journal of Applied Mechanics, Vol. 24, pp. 361-363.

James, F. Shackelford, 2000, Introduction to materials science for engineers (5^{th} edition), Prentice Hall in International Edition, pp.414-415.

Kikuchi, M. and Kuga, K., 2002, Fatigue test under Mode II+III mixed-mode condition with four point shear specimen, Experimental Mechanics, Vol.2, No.1, pp.55-60.

Mahajan, R. V. and Ravi-Chandar, K., 1989, An experimental investigation of mixed-mode fracture, International Journal of Fracture Vol.41, pp.235-252.

Makabe, C. and Darrell, F., 2001, Branching and propagation behaviors of fatigue crack propagation behaviors of fatigue crack precracked specimen, Journal of the Society of Materials Science, Vol.50, No.12, pp.1329-1334.

Makabe, C., Socie, D. F., Sueyoshi, Uehara, T., 2004, Mechanism of shear mode fatigue crack growth in pure aluminum, Trans. of the Japan Society of Mechanical Engineers, Vol.70, No.689, pp.84-92.

Murakami, Y, Nemat-Nasser, 1983, Growth and stability of interacting surface crack flaws of arbitrary shape, Engineering Fracture Mechanics, Vol.17, No.3,

Murakami, Y., and Nemat-Nasser, S. 1982, Interaction dissimilar semi-elliptical surface flaws under tension and bending, Engineering Fracture Mechanics, Vol.16, pp.373-386.

Hideki, E., Katsutoshi, A., 1989, Fatigue Strength Characteristics of High Strength Steel , Journal of the Japan Society of Machanical Engineers , Vol.55, No. 509.

Qian, j. and Fatemi, A., 1996, Mixed Mode Fatigue Crack Growth , A Literature Survey, Eng. Frac. Mech., Vol. 55, No. 6, pp. 969～990.

Sam-Hong S. and Jeong-Moo L., 2001 , Fatigue Crack Propagation Behavior in STS304 under Mixed Mode Loading, Transaction of the KSPE, Vol. 18, No. 9, pp. 131 ～139.

ASTM E647-93, Standard Test Method for Measurement of Fatigue Crack Growth Rates, Annual Book of ASTM Standards, Vol. 03. 01, pp. 565～601

Paris, P. C. and Erdogan, F., 1960, A Critical Analysis of Crack Propagation Laws, Journal of Basic Engineering, Vol. 85, pp. 528~534.

Namba, K. and Torii, T., 2004, Evaluation of stress intensity factors and fatigue crack propagation rates based on crack opening displacement distributions for part-through cracks, Japan society of Mechanical Engineers, Vol. 70, No. 692, pp. 596-603.

Neuber, H., 1961, Theory of stress concentration for shear-strained prismatical bodies with arbitrary nonlinear stress-strain laws, J. Appl. Mech. Trans, ASME, Vol.

E28, pp. 544-550.

Nishioka, T and Atluri S.N., 1983, Path Independent Integrals, Energy Release rates and, General Solutions of Near-Tip Fields in Mixed-Mode Dynamic Fracture Mechanics, Engineering Fracture Mechanics. Vol.18, No.1, (1983)

Nishioka, T. and Altluri, S.N., 1983, Analytical solution for embedded elliptical cracks, and finite element alternating method for elliptical surface cracks, subject to arbitrary loadings, Engineering Fracture Mechanics. Vol.17 pp. 247-268.

Norio, H. and Yasuhiro, K., 1978, Calculation of stress intensity factor from stress concentration factor, Engineering Fracture Mechanics, Vol. 10, pp. 215-221.

Otsuka, A. and Mori, K., 1983, Fractographic study of Mode II fatigue crack growth on 7075-T6 and 2017-T4 Aluminum Alloys, Journal of the society of Materials Science, Vol.32, No.355, pp.34-40.

Otsuka, A., Tohgo, K. and Matsutama, H., 1987, Fatigue crack initiation and growth under mixed mode loading in aluminum alloy 2017-T3 and 7075-T6, Journal of the Society of Materials Science, Vol.36, No.405, pp.38-44

Otsuka, A., Tohgo, K. and Yoshida, M., 1987, Fatigue crack growth of a mixed mode three-dimensional crack (2^{nd} Report, Fatigue crack growth behavior from a semi-elliptical surface crack under shear loading), Trans. of the Japan Society of Mechanical Engineers, Vol.54, No.505, pp.1735-1744.

Nishioka T., Yoshimura S., Nishi M. and Sakakura K., 1995, Experimental Study on Three-Dimensional Dynamic Fracture, ASME, PVP-Vol. 300.

Sakakura K., Yoshimura S., Nishioka T., 1995, Photography for Three-Dimensional Dynamic Fracture Using a High-Speed Camera", Symposium on High Speed Photography and Photonics.

Collapse of a suspended span of interstate route 95 highway bridge over the Mianus River, Greenwich, Connecticut, June 28 1983, Nat Trans Safety Board Report NTSB/HAR-84/03, July 1984

Nishioka T., Nishi M., Fujimoto T., Sakakura K., 1993, A study on the Front Shapes and Surface Singularity of Dynamically Propagating Cracks", Vol. 59-559, No. 92-1213, pp. 666-673.

Standard Test Method for JIC. A Measure of Fracture Toughness, ASTM E 813-81, Annual book of ASTM Standards, 1983

Portch, D. J., 1976, The propagation of fatigue crack from surface flaws, Report, Berkeley Nuclear Laboratories.

Raju, I. S. and Newman, J. C., 1981, An empirical stress-intensity factor equation for the surface crack, Engineering Fracture Mechanics, Vol. 15, Issues 1-2, pp 185-192.

Rice, J.R., 1968, A path independent integral and approximate analysis of strain concentration by notches and crack. Journal of Applied Mechanics, Vol.35, pp.379-386.

Schijve, J., Fraga, W. E. and Hewitt, R. L., 1986, Comparison of an engineering estimate with a numerical solution for the stress concentration factor of a hole near a circular edge notch, International Journal of Fracture, July, pp.111-118.

Shen, G. and Glinka, G., 1991, Determination of weight functions from reference stress intensity factors, Theoretical and Applied Fracture Mechanics, Vol. 15, pp. 237-245.

Sides, A. Perl, M., and Uzan, J., 1984, The effect of an inclusion or a hole on an approaching crack the three-point bend specimen, Engineering Fracture Mechanics, Vol.20, No.1, pp.83-91.

Sloan S.W. and Houlsby, G.T.,1984, An Implementation of Waston's Al-gorithm for Computing 2-Dimensional Delaunay Triangulations, Advances in Engineering Software, Vol.6, pp.192-197.

Soboyejo, W. O. and Choi, H. C., 1988, On the prediction of the fatigue propagation of semi-elliptical defects, ASTM STP 1122, pp.435-438.

Sommer, E, Hodular, L. and Kordisch, H., 1997, Growth characteristics of part-through crack in thick-walled plates and tubs, Journal of Pressure Vessel Technology, Transactions of the ASME 99, Series J, No.1, pp.106-111.

Tanniguchi, T., 1992, Automatic Mesh Generation for FEM: Use of Delaunay Triangulation, Morikita Publishing.

Tohgo, K., Otsuka, A. and Yuuki, R., 1986, Fatigue crack growth of a mixed mode three-dimensional crack, Japan Society of Mechanical Engineers, Vol.52, No.479, pp.909-918.

William, M.L., 1957, On the stress distribution at the base of a stationary crack, Journal of Applied Mechanics, Vol. 24, pp. 109-144.

Wu, S., Ivanova, E. and Chudnovsky, A., 1994, The effect of a process zone on the fracture path in a complex stress field, International Journal of Fracture, pp. R13-19.

Wouter O., Patrick D., Wim D., Failure of a large ball bearing of a dockside crane, Engineering Failure Analysis, Vol.11 No.3, pp.335-353,(2004)

Ochae K., Sangki L., Youngseok C., Jungchul P. and Kihyo J., Development of a Workload Assessment Model for Overhead crane Operation, Journal of the Ergonomics Society of Korea, Vol.26 No.2, pp.45-59(2007)

Chi-Cheng C. and Cheng-Yi C., Controller Design for an Overhead crane system with Uncertainty, Control Eng. Practice, Vol.4 No.5, pp.645-653, (1996)

Publications

Journal Papers

(1) Nishioka, T., Lee, H. Y., Won, Y. J., and Fujimoto, T., "Strength Evaluation of Marine Crane Hooks by Static-load and Fatigue Experiments", The Japan Institution of Marine Engineering, Journal of JIME Vol.45 Special Issue ISME Busan 2009, pp.91-96, (2010.11)

(2) Nishioka. T., Lee, H.Y., "3D Observation of Distorting Crack Growth in Three-point Bending Specimen", Journal of Solid Mechanics and Materials Engineering, Vol.5, No. 11-0671, (2012.06)

(3) Nishioka, T., Lee, H. Y., Won, Y. J., and Fujimoto, T., "Evaluation of Fatigue Crack Growth Behavior in Materials with Lubricating Oil Holes", The Japan Institution of Marine Engineering, Vol. 47, No5 (2012. 5)

(4) Kim. G. H., Cho, K.C., Lee, H.Y., Won, Y. J., "Characteristic of Fatigue Crack Behavior on the Mixed-Mode in Aluminum Alloy 5083-0", Journal of the Korean Society of Marine Engineering, Vol. 35, No.7, pp. 899~906, 2011. 11

(5) Lee, H. Y., Fujimoto, T., "Evaluation of Fatigue Crack Growth Characteristics about Mixed Mode Influence and Thickness Dependence Using the Three-point Bending Specimens", The Japanese Society for Experimental Mechanics (JSEM) (Prepublication paper)

International Conferences (proceedings)

(6) Nishioka, T., Lee, H.Y., Won, Y.J., Fujimoto, T., Fukui, T. and Kuroda, S., "Strength Evaluation on Marine Crane-hook by Static-load Fatigue Experiments", The Japan Institution of Marine Engineering, Journal of JIME Vol.45 Special Issue ISME Busan 2009, pp.91-96,

(7) Nishioka. T., Lee, H.Y., "3D Observation of Distorting Crack Growth in Three-point Bending Specimen", ATEM '11, Kobe, Japan, Sep.19-21, 2011

(8) Nishioka. T., Cho, K.C., Lee, H.Y., "Fracture Toughness Evaluation of Adhesive Material for LNG Ship Tank", International Symposium on Marine Engineering (ISME) 2011, Kobe, Japan, October 17-21 (2011).

(9) Lee, H.Y., Fujimoto, T., Nishioka. T., "A Study of Material Heat treatment and Multiple cracks Interaction Effect of Fatigue Growth of a Surface crack ", JSME 25th Computational Mechanics Division Conference (CMD2012), Kobe, Japan, October 6-8 (2012).

Acknowledgments

I would like to express my deepest respect and most sincere gratitude to my advisory professor Dr. T. Fujimoto, for the guidance and encouragement at all stages of my work.

His constructive criticism and comments from the initial conception to the end of this work is highly appreciated.

I am greatly indebted to his assistance and understanding in matters of non academic concern which have helped me endure some difficult times during my study period. My deep appreciation also goes to Dr. T. Nishioka, for valuable discussions and assistance.

I am very grateful to all my friends and all past and present members of *Simulation Engineering Laboratory* for helping me in many ways during my study in Kobe.

Finally, I wish to thank my parents, for their constant encouragement and moral support.